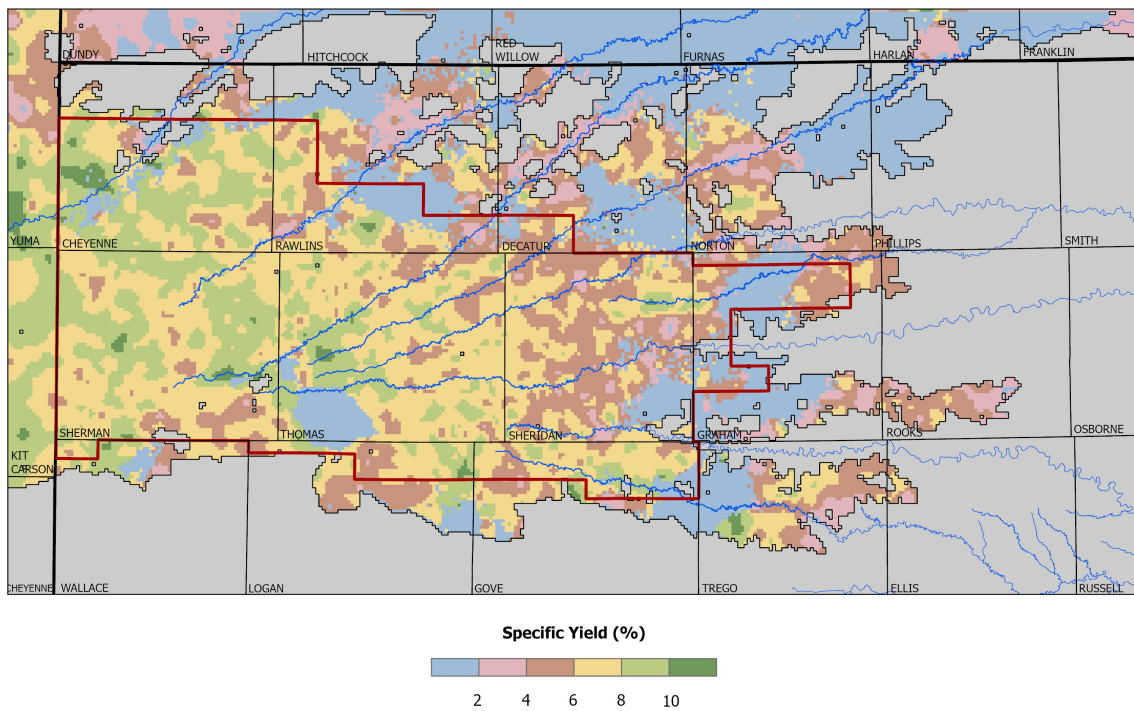


GMD4 Groundwater Flow Model

High Plains Aquifer Modeling Maintenance Project

Funded by the
Kansas Water Office (Contract 18-120)
and
Northwest Kansas Groundwater Management District No. 4



B. B. Wilson, G. Liu, G. C. Bohling, and J. J. Butler, Jr.

Kansas Geological Survey Open-File Report 2021-6

GEOHYDROLOGY

KU KANSAS
GEOLOGICAL
SURVEY
The University of Kansas

**GMD4 Groundwater Flow Model
High Plains Aquifer Modeling Maintenance Project**

**This project was funded by the
Kansas Water Office (Contract 18-120)
and
Northwest Kansas Groundwater Management District No. 4**

Kansas Geological Survey Open-File Report 2021-6

Kansas Geological Survey, Geohydrology Section
University of Kansas, 1930 Constant Avenue,
Lawrence, KS 66047
<http://www.kgs.ku.edu/>

Disclaimer

The Kansas Geological Survey does not guarantee this document to be free from errors or inaccuracies and disclaims any responsibility or liability for interpretations based on data used in the production of this document or decisions based thereon.

TABLE OF CONTENTS

Introduction	1
Description of Study Area and General Model Setup	2
Previous Geohydrologic Studies	2
Physiographic Setting	3
Model Design	3
Active and Inactive Areas	8
Review and Setup of Data Parameters	9
Precipitation Data	9
Geology and Lithology	11
Aquifer Characteristics	11
Bedrock Surface	14
Lithologic Classifications	17
Water Levels	21
Boundary Conditions	27
Stream Characteristics and Flow	27
Water Right Development	31
Kansas	31
Colorado and Nebraska	35
Irrigation Return Flow	38
Irrigated Land Fractions	40
Model Calibration and Simulation	43
Model Characteristics	43
Pumping and Irrigation Return Flows	43
Stream Characteristics	43
Drains	43
Evapotranspiration	44
Time-Varying Specified-Head Boundaries	44
Precipitation Recharge	44
Enhanced Precipitation Recharge from Irrigated Land Fractions	46
Delayed Recharge	46
Lagged Drainage from Dewatered Sediments	47
Hydraulic Conductivity and Specific Yield	48
Model Calibration	53
Sensitivity Analysis	58
Transient Model Results	59
Water Levels	59
Model Budgets	79
Model Scenarios	85
No Change in Future Water-Use Policy	85
Reduce Pumping by 20%	90
Reduce Pumping by 30%	93
GMD4 Districtwide LEMA	96
Comparison of All Scenarios	100
Acknowledgments	104
References	105

INTRODUCTION

Northwest Kansas Groundwater Management District No. 4 (GMD4) was formally established on March 1, 1976, and is the fourth of five districts in Kansas authorized under the Groundwater Management District Act of 1972. A primary purpose of GMD4 is the conservation and management of groundwater resources through policies and programs established by local landowners and water users. Overlying all or parts of 10 counties in northwest Kansas, GMD4 further supports educational and research activities while working with all levels of government to provide the best social and economic benefits from local groundwater supplies.

The Ogallala portion of the High Plains aquifer (HPA) is the primary water source for virtually all water uses; the vast majority of water is used for irrigation. Like much of western Kansas, GMD4 has experienced varying levels of declining water levels. To reduce rates of groundwater decline and extend the life of the aquifer, GMD4 was the first district to implement the Local Enhanced Management Area (LEMA) program, one in a high-priority area known as SD6 and a second, more recent one, covering large portions of the district.

Project Overview

The Kansas Water Office (KWO) and GMD4 contracted with the Kansas Geological Survey (KGS) in June 2018 to develop a numerical groundwater model for the GMD4 area. The primary objective of the model is to better understand the hydrologic system and water-level changes occurring in the underlying HPA. The model will be used to simulate future water use and management scenarios to estimate their effects on the HPA in this region.

The project funding period was January 2018 through the summer of 2021, following a delay due in part to the COVID-19 pandemic and the refinement of new modeling concepts. The calibrated transient model was completed in the winter of 2020–2021. As the model was being developed, the KGS provided progress reports at several GMD4 board meetings.

DESCRIPTION OF STUDY AREA AND GENERAL MODEL SETUP

The study area includes GMD4 in northwest Kansas and extends beyond the district boundaries in all directions (fig. 1). The model domain extends to the east (~45 miles) and south (~15 miles) to encompass the edges of the Kansas HPA in those directions and roughly 8 miles westward into Colorado and northward into Nebraska to reduce the impacts of those boundaries on model results in the district. The total area covered by the model is 16,740 square miles. Groundwater-based irrigation represents the largest use of water (about 98%), although the HPA is also the source of supply for municipal, stockwater, industrial, recreational, and domestic uses. The majority of the model area (and the entire boundary of GMD4) lie within the Upper Republican Regional Planning Area for the Kansas Water Office. Portions of the Solomon-Republican, Smoky Hill-Saline, and Upper Smoky Hill Regional Planning Areas make up the rest of the modeling area.

Previous Geohydrologic Studies

Several KGS bulletins report on the geology and groundwater resources of the model area, including Frye (1945) (Thomas County), Frye and Leonard (1949) (Norton and northwestern Phillips counties), Prescott (1952, 1953, 1955) (Cheyenne, Sherman, and Graham counties), Walters (1956) (Rawlins County), Bayne (1956) (Sheridan County), Johnson (1958) (Logan County), Hodson and Wahl (1960) (Gove County), and Hodson (1963, 1969) (Wallace and Decatur counties). In addition to characterizing the groundwater conditions in the region, these bulletins provide well records and lithologic logs that have been used to construct and calibrate the model.

All of GMD4 and the rest of the HPA in northwest Kansas are part of the much larger modeling domain used by the Republican River Compact Model (RRCM). Covering parts of Kansas, Colorado, and Nebraska, the RRCM is used primarily to simulate streamflow and baseflow components affected by pumping and recharge in the Republican River Basin in accordance with the Republican River Compact (Republican River Compact Administration, 2003). The RRCM is updated annually for compact accounting and reporting requirements.

More recently, the KGS has conducted a series of studies of the HPA involving GMD4. Whittemore et al. (2016) used regional correlations between climatic indices, water-level change, and pumping across each of the GMDs to illustrate that reasonable pumping reductions could stabilize water levels, at least temporarily, over much of the aquifer in Kansas. Butler et al. (2016) applied a data-driven, water-balance approach, which used annual water-level measurements and reported groundwater usage to determine what average level of usage is needed to stabilize water levels in the near term. Liu et al. (2021) combined the water-balance analysis with lithologic logs and developed a new approach for estimating specific yield that can be used directly in groundwater models. The methodologies outlined in these reports have been incorporated into this model.

Physiographic Setting

The vast majority of the active area of the model lies within the High Plains physiographic region. Much of the High Plains region is characterized by flat to gently rolling, eastward sloping uplands broken by relatively shallow valleys. Shallow depressions/playas are common features. Although not well supplied with surface water, GMD4 contains the headwaters to several streams, most of which are intermittent with distinctive drainage patterns. The eastern- and southernmost portions of the model domain are within the Smoky Hills region where the HPA has been eroded away, often exposing the underlying chalk formations.

Land cover classification maps compiled in Kansas in 2015 by the Kansas Biological Survey (Peterson, 2018) and in Colorado and Nebraska by the USGS (Homer et al., 2012) show cropland is the primary land-cover type within the district (fig. 2). Grasslands are typically more prevalent along stream courses and in the areas outside of GMD4, while municipal footprints (and water usage) across the model area are relatively small.

Model Design

This project used MODFLOW, the modeling software developed by the USGS based on a finite-difference approximation of the flow equation (Harbaugh et al., 2000). MODFLOW is one of the most widely used groundwater flow models in the world and can be used to simulate the effects of many processes, such as areal recharge, stream-aquifer interactions, drains, evapotranspiration, and pumping. Input files for the MODFLOW model were created with assistance from scripts written in Fortran (<https://www.fortran.com/>). The model was run by entering the executable file name in a Windows command prompt.

The model uses uniform and equally spaced square cells, 0.5 x 0.5 miles in size (0.25 mi²). It contains 186 rows and 360 columns, resulting in 66,960 individual model grid cells (fig. 3). The grid was designed to align with model cells used in the MODFLOW-based groundwater flow model for GMD1 in west-central Kansas, developed by the KGS in 2015 (Wilson et al., 2015). The GMD4 model uses one convertible layer that allows both confined and unconfined aquifer conditions to be simulated, depending on where water levels intersect the top of the HPA.

The streamflow-routing package (SFR in MODFLOW; Prudic et al., 2004) was used to compute stream-aquifer interactions by subdividing streams into a series of segments and reaches. Streams cells were set up for Beaver Creek, Big Creek, Bow Creek, Keith Sebelius Reservoir, North Fork (NF) Solomon River, Prairie Dog Creek, Saline River, South Fork (SF) Republican River, SF Sappa Creek, and SF Solomon River. Drain cells are specified for much of the aquifer's eastern edge, into which groundwater might discharge. For the drain cells, water from the aquifer can discharge to the surface depending on water-table elevations. If the water levels drop below the land surface, this connection is broken and the drains become inactive (e.g., a spring becomes dry after the water table falls below the spring outlet).

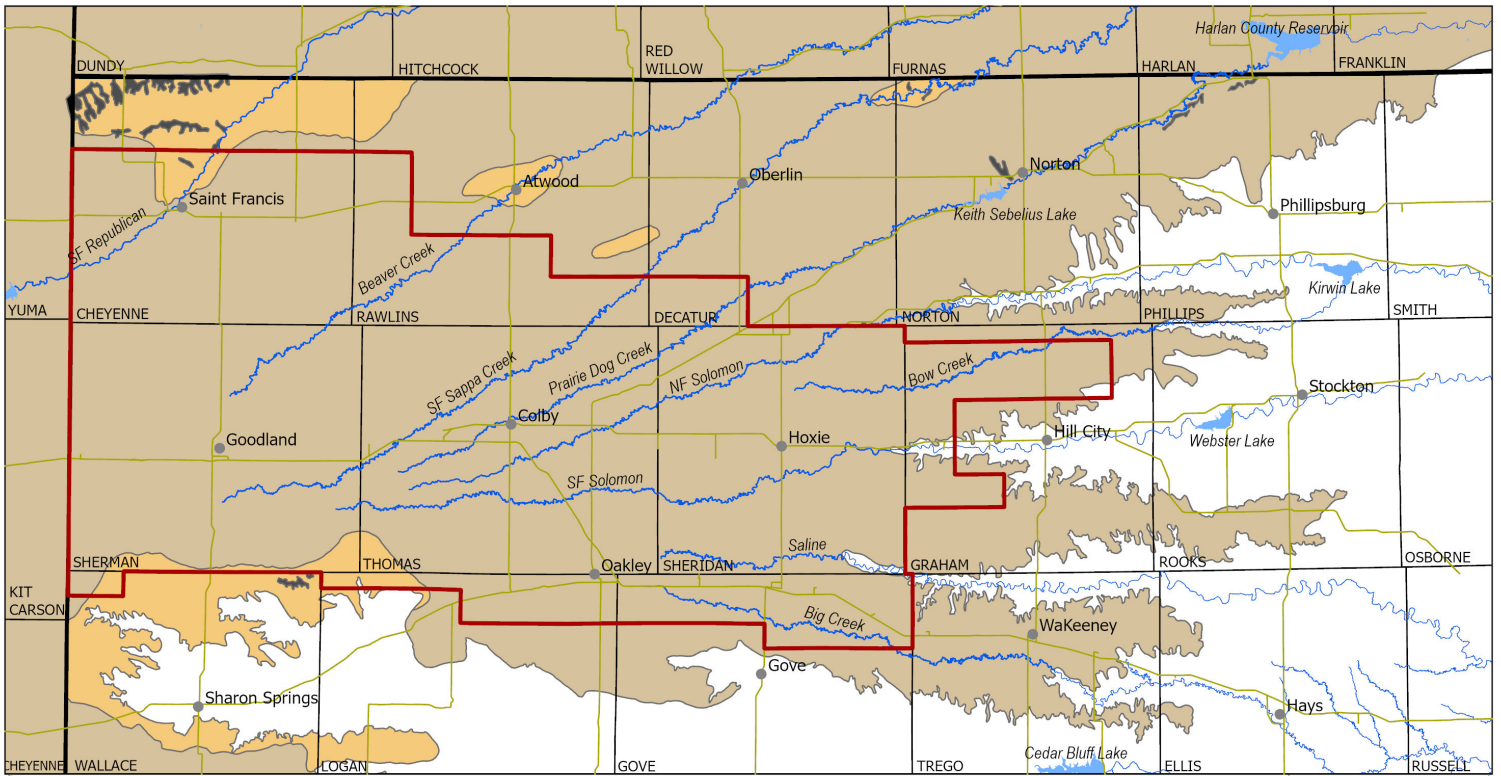
Time-varying specified-head boundaries are located along the edges of the model where the HPA is present. The head values for these boundaries are determined by a spatial and temporal interpolation of the water-level observations from nearby wells, with some adjustment from model-simulated water-level changes during preliminary model runs. Remaining boundary edges are set

to no-flow cells, which prevents flow between active and inactive areas of the model. Specified heads are also set along pockets of inactive areas found within and just north of GMD4 to prevent widespread occurrence of drying cells in the typically thinly saturated and/or less permeable portions of the aquifer.

The lower vertical boundary of the model is Cretaceous-aged bedrock (mainly shale), which has much lower permeability than the aquifer and is treated as a no-flow boundary. The upper boundary of the model is the land surface, where water may enter or leave the aquifer through areal recharge, evapotranspiration, and stream-aquifer interactions. Land surface elevations in Kansas are based on classified bare-earth LiDAR digital elevation models provided by the KGS Data Access and Support Center (DASC); those for Colorado and Nebraska are based on the USGS National Elevation Dataset.

The modeling work was divided into two major steps. First, a steady-state simulation was generated for the predevelopment period before 1945. Data used for the predevelopment simulation were typically from 1940 to 1950, before large-scale, intensive pumping activities began. Second, a transient simulation was conducted for the period between 1945 and 2020 to replicate the historic evolution of the groundwater system under intensifying pumping. The predevelopment step established the initial conditions for the subsequent transient simulation.

The model takes advantage of detailed information from the KGS HyDRA program (Bohling, 2016), for which the lithologic descriptions from thousands of drillers' logs have been digitally transcribed and categorized into common groups. The lithologic groupings were then spatially interpolated to develop three-dimensional grids of lithologic categories. Next, based on representative hydraulic conductivity (K) and specific yield (Sy) values assigned to each lithologic category, K and Sy for each model cell are computed based on where the water levels intersect the lithologic grid at a specific time. For each lithologic category, K is a calibrated parameter whose value is determined by model calibration, whereas Sy is determined from a water-balance analysis of annual water levels and pumping (Butler et al., 2016, 2018; Liu et al., 2021). Determining Sy using the water-balance analysis approach allows aquifer recharge rates to be estimated much more accurately during model calibration. The HyDRA process used 16,159 logs from Kansas, 488 from Nebraska, and 76 from Colorado.



- High Plains Aquifer**
- Saturated extent
 - Thin/little saturated thickness
 - Outcrop of older formations
 - Non-aquifer area

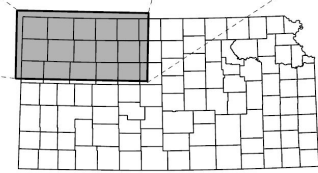


Figure 1. Map of GMD4 model area in Kansas, Nebraska, and Colorado. The red line indicates the district boundaries of GMD4. Yellow lines are major highways.

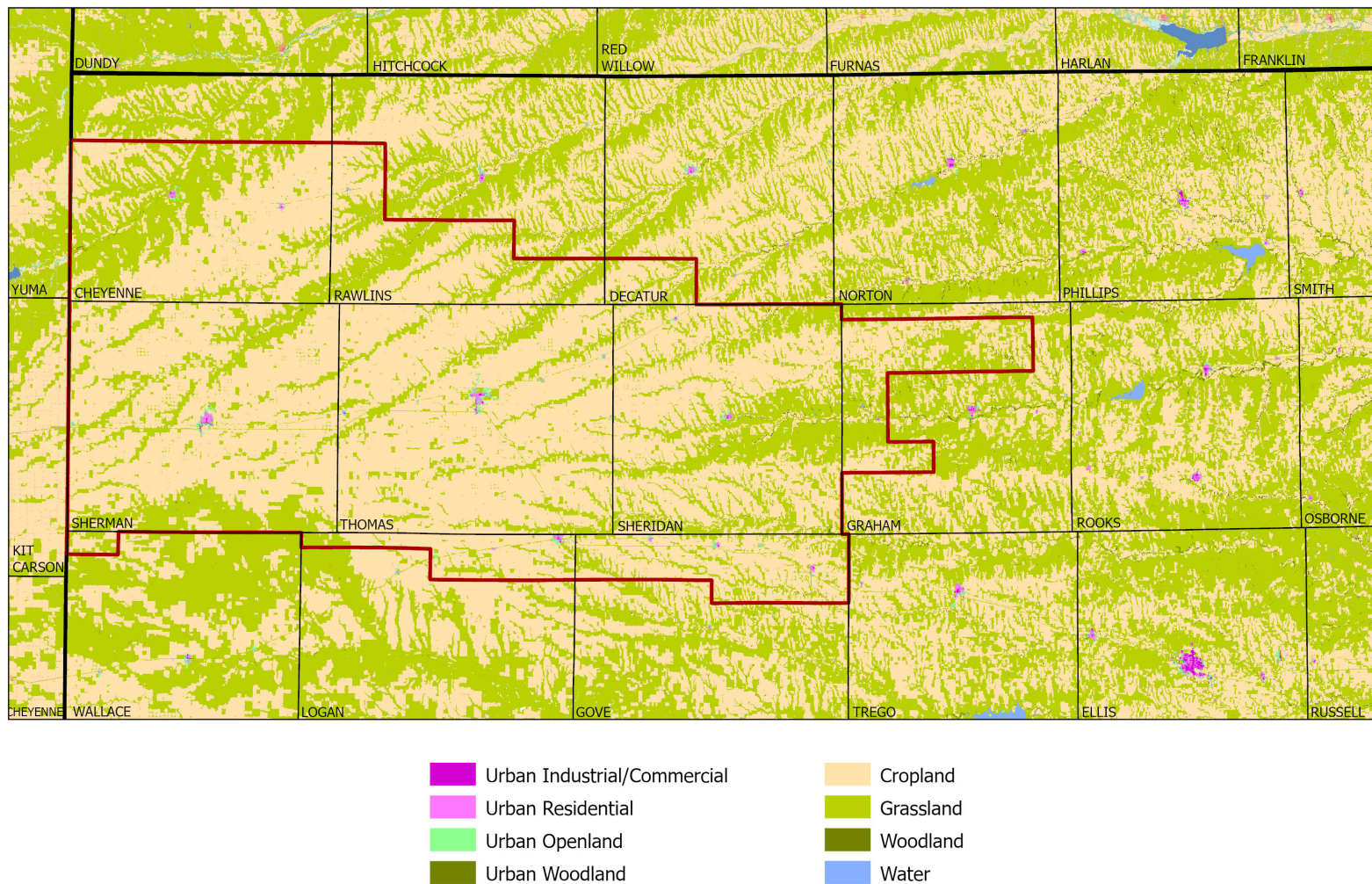


Figure 2. Land use/land cover classifications of the model area, 2015.

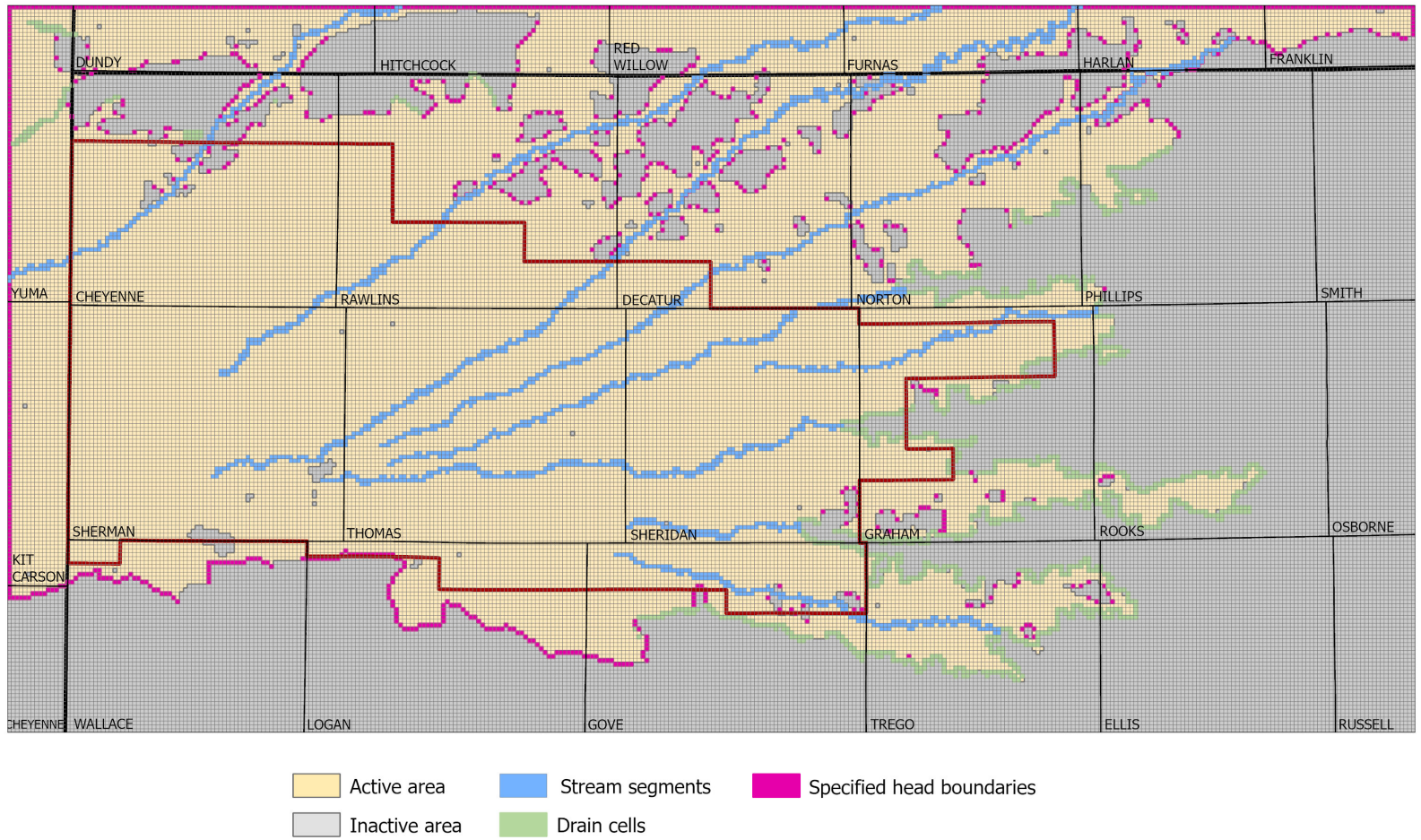


Figure 3. Model boundaries, grid cells, active area, and special model cells.

The model was calibrated to match predevelopment water levels and long-term hydrographs of selected wells, especially the water-level change over time. Low-flow conditions in the selected stream courses (average flows between January and March, during which surface runoff contributions are typically a small component of the total streamflow) were also used to assist in the calibration process. The recharge-precipitation relationship, the delay characteristics between water infiltrating below the land surface and reaching the water table, the lagged release of water from storage in dewatered sediments, and hydraulic conductivity of lithologic categories are all treated as calibration parameters due to their relatively large uncertainties and high impacts on model results.

Active and Inactive Areas

Most groundwater models include “active” and “inactive” areas. The actual groundwater flow calculations are only conducted within the active cells. In this study, the extent of the HPA in northwest Kansas, including the majority of GMD4, represents the active area. “Inactive” cells are those where the HPA is not present, that are disconnected from the GMD4 area (such as some of the southern extents of Wallace and Logan counties), or that have a substantial area of bedrock outcroppings, such as occurs in northern Cheyenne County. Additional inactive areas were assigned to cells with very thin aquifer thickness that would routinely go “dry” and cause model convergence errors during preliminary model simulations. The number of active cells in the final model is 38,463, giving a total active model area of 9,616 square miles, a little more than 57% of the model domain (fig. 3).

REVIEW AND SETUP OF DATA PARAMETERS

Precipitation Data

Monthly precipitation data were downloaded from the PRISM Climate Group at Oregon State University (<http://prism.oregonstate.edu>) in early spring of 2019 and again in the fall of 2020. PRISM provides raster-based grids (roughly 4 x 4 km) for the entire continental United States, and the data compare very favorably with similar precipitation-based data processing undertaken in past KGS activities (Wilson and Bohling, 2003; Wilson et al., 2008).

The monthly PRISM grids for each year from 1945 to 2020 were processed to compute the annual average, minimum, and maximum precipitation for each year along with averages for the “summer” period (April to September) and the “winter” period (October to March). The “summer” and “winter” periods represent the irrigation and non-irrigation seasons, respectively. The output for each of these processing steps was a new raster-based grid, which was then overlain on the model area and the values assigned to each of the model cell centers.

The average summer and winter precipitation over the model area from 1945 to 2020 is 16.08 and 5.01 inches, respectively (fig. 4). The highest summer precipitation year was 1951 followed closely by 1993, with 26.09 and 23.65 inches, respectively, and the lowest period of precipitation was in the winter of 1968 with only 1.59 inches of precipitation.

Figure 5 shows spatial patterns in the normal precipitation (average precipitation over the period of the last three full decades, 1981 to 2010) across GMD4 are similar to those at the statewide level. Typically, the area has a pronounced west-to-east gradient with precipitation levels lower along the western and southwestern edges of the model area and increasing eastward to their maximum levels, reflective of the pattern across the state.

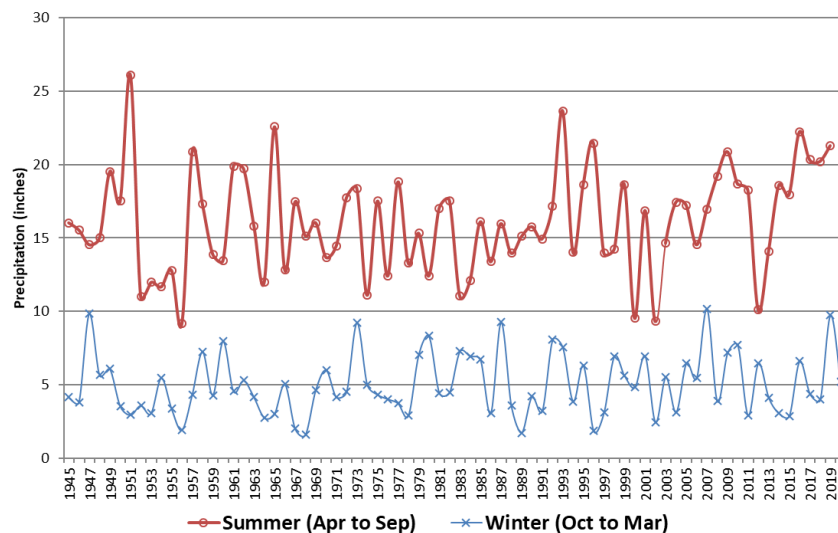


Figure 4. Average “summer” and “winter” precipitation.

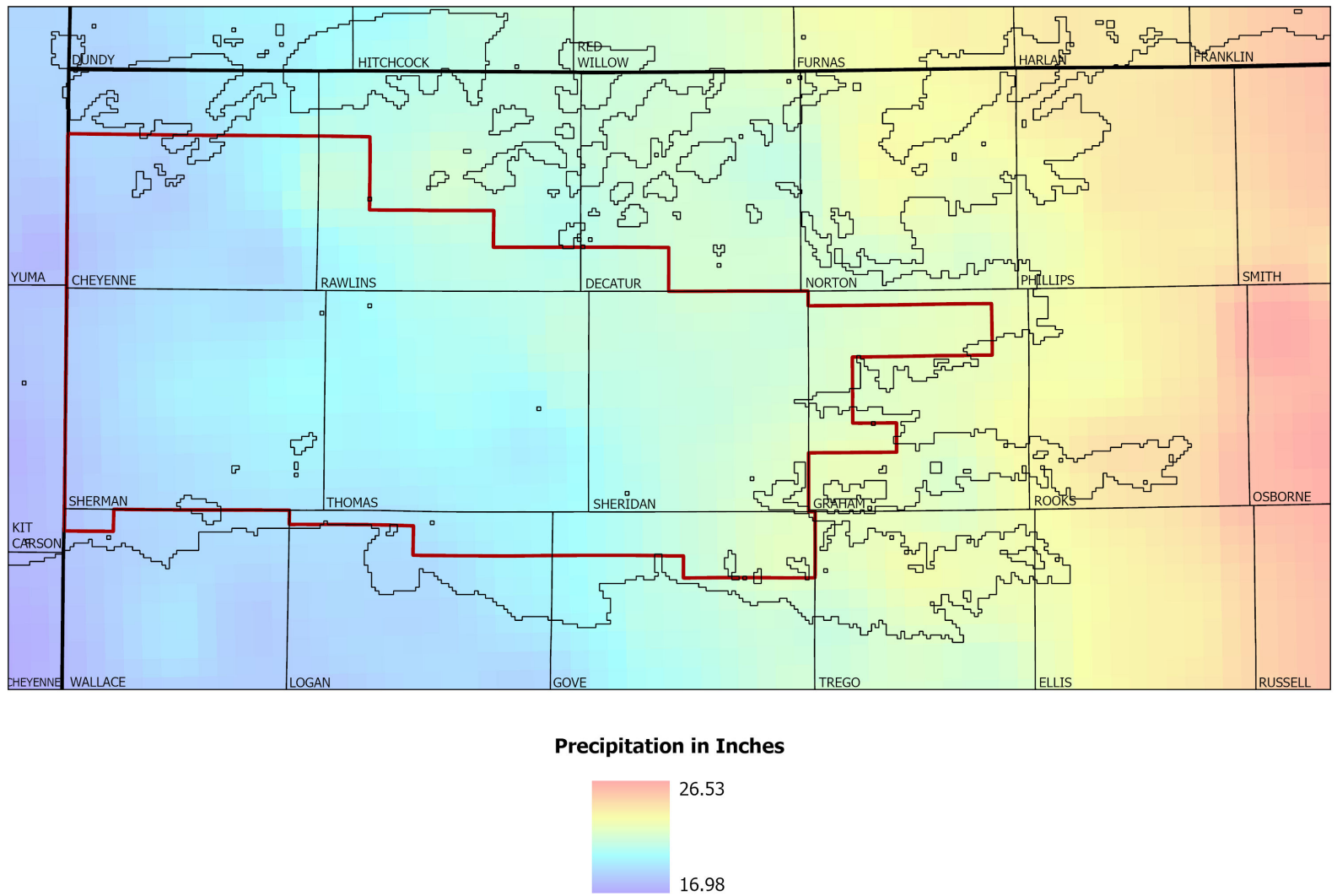


Figure 5. PRISM normal annual precipitation (average for 1981 to 2010). The irregular black line represents the active area of the model.

Geology and Lithology

Geologic formations at or near the surface across the model area are sedimentary in nature and typically range in age from Late Cretaceous to recent. The oldest of these exposed at the surface is the Carlile Shale overlain by Niobrara Chalk, generally found in eastern and southern portions of the model area. Moving westward across GMD4, the area becomes overlain by unconsolidated sediments primarily from the Ogallala Formation of the HPA, belonging to the Neogene System, and undifferentiated Pleistocene deposits, mainly loess and recent alluvial deposits (fig. 6). The Ogallala and undifferentiated Pleistocene deposits, which consist of clay, silt, sand, and gravel, accumulated as an apron of clastic (particulate) sediments that were eroded from the uplifting Rocky Mountains and carried eastward by streams (Ludvigson et al., 2009). Eolian (wind deposited) sand dunes are not common but vegetated sand hills can be found along the South Fork Republican River in Cheyenne County, Kansas. The eastern and, for the most part, southern boundaries of the active model area coincide with Ogallala/late Cretaceous outcrops. The core areas of the model are concentrated over GMD4 and the thicker portions of the unconsolidated sediments (fig. 7).

Aquifer Characteristics

The HPA is the principal aquifer in the area and provides water for almost all uses within the active model area. Although groundwater is also found in the alluvial deposits of streams, these deposits are generally limited to relatively small yields within GMD4. Alluvial deposits are more prevalent in many stream courses in the northern reaches of the model, down-gradient of the district. The intent of this project is to simulate groundwater conditions in the unconsolidated material and no distinction is made between the HPA and alluvial deposits.

Cretaceous-aged formations underlie the HPA but are not considered in this study. The Pierre Shale in most cases represents the bedrock (e.g., the bottom) of the HPA, given its relatively low permeability. The next formation in sequence is the Niobrara Chalk, which is water bearing but is not considered a principal source because the water typically is found in fractured limestone or in dissolved solution openings and thus can be highly variable in terms of availability. The Graneros Shale, Greenhorn Limestone, and Carlile Shale are found below the Niobrara but are generally of very low permeability and yield little water. The Dakota aquifer system is water bearing and underlies the entire model area. However, given its depth and higher salinity, there are no known water-right wells developed in the Dakota in the study area (Whittemore et al., 2014).

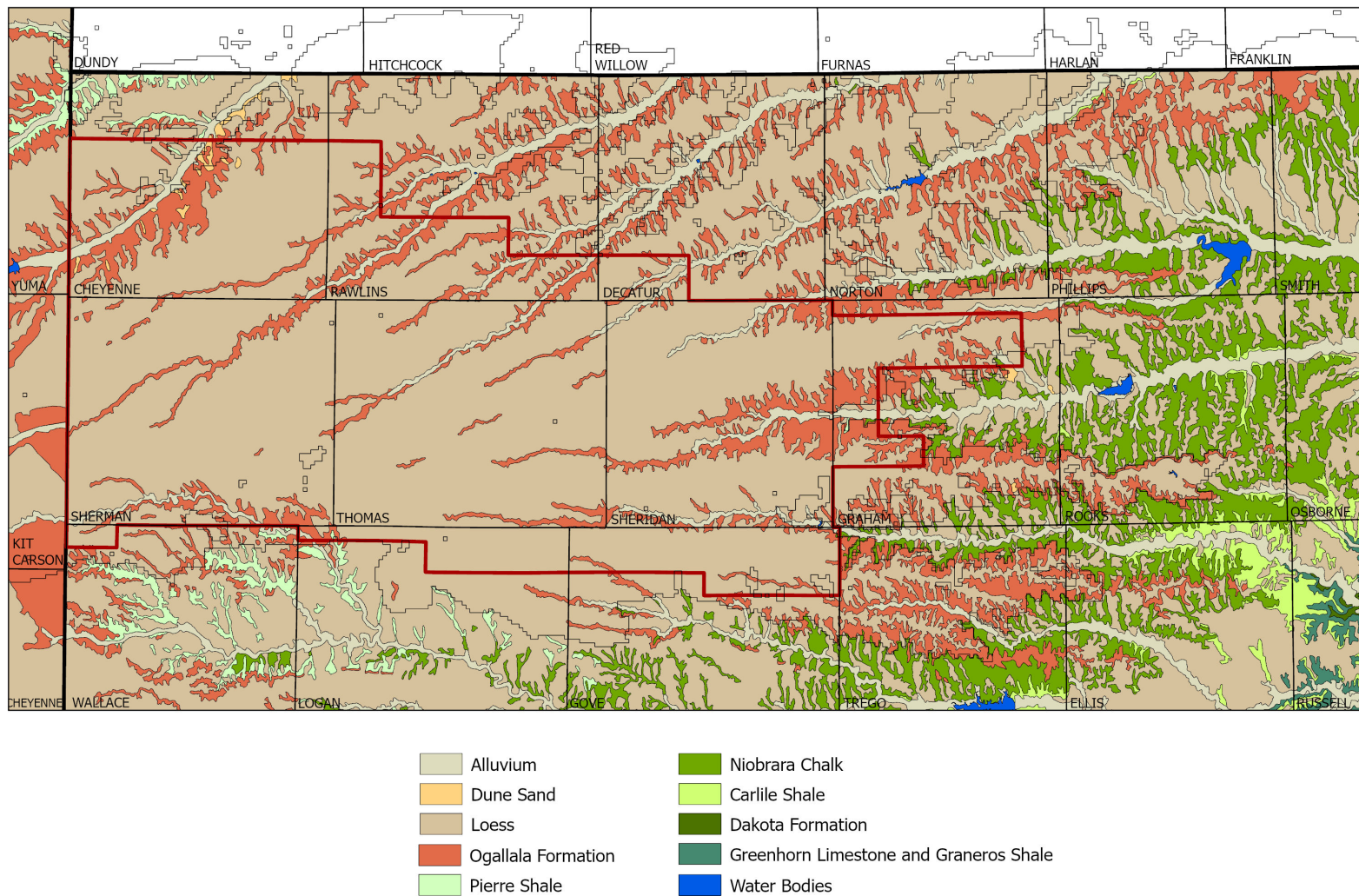


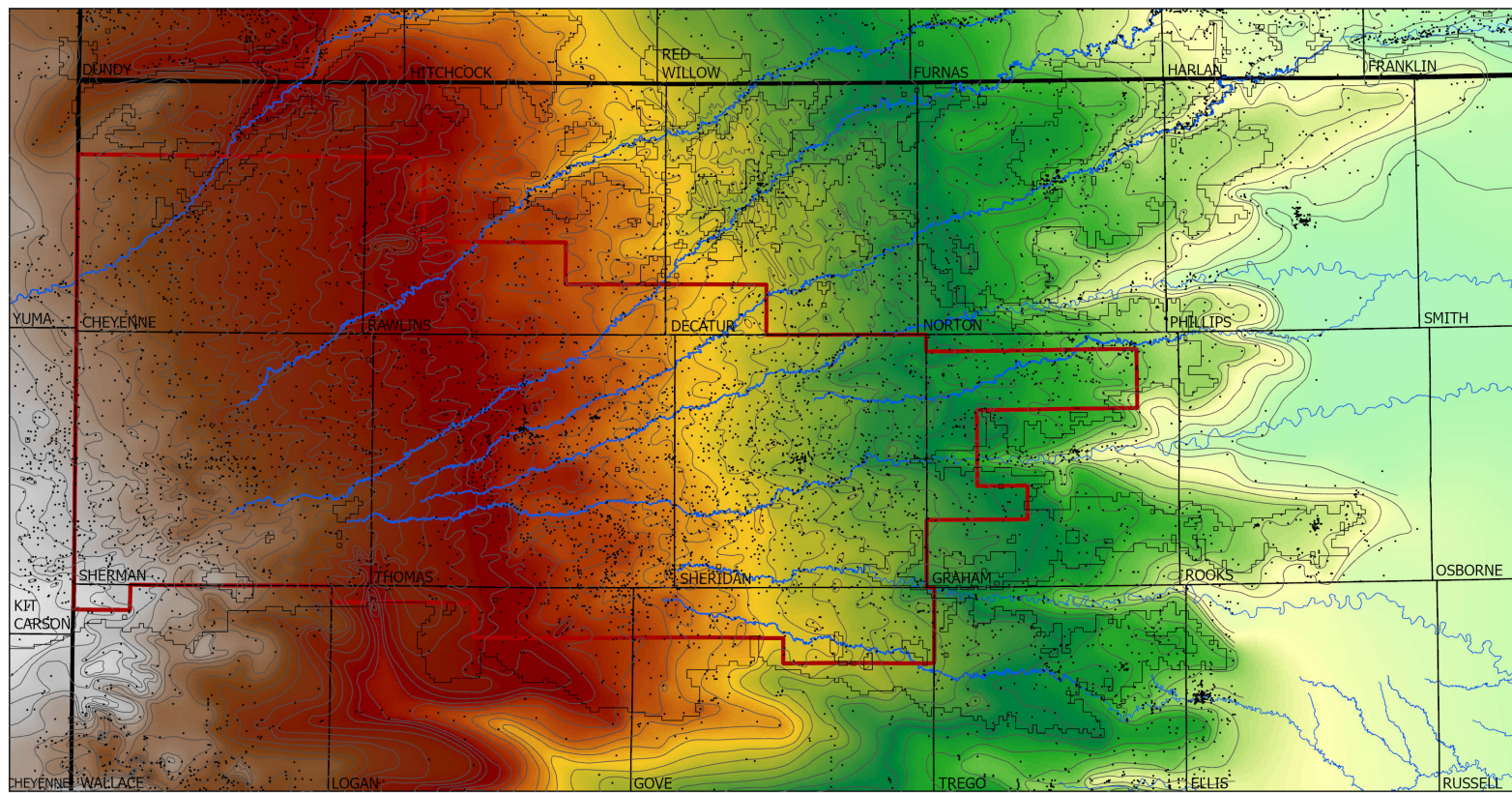
Figure 6. Surficial geology (Nebraska data not available).

Bedrock Surface

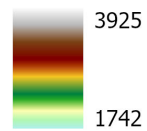
Data for the bedrock surface were obtained by updating a previous bedrock study by Macfarlane and Wilson (2006). In that study, lithologic logs were obtained from water-well completion records, county geologic bulletins, and geophysical logs stored at the KGS, along with additional data from the USGS and the Henkle Drilling and Supply Company in Garden City, Kansas. For this study, the bedrock elevation isolines were extended slightly into Colorado and Nebraska and then interpolated to form a continuous raster-based surface (fig. 8). The model cells were overlain on the interpolated surface and the average bedrock elevation within each model cell computed. Within GMD4, the bedrock elevation was manually adjusted to be at least 10 ft below the land surface for 21 cells. These cells were mostly found along stream channels near the edges of the district where the model's 0.5 x 0.5 mile grid size was too coarse to adequately capture the local elevation changes interpolated from sparse bedrock points.

The bedrock surface elevation follows the same general slope as the land surface, with higher values located along the western edge of the model and lower values to the east. Bedrock highs in GMD4 are concentrated in corners of southwest Sherman and northwest Wallace counties, with the lowest bedrock elevations found in northern Graham County. Within the district, the depth from land surface to bedrock ranges from near the land surface to 370 ft along portions of the Sherman-Cheyenne county line and southeast Cheyenne County, Colorado. The average depth to bedrock across GMD4 is approximately 200 ft below the land surface.

A three-dimensional version of the bedrock surface (fig. 9) facilitates visualization of the bedrock topography. Localized areas of bedrock highs can be seen in southeast Sherman County, which results in little to no saturated thickness in the HPA. Eroded stream channels dominate the eastern expanses of GMD4.



Elevation in Feet



Bedrock Data Source

- Macfarlane and Wilson, 2006
- ~ Bedrock isoline, adjusted

Figure 8. Elevation of the bedrock surface interpolated from well logs.

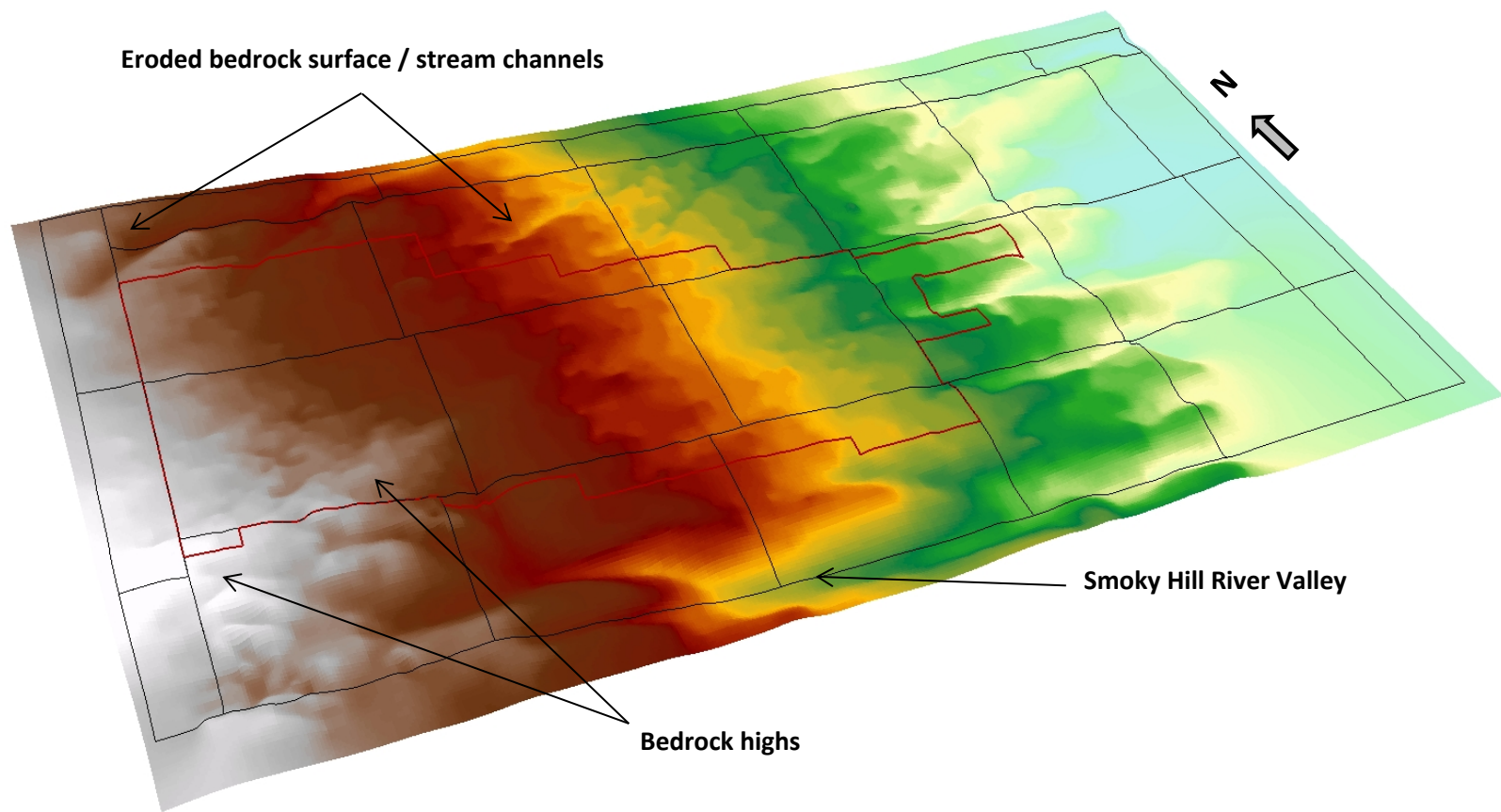


Figure 9. Three-dimensional view of the interpolated bedrock surface, looking northeast (see fig. 8 for color scale).

Lithologic Classifications

The KGS has established methods to extract and categorize information from drillers' logs with the current version of the process known as the Hydrostratigraphic Drilling Record Assessment (HyDRA) (Bohling, 2016; Bohling et. al, 2020). Lithologic descriptions and interval depths have been transcribed and stored in Oracle, an enterprise-level relational database management system, from which they are extracted and categorized into similar descriptive groupings. The lithologic groupings are spatially interpolated to produce a three-dimensional grid, with each grid cell containing the proportions of different groupings. Using representative values for each lithologic group, vertically averaged K and S_y are computed for the saturated interval between the predevelopment water table and bedrock surface or any water-level interval between two different times.

A little more than 10,700 well logs were used in the HyDRA process (fig. 10). In Kansas, water well completion forms (WWC5) are the source of the lithologic logs, while similar records were retrieved from Colorado's Department of Natural Resources' permitted wells database and the University of Nebraska's School of Natural Resources Conservation and Survey Division's test-hole database. Together, these data sources provide about 115,000 depth intervals from which the lithology is described. From these, roughly 86% matched existing lithology translations, which in turn are used to assign the intervals to 71 standardized lithology codes. Unmatched intervals, roughly 13,000 in this case, are not part of the standardized logs. The standardized lithologies are further categorized into five groups, each representing a set of lithologies expected to exhibit similar values of K and S_y (table 1).

With the lithologic groupings in place, HyDRA segments each driller's log into 10 ft intervals, starting from the interpolated predevelopment water table (described in the next section of this report) to bedrock. The proportion of each of the five lithology categories occurring within each 10 ft interval is estimated based on the driller's log. The five category proportions in the 10 ft intervals are then interpolated into a three-dimensional grid across the model's active area, so that each 3-D grid cell contains a set of values representing the category proportions within that cell. Figure 11 shows a summary representation of this information, the proportion-weighted average category. A special program was written to intersect MODFLOW-formatted water table and bedrock elevation grids with the three-dimensional proportional grids and then write out the vertically averaged K and S_y values to MODFLOW-formatted grid files, based on the category proportions within the intersected grid cells and the K and S_y values assigned to each category. Specifically, K is calculated as the average value for the entire lithologic interval between the water table and bedrock, while S_y is computed only for the water-level change interval between the start and end of a time step.

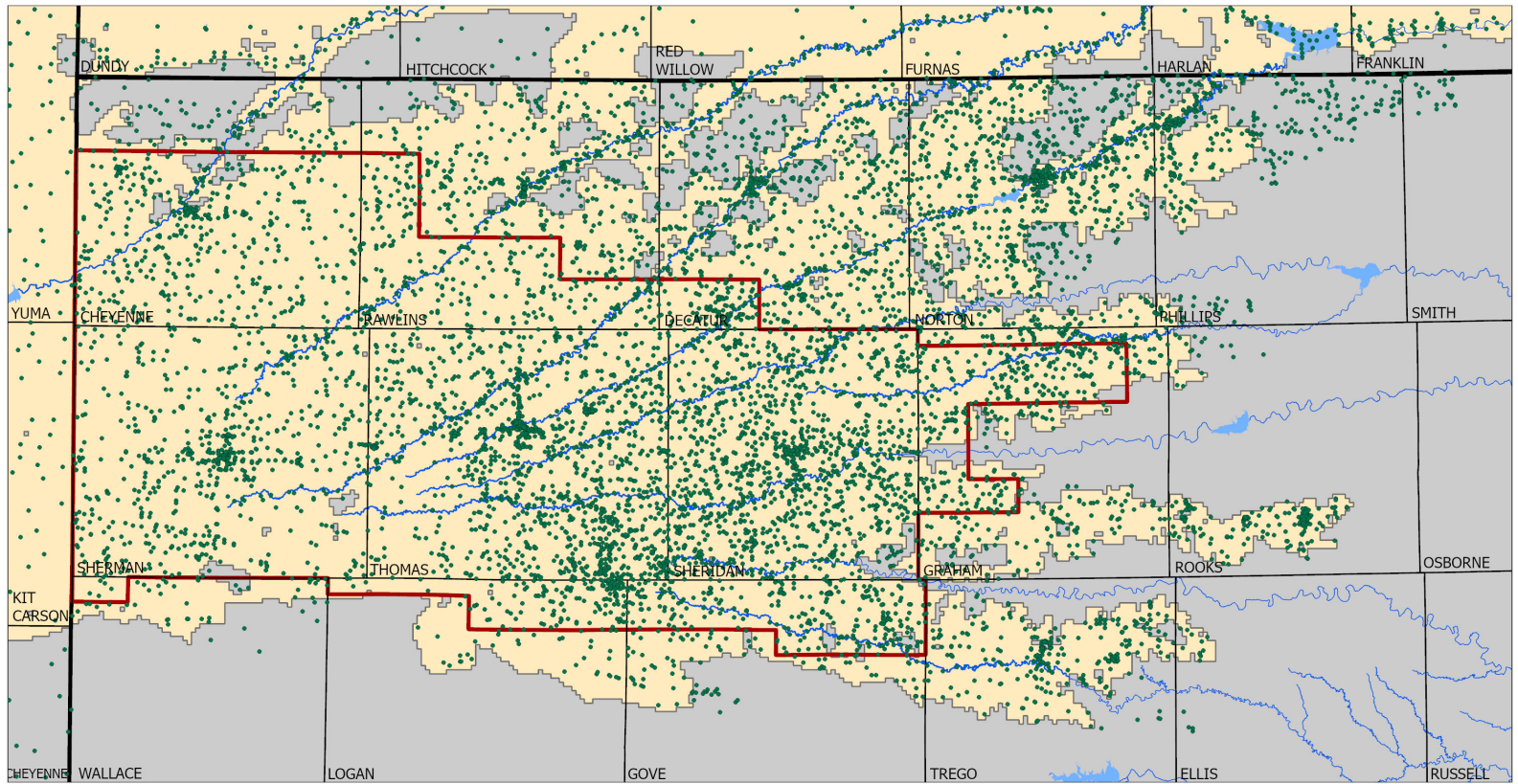


Figure 10. Distribution of lithologic logs used in HyDRA.

Table 1. Standardized lithologies and hydraulic conductivity (K) in feet-per-day and specific yield (Sy) categories with estimated values				
Category 1 "Clay" K=6E ⁻⁶ ft/d Sy= 0.01	Category 2 "Clay and Silt" K=2E ⁻² ft/d Sy=0.01	Category 3 "Silt and Sand" K=193 ft/d Sy= 0.094	Category 4 "Sand" K=336 ft/d Sy=0.1195	Category 5 "Sand and Gravel" K=638 ft/d Sy=0.1199
Shale Clay Bedrock Red bed siltstone	Silty and sandy clays Silts Top soil Marl Caliche	Sandy silts Sandstone Fine sands	Medium to coarse sands Clayey and silty gravels	Sand and gravel Fine to coarse gravels

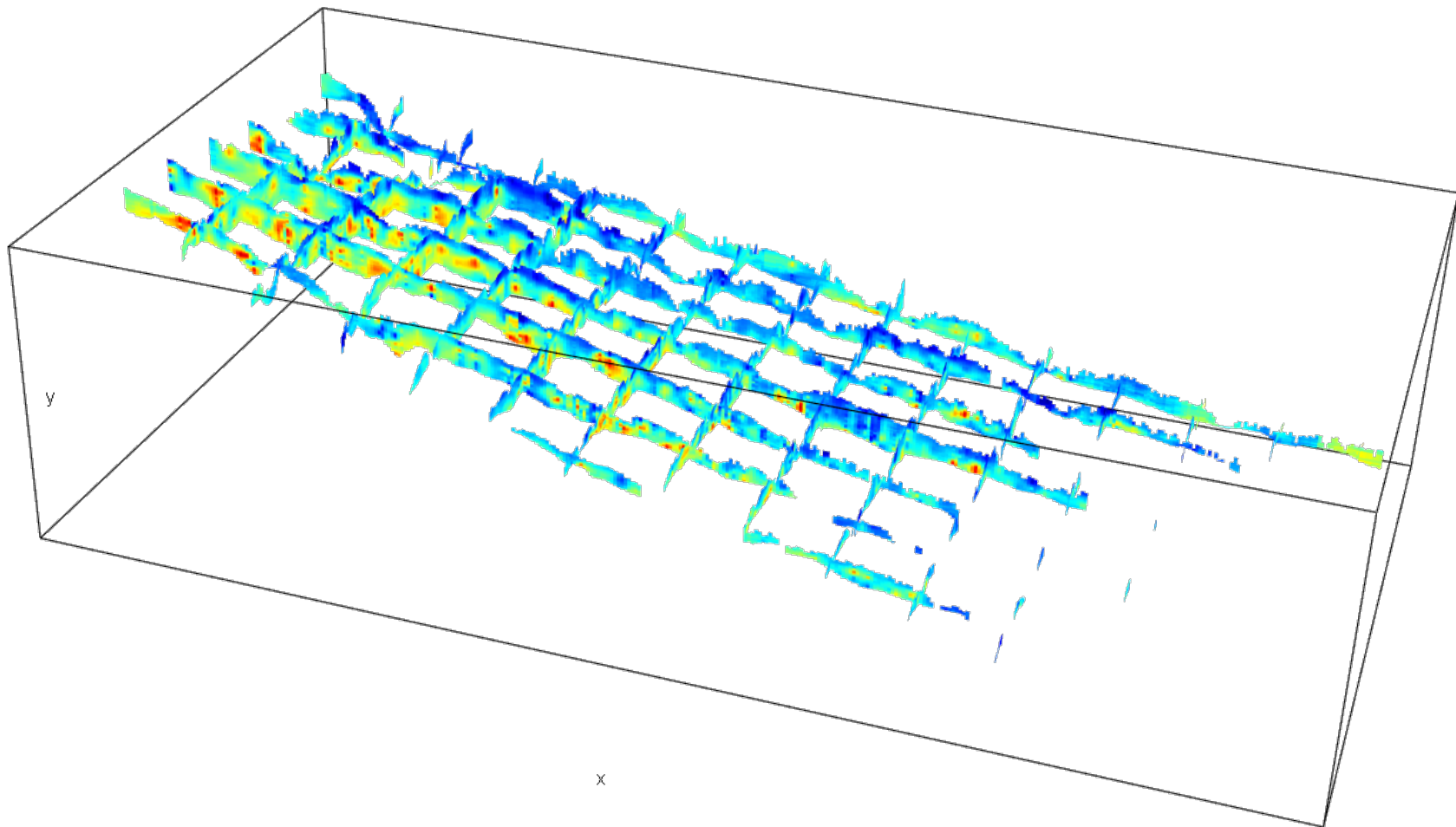


Figure 11. Proportion-weighted average lithology categories in cross sections of the 3-D grid. The dark blue colors indicate lower permeability classes whereas yellow to red represent higher permeability classes.

Water Levels

Estimates of the predevelopment water table for the HPA were compiled primarily from the “Well Records” listing of county-based geologic bulletins. Most of the depth-to-water measurements in these reports for the core GMD4 counties (e.g., Cheyenne, Rawlins, Sherman, Thomas, Sheridan, and Graham) were made from 1942 to 1952. Water-level dates for the other counties range from 1953 to 1964. Predevelopment points from a USGS map product (Becker, 1999) were used to represent conditions in Colorado and Nebraska.

The predevelopment water-table elevations were interpolated to form a continuous 2,000 x 2,000 ft gridded surface (fig. 12). The model cells were overlain on the gridded surface and the average predevelopment water-table elevation within each model cell computed. In a few areas, primarily outside GMD4 along the fringes of the active area and stream channels, the predevelopment water table was manually adjusted to be at least 5 feet below the land surface and/or 5 feet above the bedrock.

Like the bedrock surface, the predevelopment water-table elevation follows the same general slope as the land surface, trending from highs along the western edge of the model to lows in the east. The predevelopment depth-to-water varies across the model’s active area (fig. 13). The depth to water is shallowest along the stream channels, typically within 50 feet of the land surface, with the deepest values found in Cheyenne County. The predevelopment depth to water in GMD4 within the active area of the model averages 110 feet and ranges from near the land surface to 267 feet.

GMD4 has a number of wells with measurement histories going back to the 1980s (fig. 14). Depth-to-water measurements for the Kansas portion of the model were obtained from the Water Information Storage and Retrieval Database (WIZARD). The majority of these records from 1996 to present were obtained as part of the annual Kansas Cooperative Water Level Program, operated by the KGS and Kansas Department of Agriculture, Division of Water Resources (KDA-DWR). Colorado- and Nebraska-based measurements were downloaded from the USGS National Water Information System and the USGS National Groundwater Monitoring Network (NGWMN).

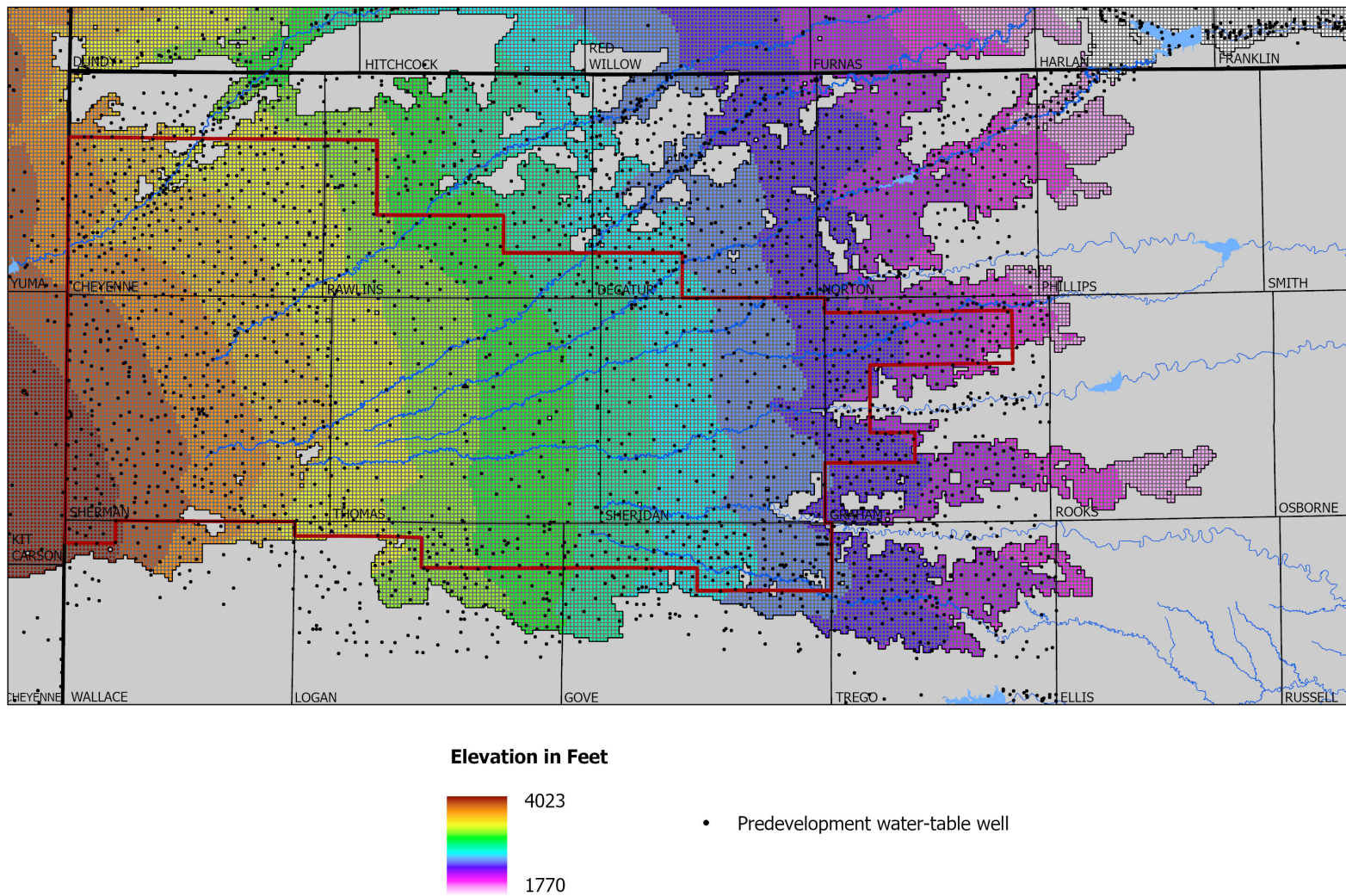


Figure 12. Interpolated predevelopment water table.

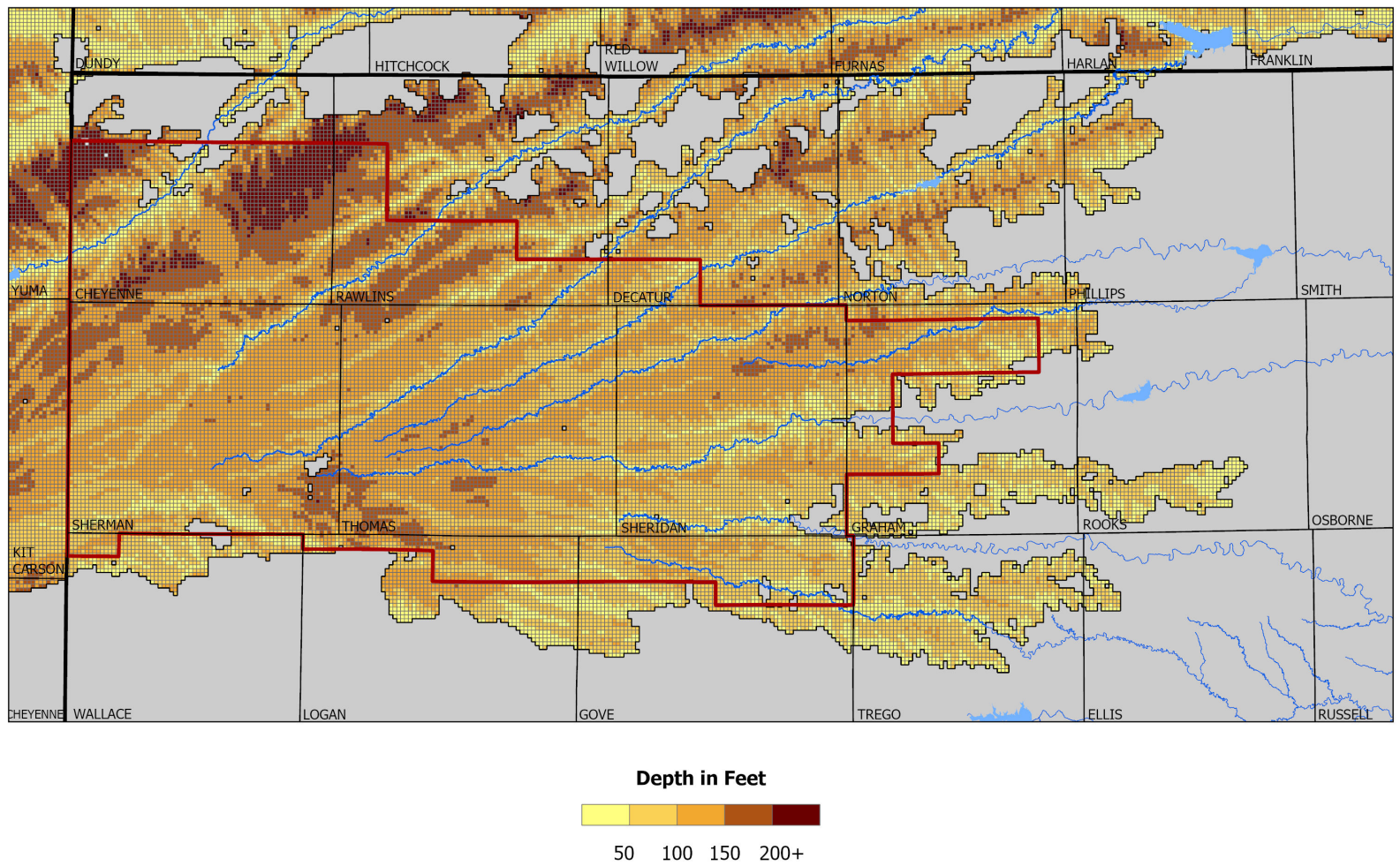


Figure 13. Interpolated predevelopment depth to water.

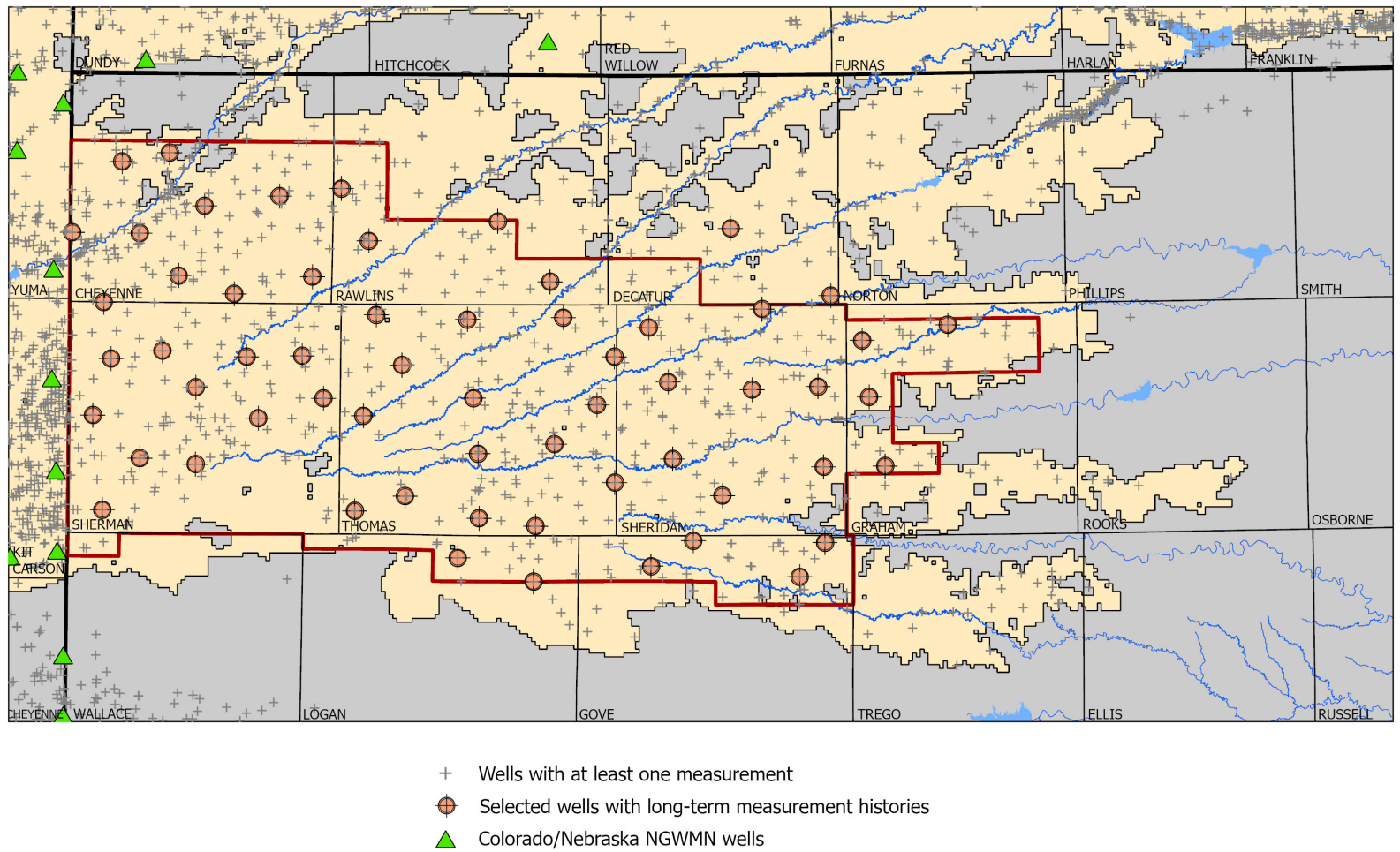


Figure 14. Distribution of water-level measurement wells during the transient period.

Water-level measurements with status codes that indicate the value might not reflect normal conditions (e.g., the well was being pumped) were removed from consideration. “Winter” measurements, those taken between December 1 and April 15, were averaged at each well to obtain a single yearly value for that well. Within GMD4, 84% of these measurements occurred in the month of January. Since the 1970s, the number of measured wells has remained fairly static, averaging 277 wells each year, while the number of measurements has a slightly decreasing trend over time (fig. 15).

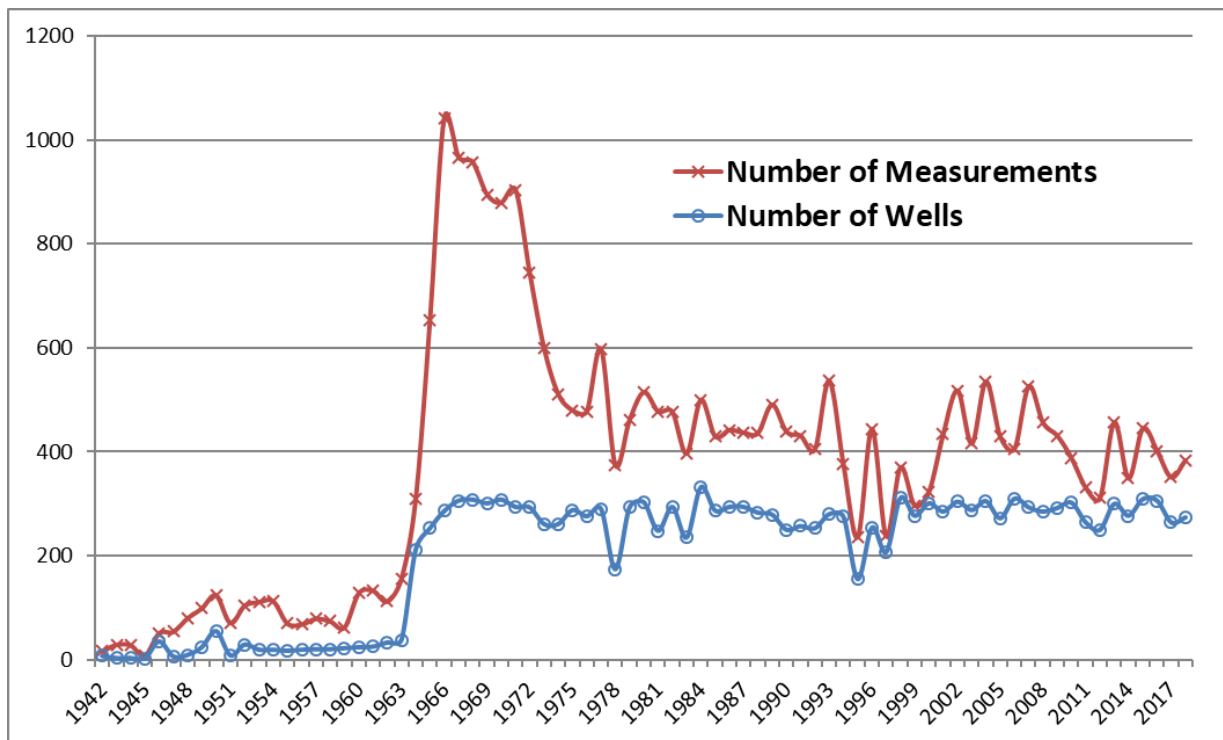


Figure 15. Number of wells in the model domain with “winter” (December 1 to April 15) measurements.

The average predevelopment saturated thickness of the HPA within the GMD4 boundary and active area of the model is 95 ft and ranges from close to 0 to just more than 235 feet, with the maximum thickness occurring in Sherman County. In comparison, saturated thickness averaged 69 ft from 2018 to 2020 with the greatest declines in southwest Sherman, western Sheridan, and southern Thomas counties (fig. 16). Many of the fringe areas outside of GMD4, where the aquifer has little thickness and little groundwater development, have seen relatively smaller changes. The thickest portions of the present-day HPA can still be found in northern Sherman County, whereas bedrock highs in the southeast and southwest portions of Sherman and Thomas counties, respectively, have greatly reduced the availability of groundwater.

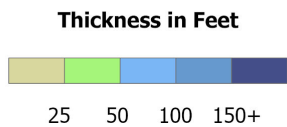
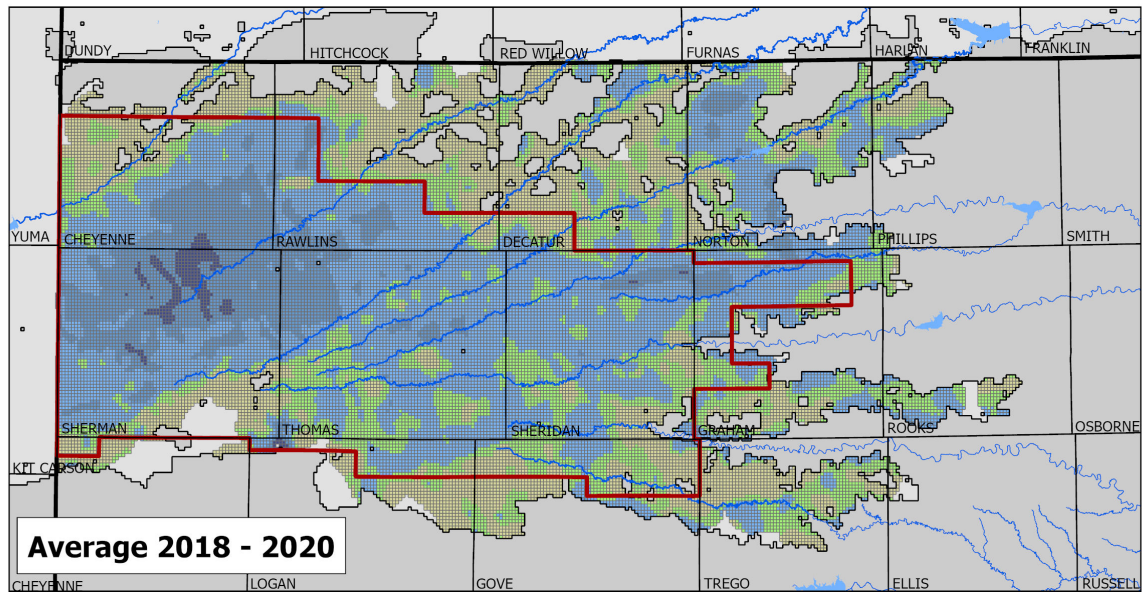
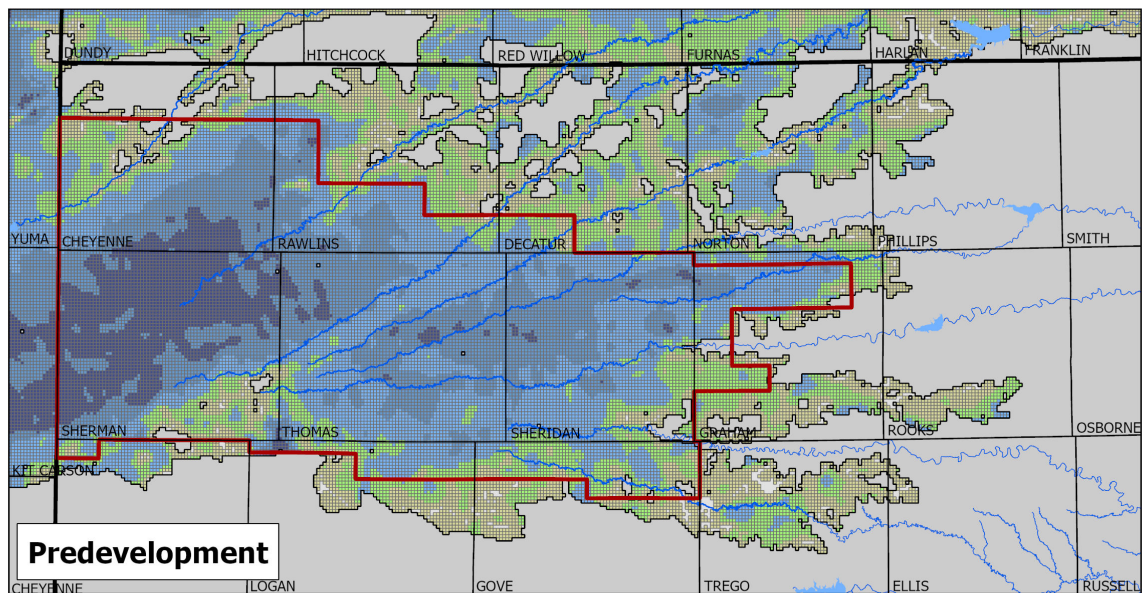


Figure 16. Interpolated predevelopment and average 2018–2020 saturated thickness.

Boundary Conditions

The model uses time-varying specified head boundaries along all but its eastern edge to represent conditions in the HPA to allow water to move in and out of the active area. Given that head boundaries in the model are not necessarily located along natural or known hydrologic boundaries, setting appropriate head values is challenging, especially in areas that lack data. Starting with the interpolated predevelopment water levels, each time-varying head cell was reviewed in relation to well measurements taken over the transient period, 1945 to 2020.

There are thousands of well measurements during the transient phase in Colorado and Nebraska, located along the western and northern edge of the model's domain (fig. 13), although the number of wells containing long, winter-based measurement histories is roughly an order of magnitude less. Colorado, Nebraska, and Kansas are participants in the USGS NGWMN, a network of selected monitoring wells across the country intended to facilitate the planning and management of groundwater resources. These wells meet a set of minimum data requirements and have been selected by each state to represent conditions and trends in various aquifer systems. In Kansas, all of the HPA wells in the annual cooperative water-level network are included in the NGWMN.

In cases where currently measured wells with long-term measurement histories are located in or near the head-boundary cells, the water-level trends shown in the measurement histories were applied to the overlapping or closest head-boundary cells. Data gaps in the measurement histories were filled by applying linear projections to existing predevelopment values or applying regional water-level changes from any available nearby wells to provide water-table elevation estimates over the entire transient period. The annual water-level changes from these cells were then applied to adjacent and nearby boundary cells with incomplete records, starting in predevelopment. The end result is the specified heads for all the boundary cells are based on actual measurements or the regional changes seen in those wells with linear projections back to predevelopment conditions.

This process of filling in temporal holes with nearby data works well where data records are present. The process is subjective in areas with little to no data, such as along the Nebraska line and thinly saturated areas of the HPA along the southern edge of the active area in Kansas.

Constant heads were also specified in thinly saturated areas where cell drying was a challenge. In those areas, initial transient model runs generated a significant number of dry cells and caused large computational errors. To overcome the dry cell problem in those areas, constant head boundaries (heads set to predevelopment heads and held constant through time) were specified to the edges of dry cell pockets. The idea is that flow from those "pockets" would maintain the water level at their edges. The majority of those dry cells are located in the thinly saturated portions of the HPA outside the district boundary to the north (fig. 3).

Remaining boundary edges are set to drains (further discussed below) or no-flow cells (prevent flow between active and inactive areas of the model).

Stream Characteristics and Flow

GMD4 is unique compared to the other Kansas GMDs in its dendritic to trellis drainage patterns formed by a number of streams that are ephemeral to intermittent in nature (fig. 17). Perennial flow typically starts near or outside the district's northern and eastern boundaries where most USGS gaging stations are located. Streams simulated in the model are the SF Republican, Beaver Creek, SF Sappa, Sappa Creek, Prairie Dog Creek, NF Solomon, SF Solomon, Bow Creek, Saline River, and Big Creek.

Mean monthly streamflow records were obtained from the USGS National Water Information System for the gaging stations in the active area of the model. Available data from the gaging stations are used as a measure of the aquifer's baseflow contribution occurring during winter periods. Gaged flow in summer months was not used for model calibration as streamflow during that period is much more significantly affected by surface runoff from precipitation events. The headwaters for all modeled streams occur within the active area except for the SF Republican River, which originates as discharge from Bonny Reservoir, located along the western edge of the model. As such, daily reservoir releases from the U.S. Bureau of Reclamation were used in place of gaged data. Bonny Reservoir was drained in 2011, but flow data are still being provided.

The stream package for MODFLOW requires all surface water courses to be broken down into individual segments and reaches. A "segment" is a longer portion of the stream that has similar properties, such as width, slope, and streambed hydraulic conductivity; a stream segment is further divided into "reaches" that represent each portion of a stream segment within individual model cells. To represent all the streams in fig. 17, the model uses 11 stream segments with 3,400 reaches. Figure 18 shows an example of the stream/reach divisions.

Streambed elevations were obtained by determining where land surface contours (10 ft intervals) from 7.5-minute USGS topographic maps crossed the stream channel. Roughly 40% of the stream cells had elevation contours crossing the channel. For stream cells without crossing topographic contours, elevations were interpolated between cells with assigned elevations based on the overall change in elevation and length of the particular stream segment.

Depending on how the streams meander over the model's 0.5 x 0.5 mile grid, the streambed elevations in relation to the bedrock elevations may not be properly represented in the model. This happens when a model cell is designated as a "stream" cell even though the cell is dominated by upland topography. In these cases, the estimated bedrock elevations for this cell are substantially above the streambed, causing computational errors in the model. A total of 115 model stream cells had bedrock elevations estimated to be above the streambed elevations, located primarily in the north extents of the model domain, outside of GMD4. The bedrock elevations for these cells were lowered to 0.1 ft below the streambed.

Most of the cells along the eastern edge of the model boundary are simulated as drain cells. As the name implies, drain boundaries allow water to discharge from the aquifer when the water levels are at or above the drain elevations. Unlike stream cells, where flow can be into or out of the aquifer, drains allow flow in only one direction, discharge out of the aquifer. If the water levels decline enough, the connection is broken and water will no longer discharge out of the system, rendering the drains effectively inactive. If water levels rise to the level of the stream bed again, the one-way drain connection is reestablished.

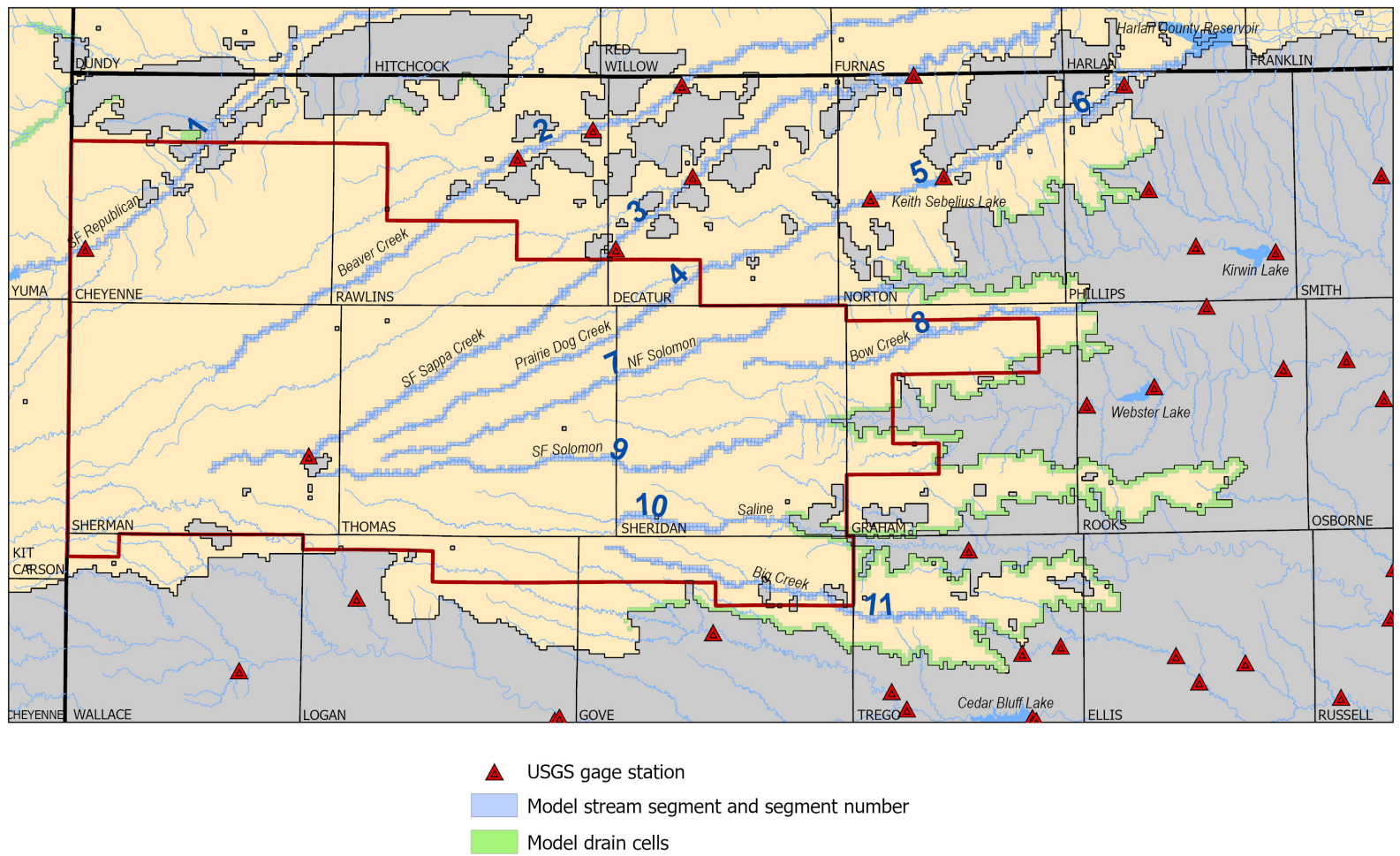


Figure 17. Model stream and drain cells and USGS stream gaging stations.

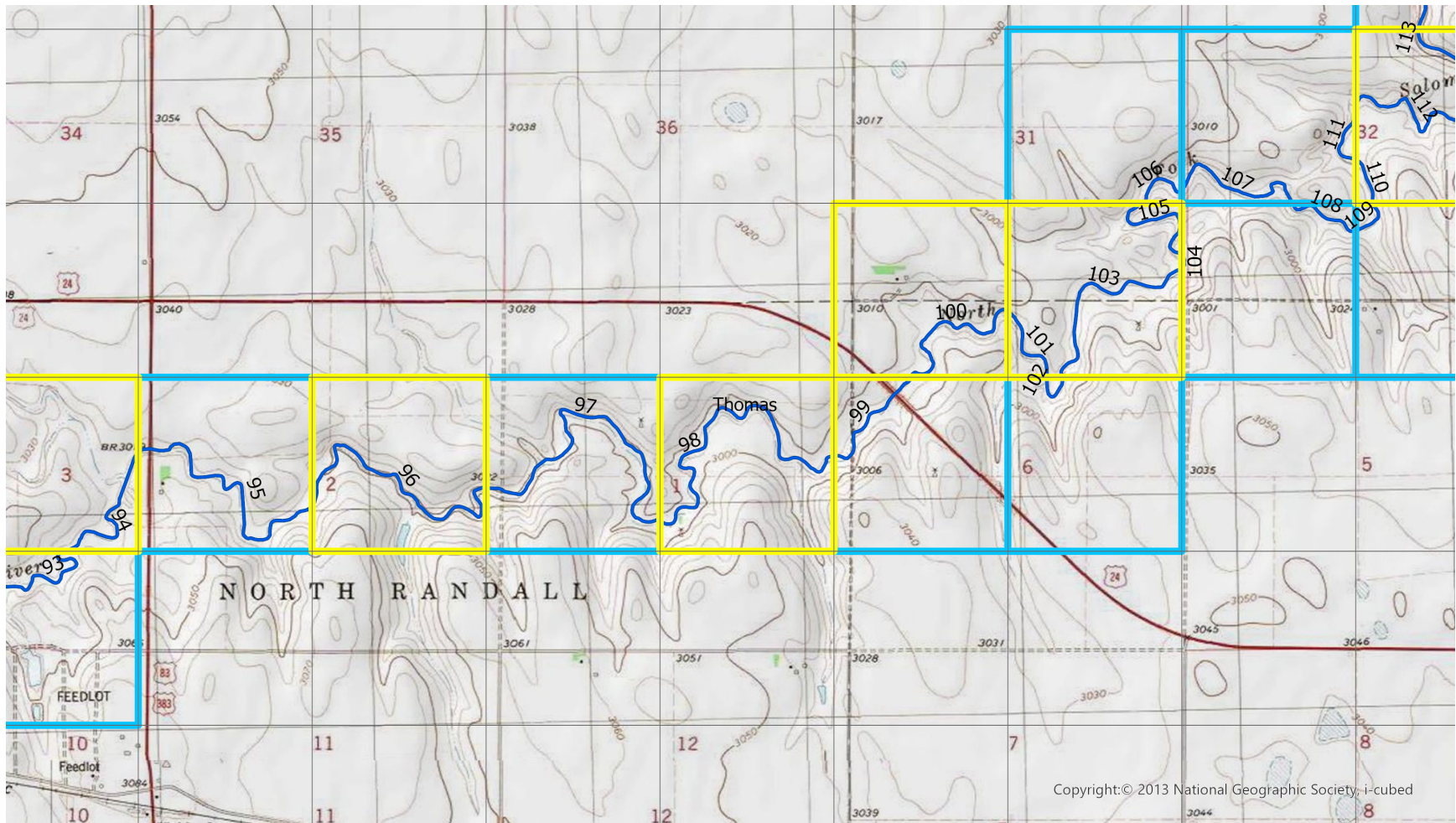


Figure 18. Selected area of the model showing a stream course segmented by reach designations.

Water Right Development

In the United States, regulation of groundwater has traditionally been left to the states. As with Kansas, the states to the immediate north, south, and west follow some version of the appropriation doctrine (first in time, first in right) involving water-right permits or certificates. Water rights in Kansas are highly regulated in terms of how much water can be used annually and where that water is applied. Kansas is also one of the few states that maintains a long-standing, self-reporting water-use program. A substantial amount of Kansas water-right data is online. Colorado-based permitted wells and Nebraska-based registered wells also have similar data available online. The KGS has a strong working knowledge of the Kansas water-right system, including the intricacies of the underlying data structure and the business rules used to represent the data. Permitted well data from Colorado and Nebraska are not as high quality as the Kansas water-use data.

Kansas

Water rights in Kansas are dynamic entities whose characteristics can change over time. The authorized quantities and water-right locations used in the model represent conditions in Kansas as of October 12, 2020. Data were accessed from the Water Information Management and Analysis System (WIMAS) (<http://hercules.kgs.ku.edu/geohydro/wimas/index.cfm>). Within GMD4, there are 3,331 unique appropriated and vested water rights and 3,735 active points of diversion. The majority of Kansas water rights in GMD4 are groundwater based (fig. 19), with irrigation making up 98 percent of that total (table 2). Although some surface-water-based appropriations exist, most have been limited by water availability and are insignificant relative to the total authorized quantities. None of the surface-based water rights have had significant levels of reported water use for decades and, as such, are not considered in this model.

Table 2.							
Total authorized quantity, in acre-feet, for appropriated and vested water rights, by use made of water and source of supply for GMD4							
Represents conditions as of October 12, 2020							
	Domestic	Industrial	Irrigation	Municipal	Recreation	Stockwater	Total
Surface	0	0	1,310	0	1,749	25	3,084
Ground	80	2,578	829,834	8,978	535	4,596	846,221
Total	80	2,578	831,144	8,978	2,284	4,621	849,305

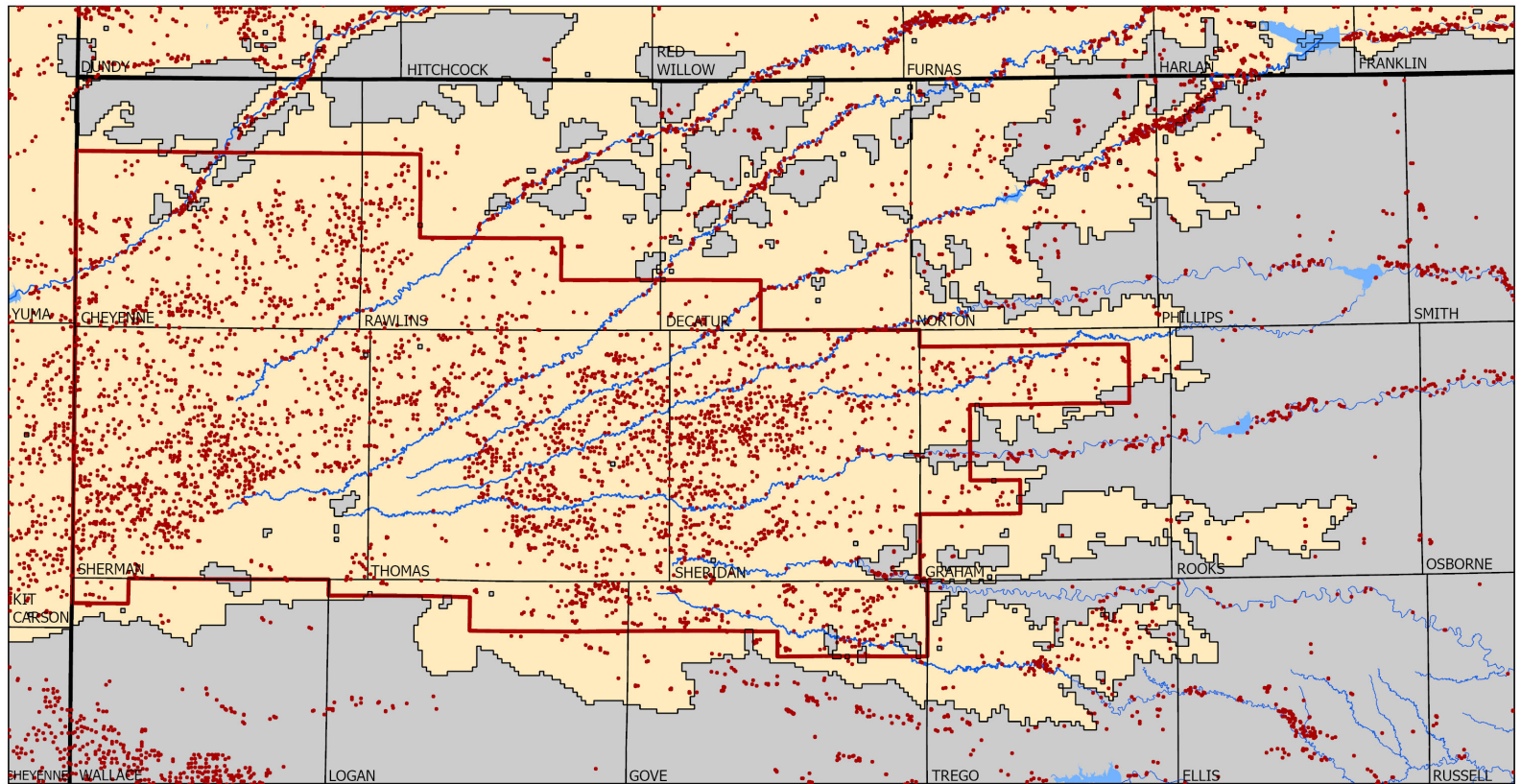


Figure 19. Groundwater-based water rights and permitted wells in Kansas, Colorado, and Nebraska.

The WIMAS database only stores a water right’s present authorized quantity. Although quantity values can change as a water right goes through the certification process or by other administration actions (generally becoming less), the historic trends used in the model are based on the appropriated quantity values at the time of the download (October 12, 2020) and in relation to the priority date of the water right.

A common complexity with Kansas water-right quantities is that the annual appropriation can be associated with the water right itself (regardless of how many uses or points of diversion it might have), with the water right’s uses of water, or with the water right’s multiple points of diversion. Because the points of diversion for a particular water right could be located across multiple model cells, the total annual authorized quantities for water rights that had their appropriations stored by the water right or use made of water were divided equally among the water right’s point(s) of diversion. Each point of diversion would then have an associated quantity that when added with the other points of diversion under the water right would equal the total quantity authorized. If the quantity was already stored by the point of diversion, it remained unchanged.

The trend in authorized quantity over time, based on priority dates, in the active portion of the model’s area (fig. 20) has similar characteristic to the rest of the HPA in western Kansas. Kansas water law started with the passage of the 1945 Water Appropriation Act. Water users in place before that time could apply for a “vested” water right. Water rights issued after 1945 are referred to as “appropriated” rights. The number of water rights started increasing sharply in the early 1960s and then gradually leveled out around the mid-1970s/early 1980s.

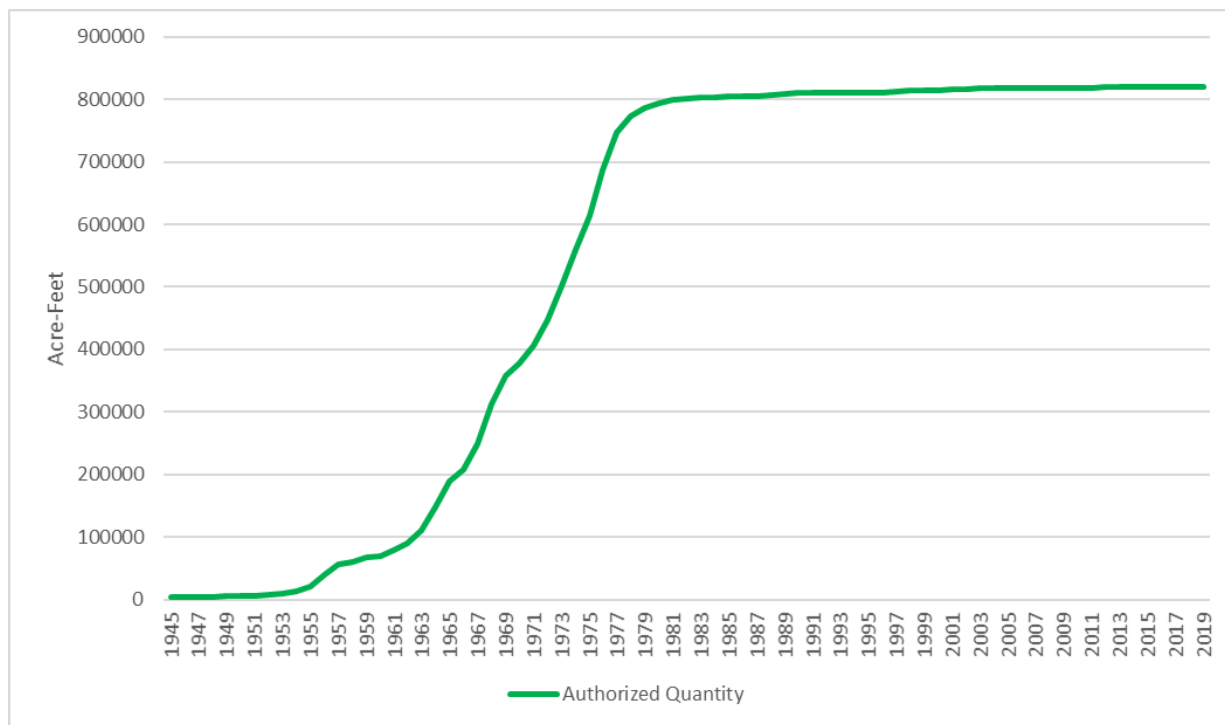


Figure 20. Total authorized quantity of Kansas groundwater-based water rights in the model’s active area within GMD4 that reported some amount of use from 1990 to 2019.

Estimation of Historic Water Use

Although Kansas water-use reports go back to 1958, actual water usage as a whole, across large areas, was probably much higher than these reports would indicate in the early period, since it wasn't until 1978 that water rights were required to be obtained before diverting water for beneficial use. Even then, it wasn't until the early 1980s that water-right holders were required to submit annual water-use reports and not until 1987 that the KDA-DWR had the regulatory authority to fine water-right holders for lack of submission or knowingly falsifying reports. The Water Use Program of the Kansas Water Office was initiated in 1990. Now operated through the KDA-DWR, this program provides quality control and assurance for the submitted water-use reports. As such, reported water-use records were downloaded only from 1990 to 2019 (at the time of the model development, 2019 was the most recent year available for access as the 2020 reports were still under review).

To estimate historical pumping levels before 1990, linear regression equations were determined based on the ratio of water use/authorized quantity versus precipitation between 1993 and 2019, similar to past KGS modeling projects (Wilson et al., 2020; Wilson et al., 2015; Liu et al., 2010; and Wilson et al., 2008). Various iterations found the regression of the water use/authorized quantity ratio against summer precipitation (April to September) from 1993 to 2019 to be statistically significant ($P < 0.001$) and highly correlated for total groundwater use (R-squared value of 0.74).

Figure 21 shows the results of the regression-based water-use estimates against the authorized quantity and the 1990–2019 reported water use for cells in the model's active area within GMD4. The ratios of water use/authorized quantity for total groundwater use and total irrigation groundwater use are computed for every model cell based on the variations in summer precipitation. The ratios are then multiplied against their respective authorized quantities for a given year to yield an estimate of the actual amount of water used. The transient model uses the regressed water use from predevelopment until 1992, the actual reported water-use data for 1993–2019, and regressed water use for years going forward after 2019 (in future scenarios).

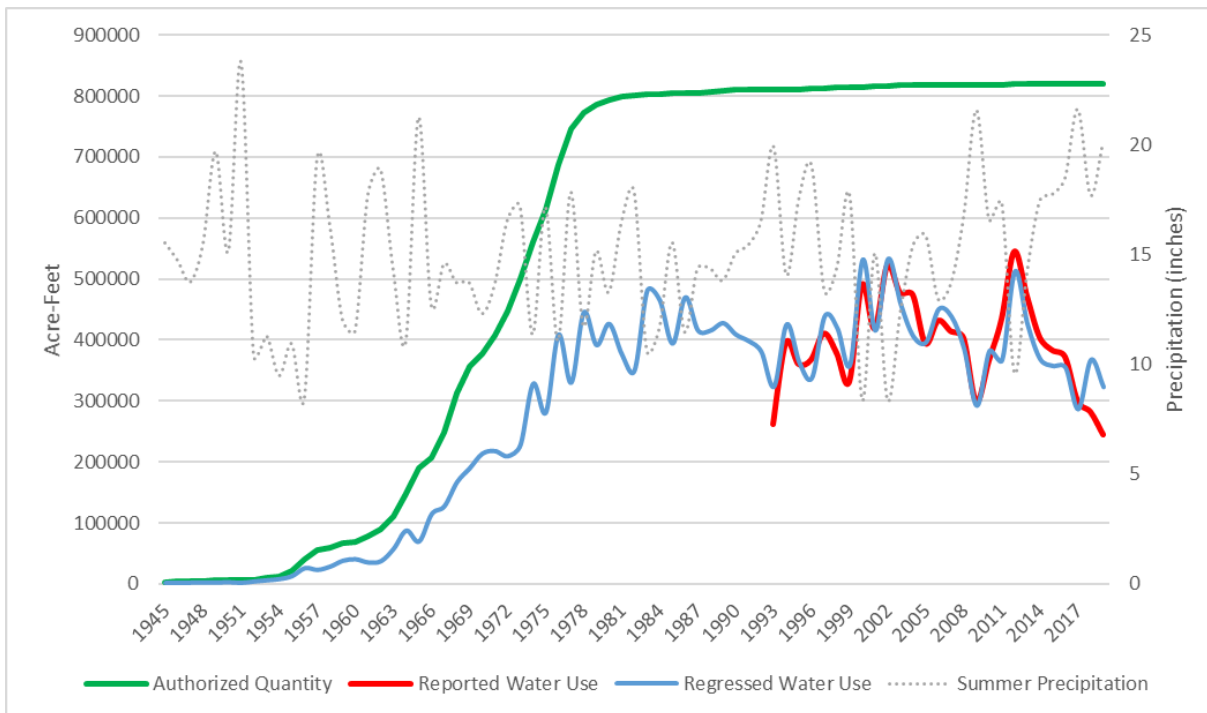


Figure 21. Total authorized quantity, regressed water use, summer precipitation, and reported water use.

The geologic bulletins note that pumping during predevelopment periods was mainly for municipal, stock water, and domestic purposes with irrigation being relatively small to non-existent. To create a steady-state or predevelopment pumping file, both present-day active and inactive vested water rights (those permitted water rights that had verified water uses in place before the 1945 Kansas Water Appropriation Act) were queried from the WIMAS data. Vested water-right wells that were known to have been re-drilled since 1945 were removed from consideration.

Average reported pumping, by use, from 2008 to 2017 (a period where the installation of totalizing flow meters were required within GMD4) was used to represent historic predevelopment pumping for 90 identified vested wells. Within GMD4, the 53 municipal vested water right wells were assigned an annual predevelopment usage of 21 acre-feet, while 36 vested irrigation wells were assigned 53 acre-feet of usage. The lone domestic vested well within GMD4 was assigned a predevelopment usage of 0.08 acre-feet.

Colorado and Nebraska

Estimating water usage and groundwater development in other states has its challenges as the data are based on complex rules and procedures, much like Kansas water-right data. Consequently, the processing results for water usage outside of Kansas should be viewed with a certain level of caution. For this project, permitted well data from the Colorado Decision Support System (CDSS), developed by the Colorado Water Conservation Board and Colorado Division of

Water Resources, and registered wells from the Natural Resources Data Bank (NRD) administered by the Nebraska Department of Natural Resources were used.

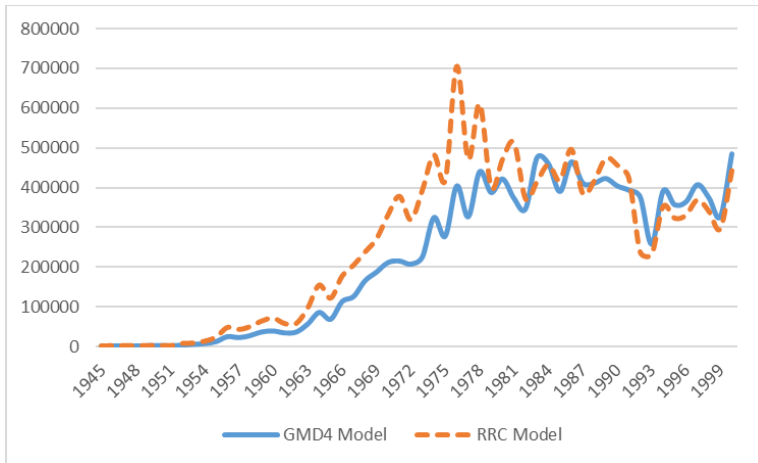
The CDSS “Final Permit” database contains information related to permit numbers, annual permitted quantities, use(s) of water, aquifer sources, and priority dates. The data set represents larger uses of water (e.g., non-domestic) with irrigation being the dominant type, accounting for 98% of the records in the model domain. Other listed uses are for municipal (three records), stock (two), and augmentation (two). Similar to Kansas, the database has the permitted well’s listed priority dates and annual appropriation.

The registered well data from the NRD is much more expansive as it inventories groundwater diversions associated with a wide range of uses, including non-consumptive uses such as wells drilled solely for observation or monitoring. Within the model domain, irrigation is the only active “larger” use of water listed. Unlike the Kansas and Colorado data, there are no permitted/authorized amounts or priority dates assigned to wells. However, the NRD data do contain proxy items that can be used to mimic those particular data items. The year of the well’s completion was used to replicate priority dates, and an authorized or maximum annual allocation was replicated by multiplying the listed number of acres the well irrigated by an application rate of 2.5 acre-feet per acre.

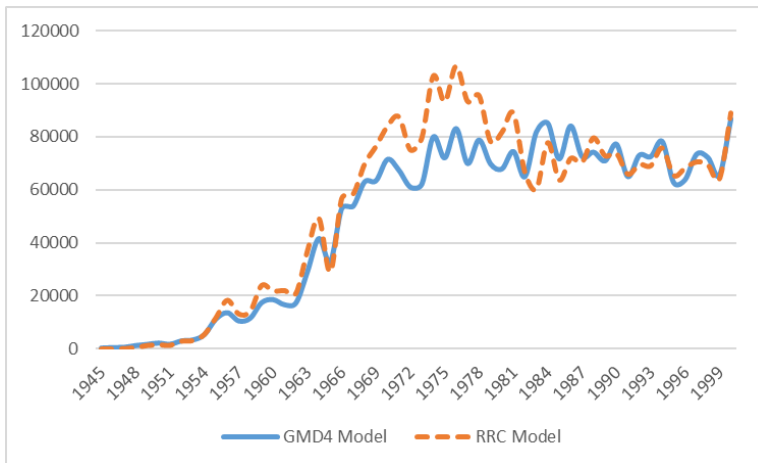
Estimation of Historic Water Use

Given the lack of extensive estimates of actual water use in Colorado and Nebraska (like most western states), the regression equation used to estimate water use in Kansas (based on summer precipitation) was applied to model cells in the bordering states using the listed permitted quantities and priority dates (Colorado) or year of the well’s completion and an estimated representative authorized amount (Nebraska).

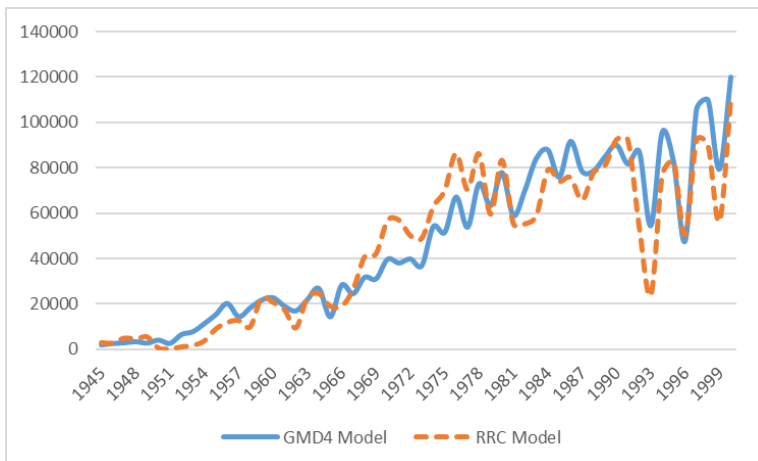
As a means of comparisons, the regressed water use was compared to the pumping files used by the Republican River Compact Model (RRCM). Completed in 2003, the RRCM was developed by Kansas, Colorado, and Nebraska with participation of federal agencies to simulate the physical and hydrogeological characteristics of the Republican River Basin from 1918 to 2000. Figure 22 illustrates a comparison between the GMD4 and RRC models in three overlapping areas and shows the two models compare favorably, both in terms of absolute volumes and regional trends.



(a) Kansas- GMD4



(b) Colorado



(c) Nebraska

Figure 22. Comparison of estimated groundwater usage, in acre-feet, between GMD4 and RRC models for Kansas (GMD4), Colorado, and Nebraska.

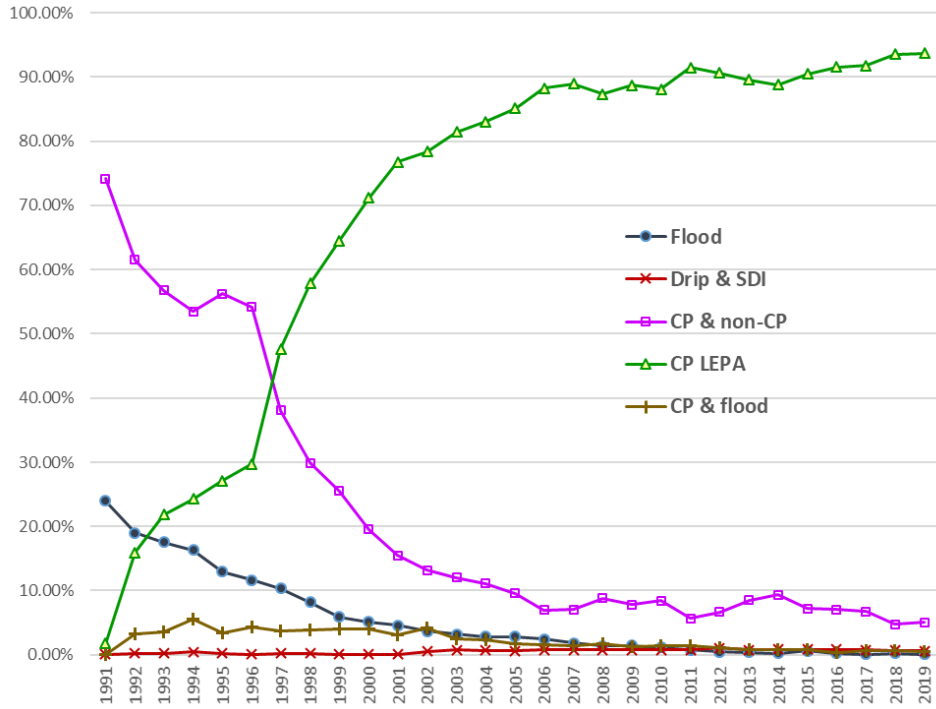
Irrigation Return Flow

A certain amount of water applied by irrigation systems makes its way back to the aquifer in the form of irrigation return flow. The rate of this aquifer recharge is determined by a variety of factors, one of which is the efficiency of the irrigation system. Irrigation system types were added to KDA-DWR water-use reports in 1991. The reported ratios of systems types each year were compared across GMD4 using north-south trending columns of counties (e.g., “Cheyenne, Sherman, and Wallace”; “Rawlins, Thomas, and Logan”; “Decatur, Sheridan, Gove, and Graham”) to see whether the west to east precipitation gradient had any influence on system types.

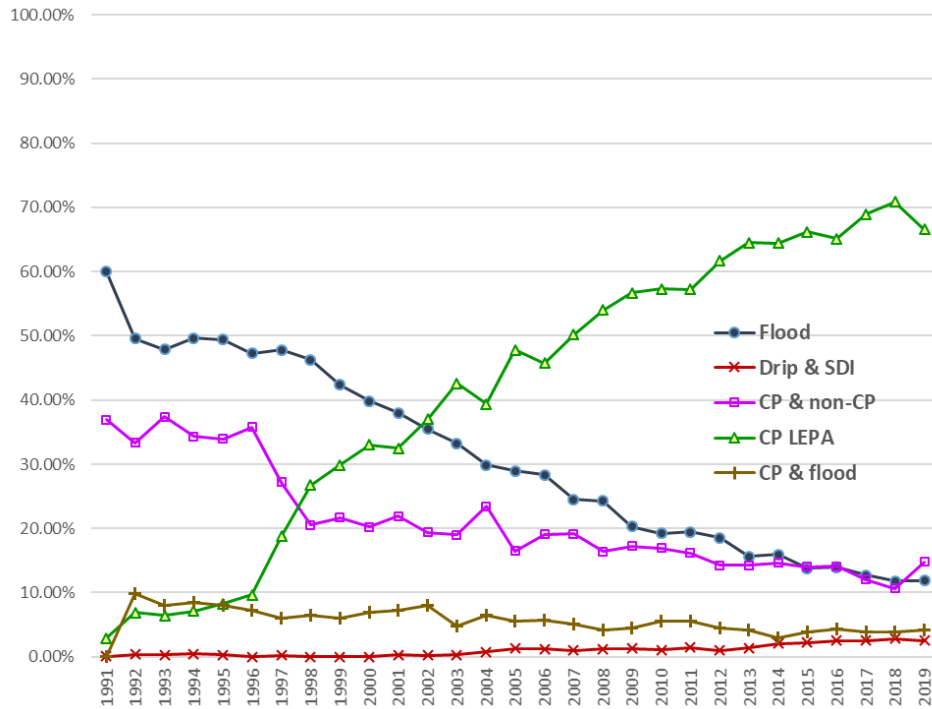
The comparisons show no obvious spatial trends within GMD4 but a slight difference compared to areas outside the district. Figure 23 shows a typical example in which flood and early generation pivot systems are the most common in the early 1990s across the model domain, with a shift to more efficient systems over time. Overall, the data show that irrigation systems inside GMD4 tend to be more efficient than those outside.

The irrigation return-flow percentages (relative to the total irrigation water pumped) used in past models were assigned to the system types reported in the water-use data. In order of decreasing return-flow percentages, those are the following: flood irrigation 25%, center pivot and flood 17%, center pivot 9%, sprinkler other than center pivot 9%, center pivot with low energy precision applicators (LEPA) 7%, and subsurface drip (SDI) in combination with other type 4%. As farming operations have improved with technological advancements, so have irrigation efficiencies, thus reducing the amount of return flow over time.

The average return-recharge percentage was then computed in GMD4 and areas outside for each year from 1991 to 2019 based on the number of each system type and its assigned return-flow percentage. It was assumed that flood irrigation was the only system type in use before 1955. Between 1955 and 1991, a smooth transition from flood to center pivot types for each county area was then applied. Water use occurring within GMD4 and areas outside is multiplied by the average return-flow percentage to determine the total amount of water returning to the aquifer (fig. 24). Water use in Colorado is multiplied by the GMD4-based percentages, whereas water use in Nebraska is multiplied by the percentages for areas outside GMD4. Return flows are combined with natural precipitation recharge to form the total recharge at the land surface in the model.



(a) Rawlins, Thomas, and Logan counties within GMD4



(b) Counties outside of GMD4

Figure 23. Examples of reported irrigation system types for (a) the portions of Rawlins, Thomas and Logan counties inside GMD4 and (b) areas outside GMD4, 1991 to 2019.

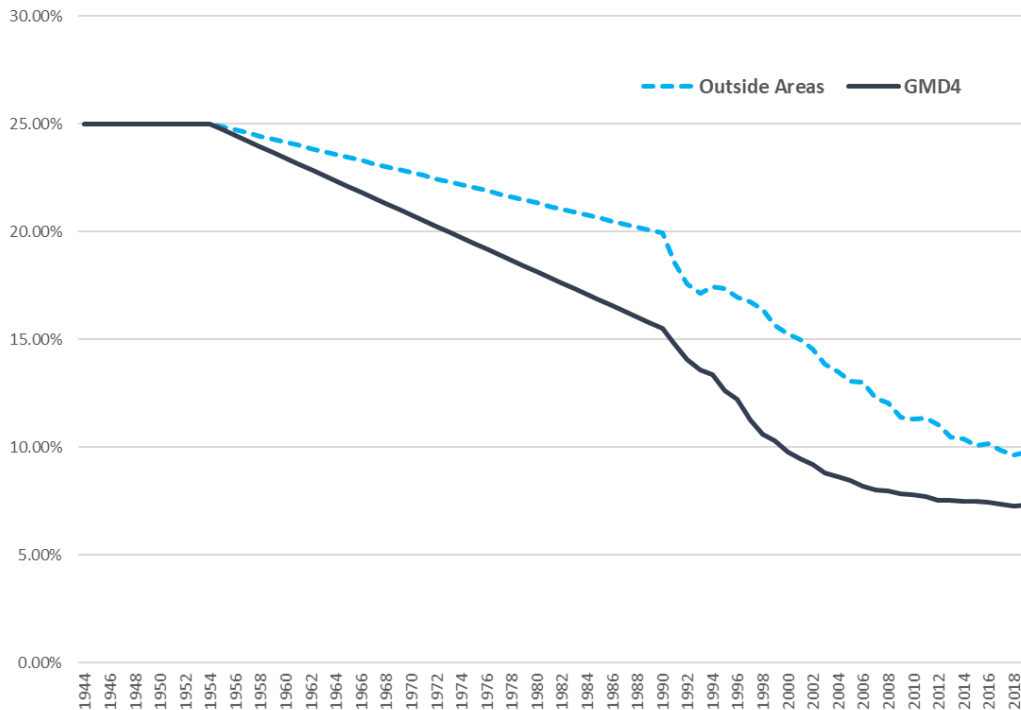


Figure 24. Average percentage of irrigation return flows for GMD4 and areas outside the district, 1945 to 2019.

Irrigated Land Fractions

The rate of precipitation-based recharge to the aquifer is often higher for areas under irrigation, relative to adjacent dryland areas, as the soil horizons are at or near saturation during the irrigation season. In early KGS modeling projects, the precipitation-based recharge was adjusted within model cells containing irrigation points of diversion. In reality, irrigation water is applied to field boundaries that can cross into model cells that may not contain pumping wells. To better estimate the irrigation-enhanced precipitation recharge, irrigated land fraction within each model cell is calculated based on where water is applied, commonly referred to as the place of use.

Although KDA-DWR water-use reports contain information about the total number of acres irrigated each year, the location of the field boundaries is unknown. However, each water right's permit or certificate specifies the authorized place(s) of use and, for irrigation uses, the authorized boundaries are spatially categorized by 40-acre Public Land Survey System (PLSS) tract(s). The total net (referred to as "additional") acres for each 40-acre tract was summed and joined to a GIS layer representing 40-acre PLSS boundaries to spatially map the authorized places of use across the model area.

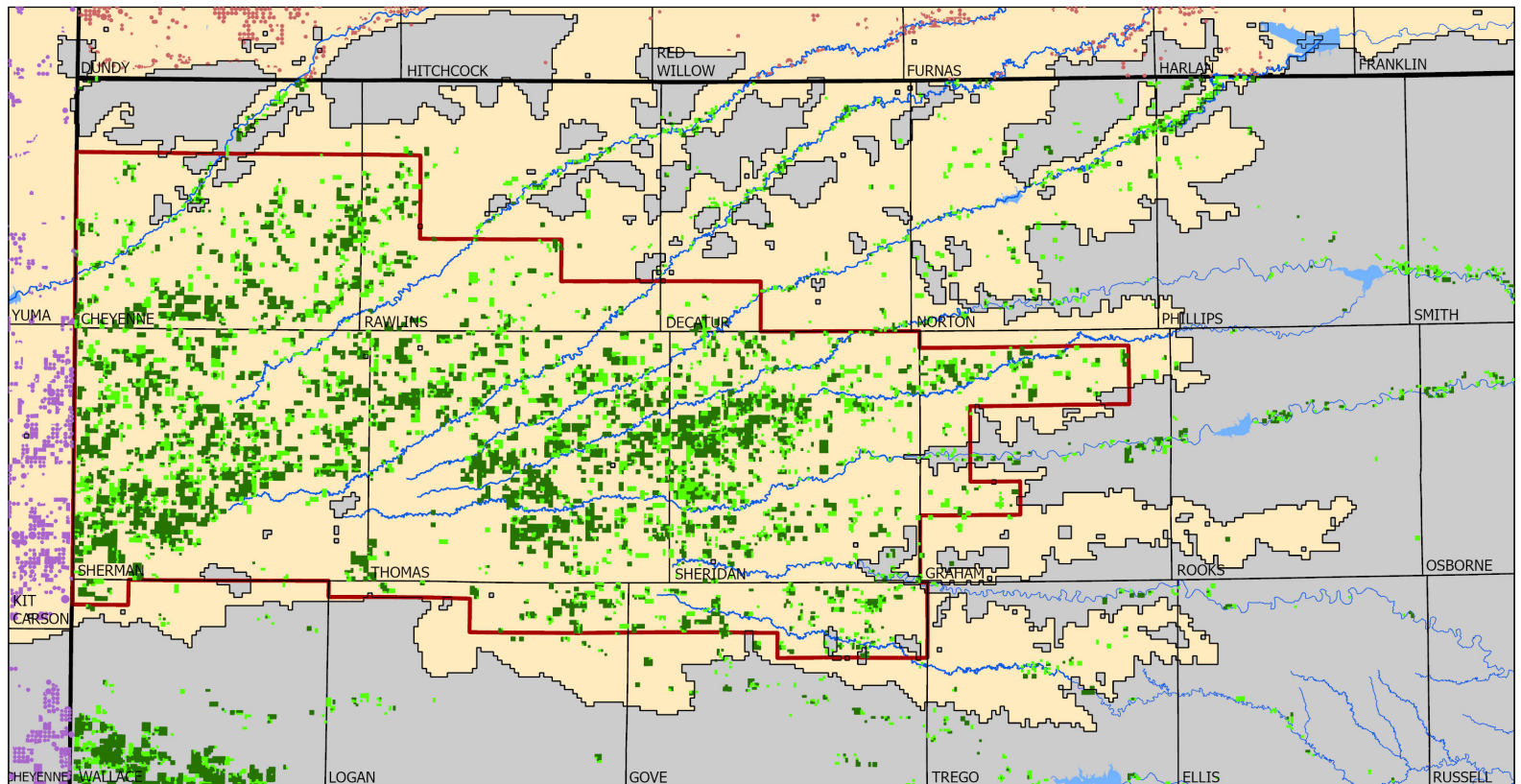
Figure 25 shows the distribution of 40-acre tracts symbolized by the total net acres authorized. For a tract with 40 acres (or more), it is assumed the entire tract is irrigated. For tracts with less than 40 acres ("partial" tracts), irrigation is authorized within that tract but the exact location and field boundaries can only be determined by looking at the original water-right permit or certificate on file with the KDA-DWR. The average acres authorized for partial tracts in GMD4 for PLSS is 26. For analysis purposes, partial tracts of less than 30 acres were deleted and not considered.

A single water right often has multiple places of use, whereas a single place of use can be authorized under multiple water rights. Water rights in the model domain were grouped based on how they overlap each other by point(s) of diversion or place(s) of use. The earliest priority date within the water-right group was assumed to represent the first point in time irrigation water was applied to the 40-acre places of use authorized under the group. It was assumed the senior water right covered all the acres listed under the 40-acre tracts and the junior water rights in the group did not add any additional acreage.

Mapped field boundaries representing irrigated lands in 2017 were downloaded from the Colorado CDSS for the Division 1 — South Platte management area. The data set contained the permit ID number that matches the final permit well data used in the pumping file. The priority date of first use associated with the permitted wells was then assigned to their respective place(s) of use to represent when water was first applied. Subsequent CDSS datasets showing irrigated places of use for 2016, 2015, and 2010 were reviewed to account for any missing fields.

Nebraska's Institute of Agriculture and Natural Resources, Center for Advanced Land Management Information Technologies provides GIS-enabled data layers that mapped irrigated fields from center pivots and non-pivots in 2005. The only attribute provided from the data layers was the irrigated area. The two data layers (pivot and non-pivot) were merged together and spatially intersected with the registered wells file used in the Nebraska water use estimates. The priority date of first use associated with the overlapping permitted wells was then assigned to their respective place(s) of use to represent when water was first applied. Places of use that did not have spatially intersecting well points were subjectively assigned a year based on the closest adjacent registered well or the average first year of use from other surrounding polygons.

The place of use tracts from Kansas, Colorado, and Nebraska were merged together (fig. 25) and overlain with the model grid to calculate the percentage of overlap, yielding an estimate of the irrigated land fraction in each year.



- Kansas tract with 40 or more acres
- Kansas tract with less than 40 acres
- Colorado irrigated land
- Nebraska pivot and non-pivot irrigated areas

Figure 25. Irrigated places of use.

MODEL CALIBRATION AND SIMULATION

Like past KGS modeling projects, the GMD4 model is divided into two major simulation periods: a steady-state predevelopment period during which water levels remain relatively stable and a transient period during which groundwater development increases and water levels change over time. The predevelopment simulation establishes the conditions from which the subsequent transient model starts.

The major data sources for the predevelopment period are from the years before 1946, although some of the water-level data extends into the early 1950s. Contrary to the implications of the term “predevelopment” (a period of time representing the aquifer before it was extensively developed), the steady-state GMD4 model includes a relatively small amount of pumping, generally clustered around county seats. The transient period simulates groundwater conditions from predevelopment to 2020 (simulation ended in spring 2020 as 2020 water use was not available at the time of model calibration), during which time groundwater pumping increased. The transient period is based on six-month time steps—a “summer,” or growing, season from April to September and a “winter” period representing the months of October to March.

Model Characteristics

Pumping and Irrigation Return Flows

The “Water Right Development” section of the report describes how groundwater pumping is determined for the Kansas, Colorado, and Nebraska portions of the model. The reported and regressed water usages are on an annual basis. For the model’s six-month time steps, all irrigation usage was assigned to the “summer” period representing conditions from April to September. All other groundwater usage was proportioned with 60 percent occurring in the summer period and 40 percent occurring during the winter period. Irrigation return flows were added to the overall recharge input file used by the model for the summer period.

Stream Characteristics

All surface water streams are simulated in this project as rectangular channels with an underlying streambed. The streambed widths are set to a representative value of 15 ft throughout the model area. The streambed thickness is assumed to be 1 ft for all simulated streams. For SF Republican River, which is perennial, the streambed K is expected to be higher than that for the ephemeral streams. As shown later, the streambed K for SF Republican River is estimated to be 0.03 ft/d by model calibration, and the streambed K for all other streams within the district is estimated to be 0.02 ft/d. Flow data from the USGS and Bureau of Reclamation were used in calibrating stream-aquifer interactions.

Drains

Drains are used along most of the eastern extent of the model’s active area where the headwaters for numerous tributaries have cut into the HPA. Drains allow water to discharge from the aquifer based on water-table elevations relative to the drain cell’s elevation. The elevation for each drain cell was set to land surface and a drain conductance of 2,000 ft²/d was used.

Evapotranspiration

Evapotranspiration (ET) could be a significant groundwater outflow in stream channels (fig. 26) where the water table is close to the land surface. The maximum ET rate at the land surface was set to 2 ft/yr (Hanson, 1991). The extinction depth was set to 10 ft below land surface, at which point the ET rate becomes zero. When the depth to water is between the land surface and extinction depth, the ET rate is linearly interpolated based on the depth to water relative to the extinction depth. In the model cells with streams, the land surface that controls ET should be that of the stream valley where the depth to water is the shallowest. In the GMD4 model, unlike previous KGS modeling projects, stream elevations are used as the surface elevation for ET calculation in those cells. This is considered to be more accurate than the average land surface elevation for a stream cell, which is dominated by the high elevations in the terraces (the length of each model cell is much larger than the stream width). For model cells without streams, as with previous KGS models, the average land surface elevation is directly used as the surface elevation in ET calculation.

Time-Varying Specified-Head Boundaries

Time-varying specified-head boundaries are used for active model cells along the western and southern border of the model's active area. Time-varying specified heads were established based on a time- and labor-intensive process of reviewing each model cell in relation to any surrounding water-level measurements. Water-level trends shown in the measurement history of wells were applied to the head-boundary cells.

Precipitation Recharge

Precipitation-based recharge was calculated based on the power-function used in the GMD3 model (Liu et. al., 2010),

$$R = \begin{cases} 0, & P < P_0 \\ a(P - P_0)^b, & P \geq P_0 \end{cases}$$

where R is precipitation recharge (infiltration), P is precipitation at a given model cell in each six-month time step, P_0 is threshold precipitation above which groundwater recharge occurs, and a and b are the coefficients of the power function. The precipitation recharge calculated above represents the amount of infiltration through the surface soil of non-irrigated lands. The enhancement to precipitation recharge in irrigated fields is computed as an additional source of recharge water as discussed in the next section.

The model divides the recharge-precipitation power functions into two zones (fig. 26) and two time periods (summer and winter). Recharge in the main aquifer generally averages less than half an inch per year, while the stream channels have higher recharge rates, accounting for enhanced recharge that occurs during runoff events. The actual recharge rate varies for each model cell as the precipitation amounts change between different cells and time steps. For the same precipitation, the recharge rate is higher in the non-growing season than in the growing season as surface evapotranspiration is much more significant in the growing season (higher temperature and more consumptive use by plants). The power-function parameters P_0 , a, and b are calibrated by matching observed water levels and streamflows to simulated values.

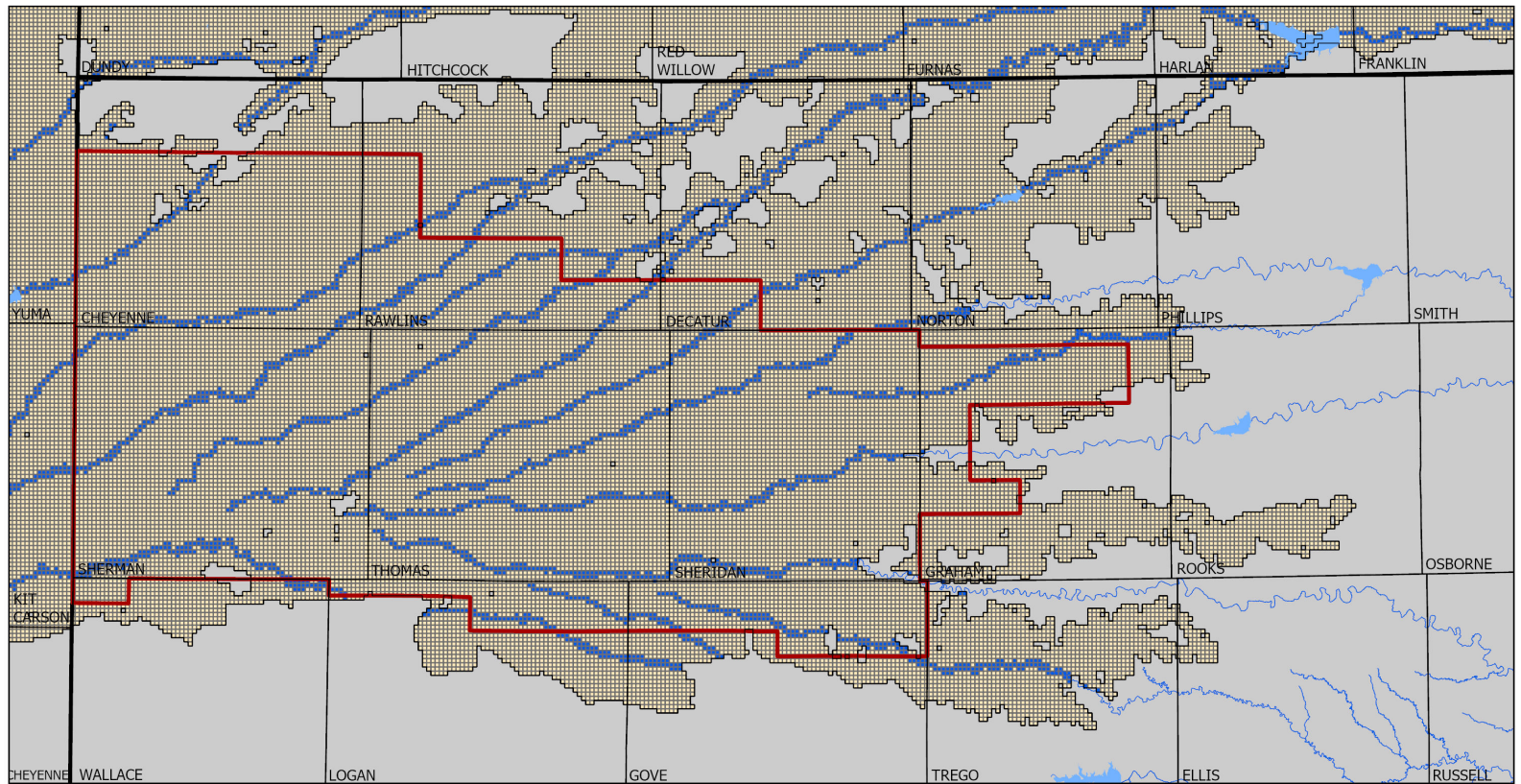


Figure 26. Recharge zones for precipitation-based recharge. The main aquifer is shown in tan while stream channels are shown in dark blue. Recharge curves are calibrated separately in each zone.

Enhanced Precipitation Recharge from Irrigated Land Fractions

The enhancement of precipitation recharge by irrigation is computed by multiplying the precipitation recharge by a constant factor for the irrigated acreage in each cell over time, based on the priority date of the most senior water right. That factor is set to 1.0 based on the previous model study in southwest Kansas by Liu et al. (2010). Because the enhanced precipitation recharge by irrigation is added to precipitation recharge computed using the calibrated precipitation-recharge curve (assuming no irrigation), the total precipitation recharge in the irrigated fields is twice that if the fields were not irrigated.

Delayed Recharge

All recharge originating from the land surface is subject to a delay function, first used in the GMD1 model (Wilson et al., 2015), to simulate the vertical distance that water must travel in the vadose zone before reaching the water table. To simulate the vertical movement of water through the vadose zone, all surface-based recharge, either from precipitation over a non-irrigated area, enhanced precipitation recharge over irrigated lands, or irrigation return flows, is assumed to move down through the vadose zone at a constant velocity and diffusivity (diffusivity describes how water molecules spread out about the average velocity and is illustrated in fig. 27). This movement can be expressed by the following function:

$$R(z,t) = \frac{R_0}{2\sqrt{\pi Dt}} \exp\left(-\frac{(z-ut)^2}{4Dt}\right),$$

where $R(z,t)$ is the recharge rate (L) at time t and depth z in the vadose zone resulting from a recharge event at the surface R_0 (L). The parameters u (L/T) and D (L²/T) are the velocity and diffusivity of water movement in the vadose zone, respectively, both of which are dependent on properties of vadose zone materials. In this work, u is determined by model calibration, while D is set to 1.0 ft²/d based on initial model simulations. R_0 includes precipitation recharge, precipitation recharge enhancement by irrigation in the irrigated lands, and the irrigation return flows; it is computed for each model cell and six-month time step. For water-table depth L and model time step t_L , the amount of water that has reached the water table from R_0 is calculated as

$$R_T = \int_0^{t_L-t_0} R(L,t)u dt,$$

where R_T is water-table recharge from R_0 and t_0 is the time step at which R_0 is computed. To compute the total water-table recharge from the surface at a given time step, the model considers R_0 over all previous time steps that have $R_T > 0.0001R_0$ (i.e., time step t_0 is included in the calculation if greater than 0.01% of surface recharge R_0 reaches the water table). The water that enters the water table from R_0 during a given time step is the difference between the R_T computed at the end of that step and the R_T computed at the beginning of that step.

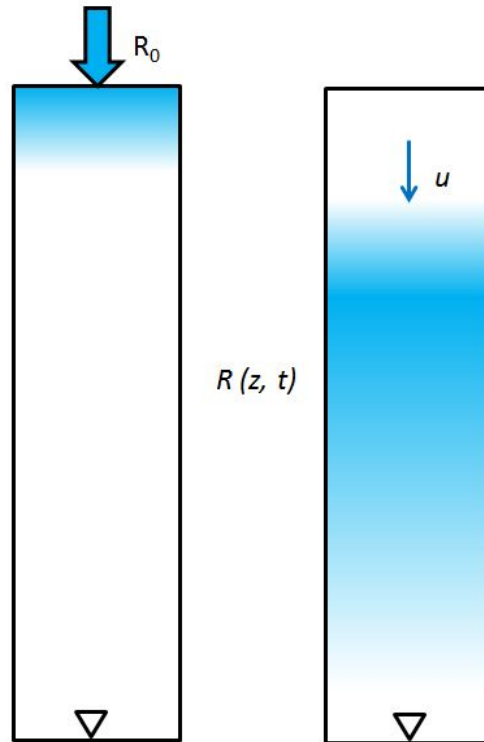


Figure 27. Schematic of the movement of surface recharge in the vadose zone.

Lagged Drainage from Dewatered Sediments

As the water table declines, the previously saturated material composing the aquifer still retains some water that is held in place by capillary forces. Part of this water will eventually drain down to the water table. This phenomenon is different from perched water, where some volume is being held up by an underlying aquitard. Here, both high and low permeability units become exposed as the water table drops and those units still retain water. Over time, a portion of that held water drains out under the influence of gravity. The amount of water being held and how readily it drains out depends on the material in question. The lower-permeability materials typically have finer grain sizes and can hold significantly more water after the water table falls; it will take a much longer time for that water to drain out than from the higher-permeability sediments.

For this modeling work, the lagged drainage of water after the water table fall is simulated with the following function:

$$W(t) = cd \exp(-d(t - t^*)), \quad t > t^*$$

where $W(t)$ is the amount of water draining out at time t , t^* is the time when the water table fell below the geological unit, c is the total amount of water for delayed drainage per unit volume of dewatered sediment, and d is the exponential decay coefficient (the later, the smaller the amount of drainage). Both c and d are treated as model calibration parameters whose values are determined by matching the simulated water levels to observations.

Figure 28 shows the curves of lagged drainage for five different geological units (see table 1 for the detailed information about each categorical unit). Sand and gravel layers drain quickly and do not hold a significant amount of capillary water. Silt and clay layers can hold a sizable amount of water that may be retained for decades because of the small pore space.

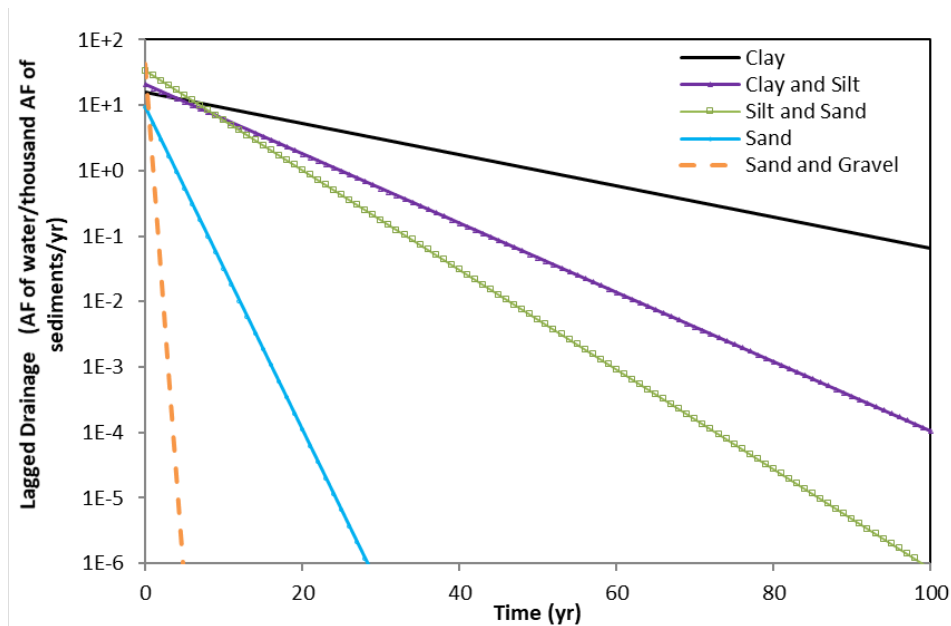


Figure 28. Lagged drainage of water for different geological units. Time zero represents the time when a lithologic unit becomes dewatered (water level declines below the unit). The vertical axis represents the amount (AF) of water released from a thousand AF of a lithologic unit after initial dewatering.

Hydraulic Conductivity and Specific Yield

As described earlier, the code developed for the HyDRA project was used to develop a three-dimensional grid describing the proportional distribution of five different categories of the material composing the aquifer throughout the model domain, based on drillers' logs contained in the WWC5 database and other sources in Colorado and Nebraska. A special program was developed to allow water levels generated for each time step in MODLFOW to intersect with this three-dimensional grid to compute proportion-weighted averages of K and Sy in each cell of the two-dimensional flow model.

Figure 29 shows the HyDRA lithology-based estimated K for the interval between the predevelopment water levels and the bedrock surface based on the estimates of K for each of the lithology categories listed in table 1. The average K across the active area in GMD4 was approximately 269 ft/day. The highest of these estimates occur in western Sherman County, Kansas, and eastern Kit Carson County, Colorado, where K values were manually doubled to allow the model to better match observed water levels in the area. Excluding this area, the estimated average K in GMD4 was 237 ft/day. During the transient portion of the model, two water levels are associated with each model cell, representing the start and end water levels at each transient time step. K is computed for the lithological units between the average of the two water levels and bedrock.

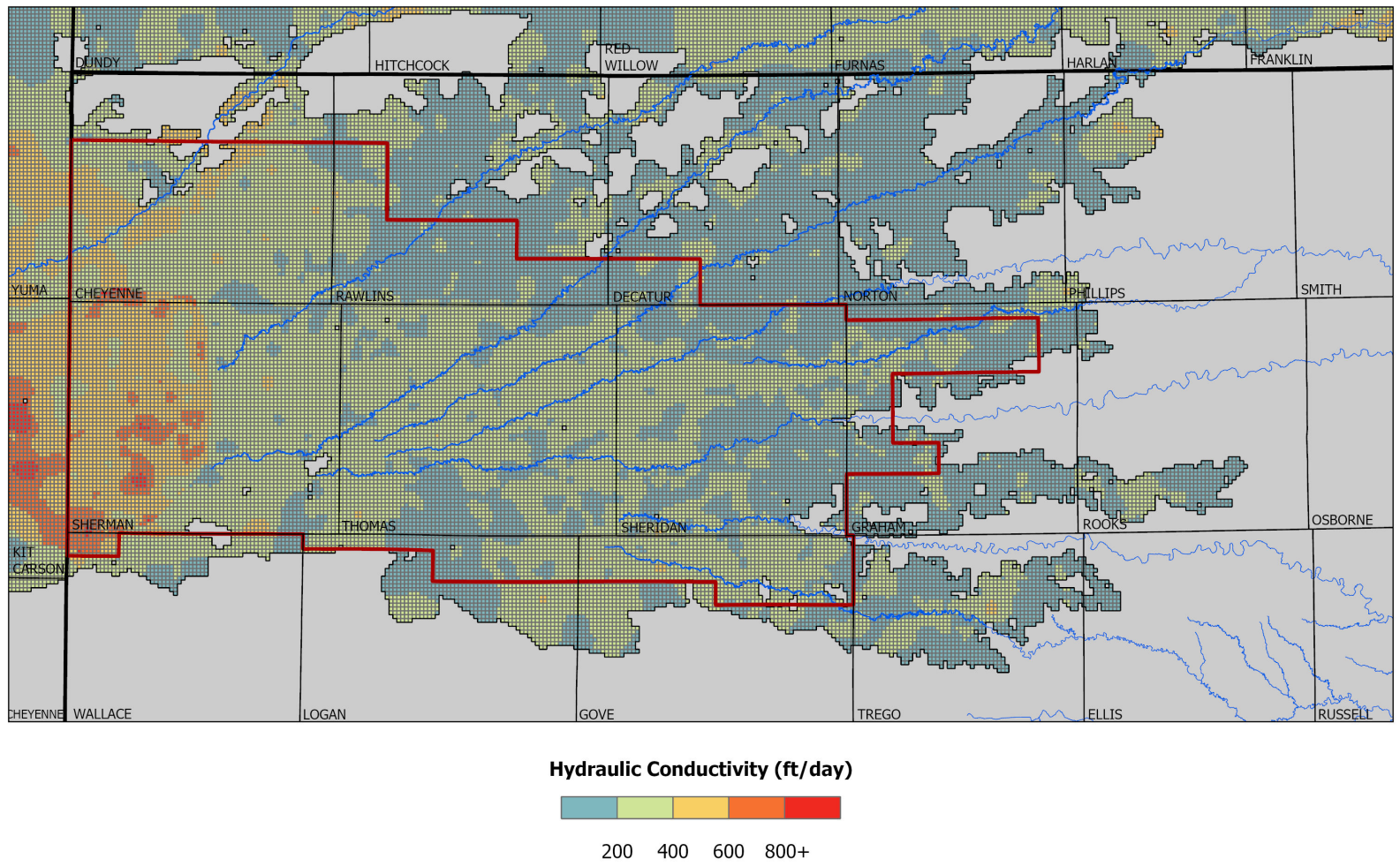
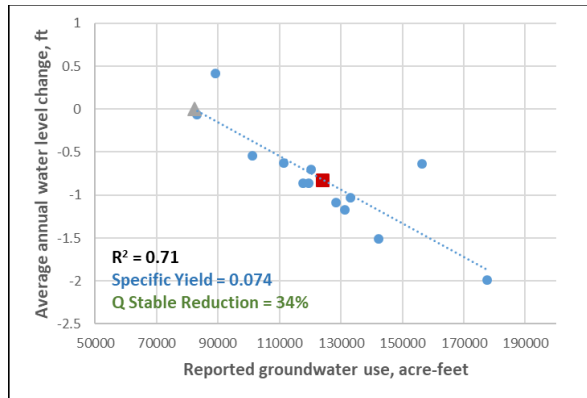


Figure 29. Vertically averaged K based on five calibrated HyDRA lithologic classifications for the interval between the predevelopment water table and the bedrock surface.

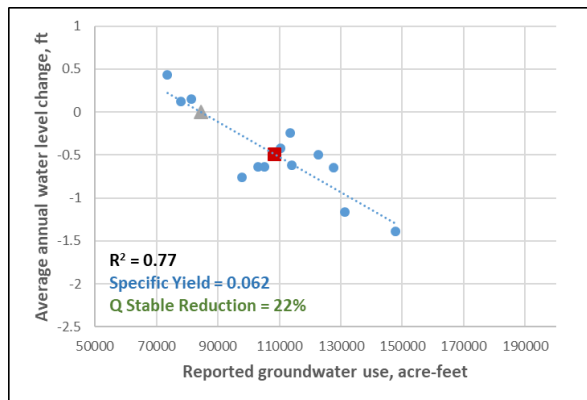
Using a method developed from Liu et al. (2021), S_y was estimated from the Hydra lithology categories combined with a data-driven, water-balance approach developed by Butler et al. (2016) for estimating the average S_y over an area from a linear relationship between annual water use and annual water-level change. Individual water-balance analyses based on data from 2005 to 2018 were conducted for Sherman, Thomas, and Sheridan counties (fig. 30), representing the western, central, and eastern regions, respectively, across the district. For all county analyses, the water-level change for 2006 and 2007 are averaged since heavy snows delayed the 2007 water-level measurements until April. The computed S_y in each county is used to compare with the overall estimated S_y values derived from each of the lithology categories.

In GMD4, the lithology percentage distributions across the three core counties are very similar, which makes isolating specific lithology categories (e.g., “Sands and Gravels”) difficult. To compensate, the first three categories were assigned a series of representative S_y values, and the overall county S_y estimates are used to solve for the last two categories, “Sands” and “Sands and Gravels.” From these series of calculations, reasonable estimates of the S_y representing the last two categories were obtained: 0.119 for “Sands” and 0.12 for “Sand and Gravel.” The first two categories were then assigned S_y values of 0.01 due to their insignificant water yield, and the S_y for the last remaining category, “Silts and Sands,” was solved to 0.094.

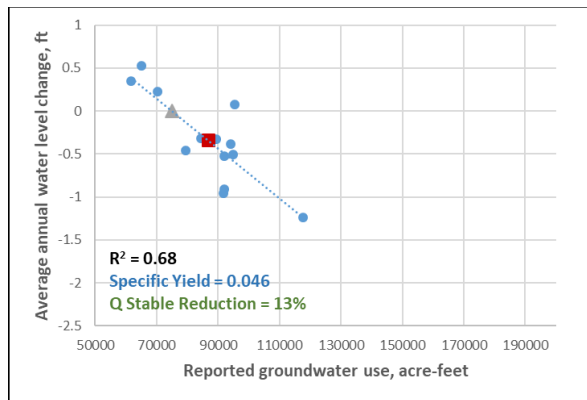
Figure 31 shows the S_y derived from the lithology category-water balance approach from the predevelopment water table to the bedrock surface. The average S_y across GMD4 is 0.0629. This is substantially less than traditional estimates of S_y for numerical models but within ranges established through the water-balance relationships computed for the GMD2 sustainability assessment (Butler et al., 2017). For the transient portion of the model, the vertically averaged S_y values representing the interval between the upper and lower water levels during each model time step were computed.



(a) Sherman County



(b) Thomas County



(c) Sheridan County

Figure 30. Average annual water-level change versus annual water use from 2005 to 2018 for selected counties in GMD4. Dashed line is the best-fit line to the plot. Overall average conditions for both water use and water-level change are represented by the maroon squares. The estimated water use under stable water-level conditions is shown by the olive-colored triangle (i.e., net inflow). Sy is calculated from the inverse of the slope of the best-fit line times the area of the county. Total pumping at which stable water levels could be achieved, termed Q-stable, is calculated as the difference between the average reported use and the net inflow.

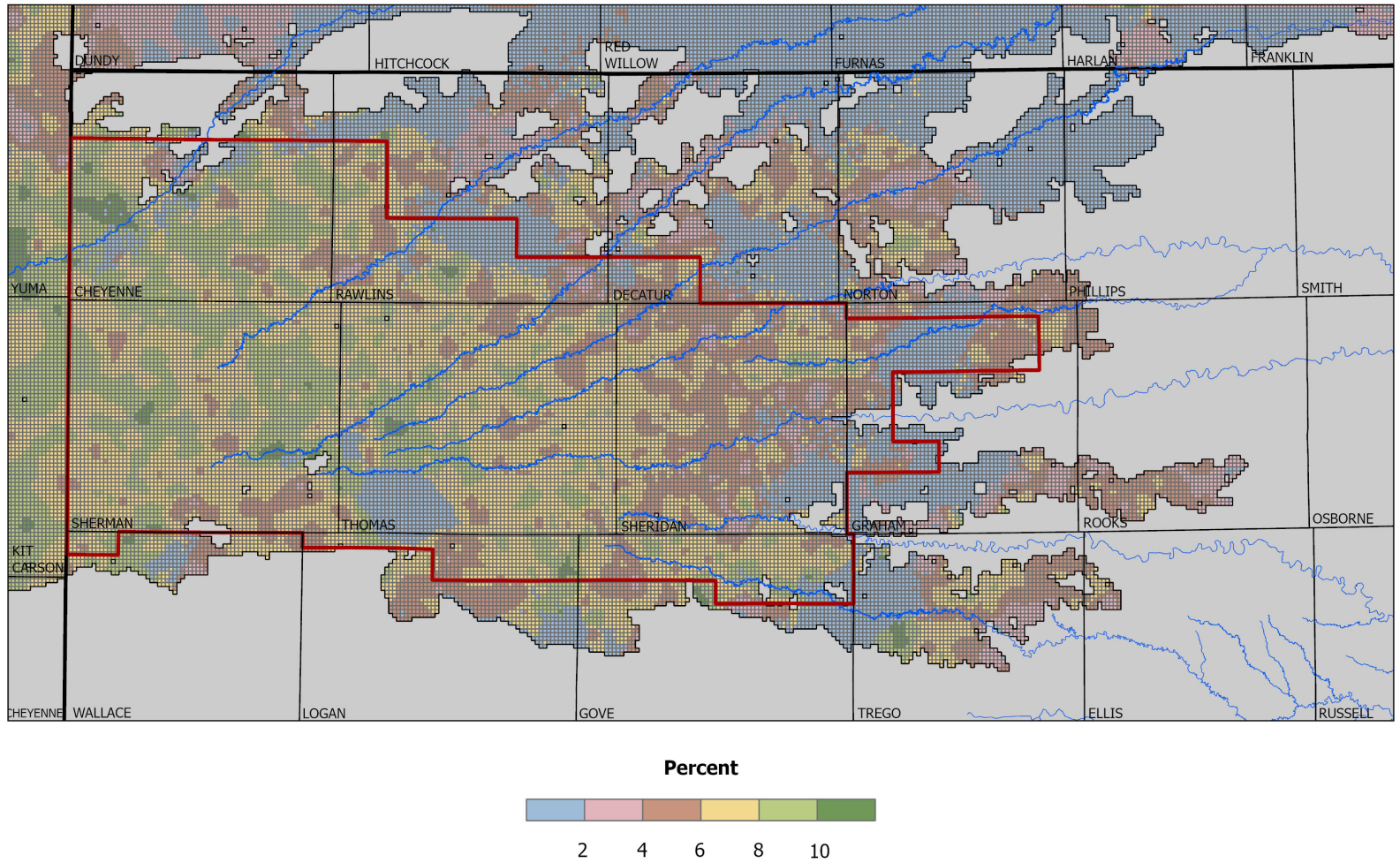


Figure 31. Vertically averaged SY solved from HyDRA lithologic classifications and county-based water-balance analyses between the predevelopment water table and bedrock.

Model Calibration

Because of our imperfect understanding of the hydrologic conditions in the field, some model parameters, especially those that are key contributors to aquifer budget calculations (e.g., K and recharge rate), need to be adjusted so that the simulated results match the observed data to the best extent possible. This process is generally referred to as model calibration. For GMD4 model calibration, data for comparison with the simulated results include water levels for a number of wells in the active model area from predevelopment to January 2020. For the wells that have multiple water levels during the transient period, the first value (i.e., the water-table elevation) is directly used in model calibration; for the subsequent years, the change between consecutive measurements is used instead. The water-level change provides a more sensitive indicator of aquifer response to different hydrologic processes during the transient simulation.

The model parameters whose values were adjusted during calibration are 1) the threshold precipitation P_0 for recharge and power function coefficients a and b for the two recharge zones, 2) the velocity of water movement in the vadose zone, 3) the lagged drainage function coefficients c and d for all five lithologic categories, 4) the hydraulic conductivity for five lithologic categories, and 5) the streambed hydraulic conductivity. The calibration process was performed with the parameter estimation program (PEST; Doherty, 2004).

Figure 32 shows the calibrated precipitation recharge curves for the recharge zones. Note that in the non-growing season, the threshold precipitation at which water starts to infiltrate through the topsoil (i.e., recharge starts) is lower, resulting in a larger recharge rate than that in the growing season for the same precipitation amount. For a given precipitation amount, precipitation recharge is low in the main aquifer and much higher in stream channels.

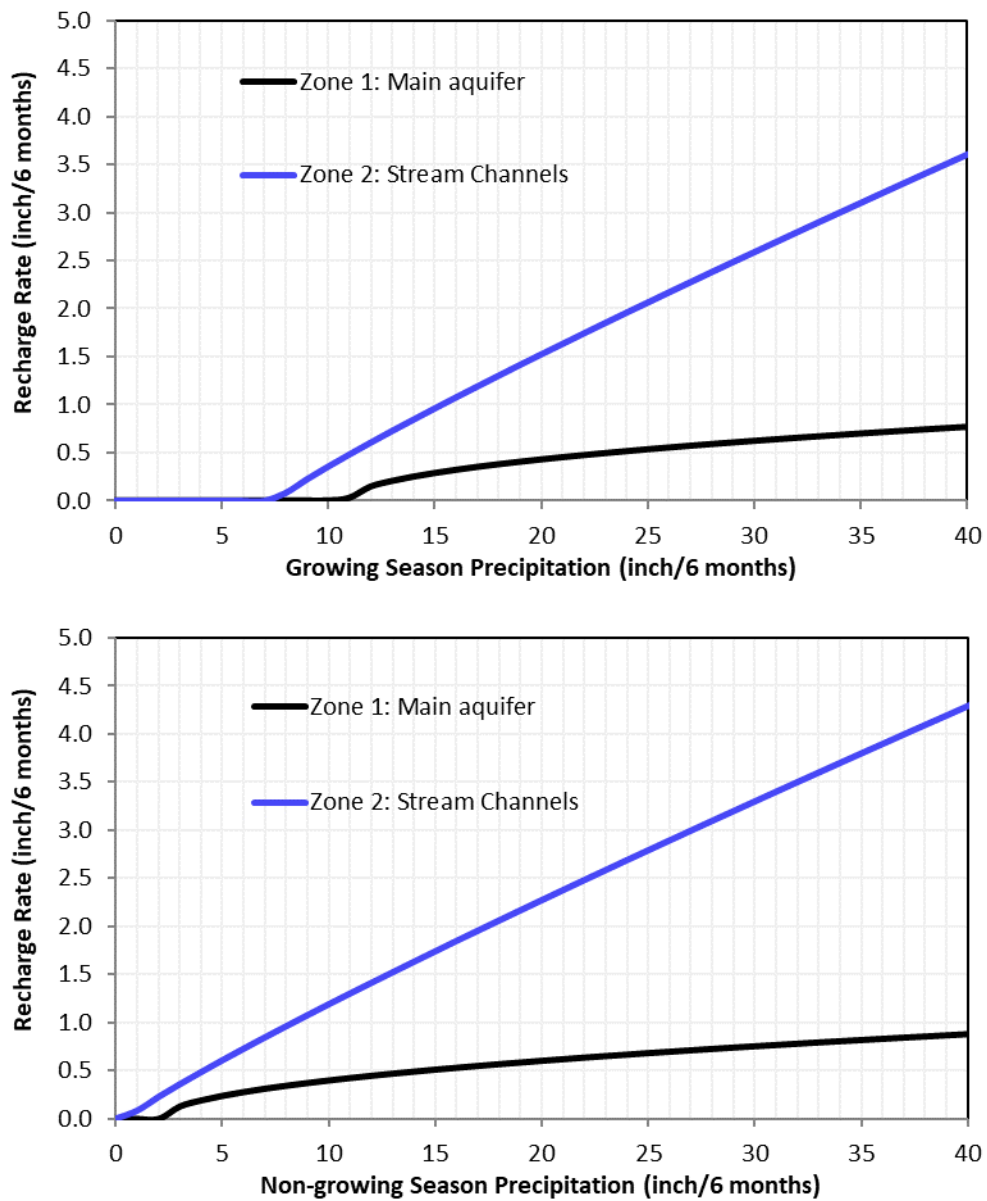


Figure 32. The calibrated precipitation recharge curves for different recharge zones in the growing (top) and non-growing (bottom) seasons.

The calibrated velocity of water movement in the vadose zone is 29 ft/year. This indicates that in predevelopment time when the average depth to water was 108 ft, it took about 4 years for the main portion of surface recharge to reach the water table. In 2019, when the average depth to water increased to 137 ft, the average travel time of surface recharge to the water table increased to 5 years. Table 1 lists the calibrated values of K, and fig. 28 shows the calibrated lagged drainage curves for each of the five lithologic categories.

Figure 33 (top) shows the simulated versus observed heads from the PEST calibration. These heads are the first water levels recorded at each well. Most of these head measurements are for the predevelopment period. If predevelopment data are not available, the earliest water-level records from the transient period were used. As the figure illustrates, the simulated heads align well with the observed values. Figure 33 (bottom) shows the simulated versus observed transient water-level changes from the PEST calibration. Water-level changes were computed by subtracting the later water levels from their corresponding earlier values, so that positive values indicate a decline of water table with time. Figure 34 shows the simulated versus observed streamflows at different USGS gages. Although most gages are located outside the district boundary, the streamflows are an accumulation of all stream-aquifer interactions upstream of the gages, and are therefore determined by the simulated water levels along the streams as well as the streambed conductivity.

Table 3 lists the mean residual, mean absolute residual, and root mean square of residuals of the PEST calibration data targets. The mean residual is given as the mean of observed minus simulated values, whereas the mean absolute residual is the mean of the absolute values of observed minus simulated values. All the different error statistics for the water-level change during the transient period are relatively small compared to past KGS models, indicating the model provides a good match for the change of aquifer conditions between predevelopment and 2020 across the entire district. The errors for predevelopment water levels are slightly larger than previous KGS models. The simulated streamflows are also larger than observed values.

Table 3. Mean residuals, mean absolute residuals, and root mean square of residuals for model calibration targets.				
	Number of data	Mean residual	Mean absolute residual	Root mean square (RMS) of residuals
Water level (ft)	1,166	6.42	18.43	23.19
Transient water-level change (ft)	2,675	-0.07	1.37	2.19
Streamflow (ft³/sec)	448	3.75	10.76	18.03

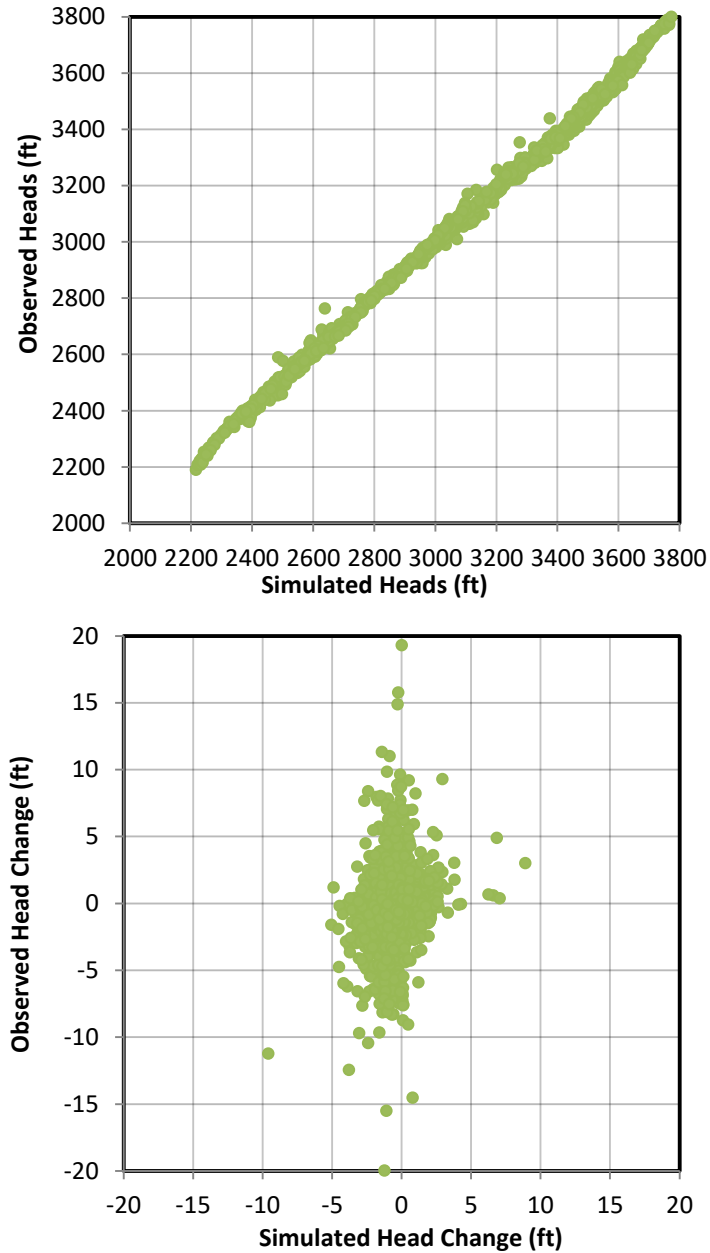


Figure 33. Observed versus simulated heads from the calibrated model: initial water levels recorded at each well (top) and water-level change during the transient period (bottom). Predevelopment water levels, if available, are treated as the initial water levels at the wells. If predevelopment water levels are not available, the earliest water-level records in the transient period are used. Transient water-level changes are computed between two adjacent winter water-level measurements (separated by one or more years for each well).

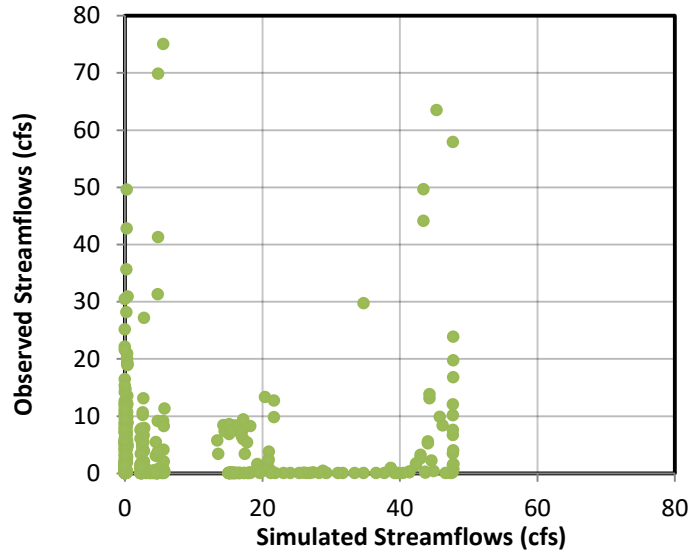


Figure 34. Observed versus simulated streamflows from the calibrated transient model. Plotted values are the average streamflows between January and March when the effects of surface runoff from precipitation are minimal.

Sensitivity Analysis

Table 4 lists the sensitivities of simulated responses to different model parameters during calibration. The relative sensitivity of a parameter p is computed as

$$RS_p = \sqrt{\frac{1}{N} \sum_{i=1}^N \left(\frac{\partial d_i}{\partial p / \dot{p}} \right)^2}$$

(Liu et al., 2010), where ∂p is the small perturbation around the calibrated parameter value \dot{p} ; ∂d_i is the change in the model-simulated groundwater level or streamflow at observation i , and N is the total number of observation data points used in the sensitivity calculation. In table 4, p11 and p14 are the threshold precipitation for recharge to start during the growing and non-growing seasons in the main aquifer, respectively, and p12 and p13 are the precipitation recharge power function coefficients for the main aquifer. Similarly, p21 through p24 are the precipitation recharge parameters defined for the stream channels. Parameters hy1 through hy5 are the hydraulic conductivity for the first through fifth lithologic categories. Parameters g11 and g12 through g51 and g52 are the lagged drainage function coefficients for the first through fifth lithologic categories, respectively. The parameter vzv is the velocity of water movement in the vadose zone. Compared to other parameters, the hydraulic conductivities of lithologic categories 3 (silts and sands), 4 (sands), and 5 (sands and gravels) have a much higher sensitivity, indicating the calibrated values of those three parameters have a much more significant impact on the match between the simulated and observed heads.

Table 4. Relative sensitivities of different model parameters during the PEST calibration.					
Parameter	Relative Sensitivity	Parameter	Relative Sensitivity	Parameter	Relative Sensitivity
p11	0.28	hy1	0.00	g22	0.03
p12	0.08	hy2	0.00	g31	0.20
p13	0.31	hy3	32.7	g32	0.04
p14	0.22	hy4	113	g41	0.01
p21	0.22	hy5	263	g42	0.00
p22	0.07	g11	0.23	g51	0.03
p23	0.13	g12	0.08	g52	0.01
p24	0.21	g21	0.14	vzv	0.05

Note: Streambed K is calibrated with streamflow data after precipitation recharge, hydraulic conductivity, lagged drainage, and vadose zone velocity are calibrated with head data. The relative sensitivity of streamflow data to the NF Republican streambed K is 0.01, and the relative sensitivity of the streambed K of remaining streams is nearly zero ($<1e^{-5}$).

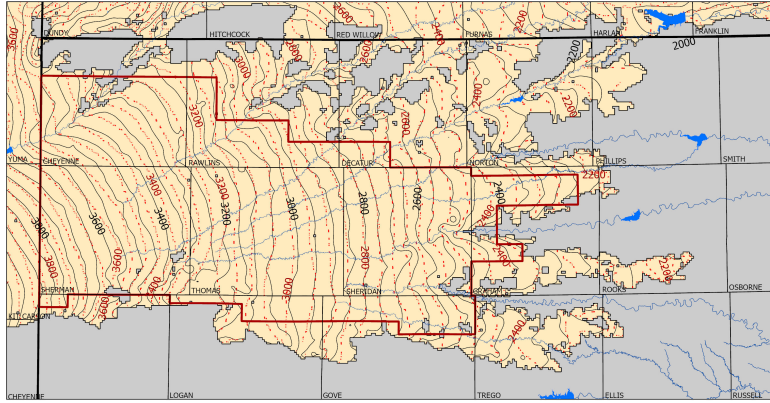
Transient Model Results

Water Levels

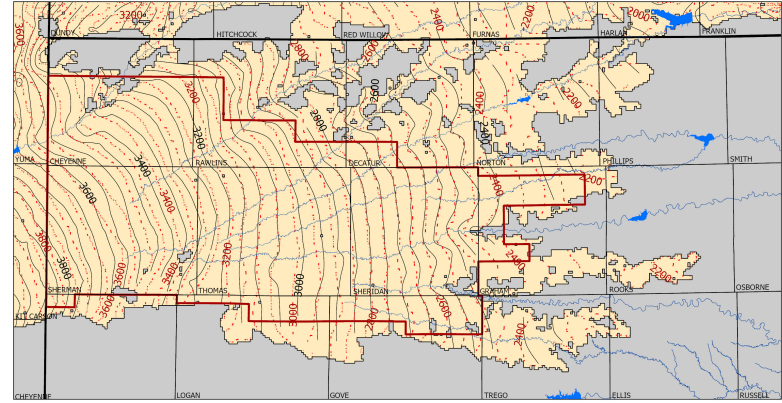
Figures 35 to 38 show a series of comparisons of the simulated groundwater elevations from the calibrated model to interpolated observed data for predevelopment, 1970, 1980, 1990, 2000, 2010, and 2020. The contour maps (top) are an indication of flow directions and water-level gradients, while the cell-based shaded maps (bottom) show absolute differences between the simulated and observed water levels. In all years, the majority of the GMD4 area has model-estimated water levels within 25 ft of observed values, although there are local mismatches in certain areas. This is especially true in Sherman County, where the model consistently underestimates water-table elevations along the western portions of the county, while it overestimates them in the eastern portions of the county (along with western Cheyenne County). Overall, through the core of the district, the simulated water levels agree favorably, relative to past KGS models, with the observed values throughout the transient period.

Figures 39 to 42 compare the model's simulated water-level changes between predevelopment and 1970, subsequent 10-year intervals up to 2020, and predevelopment to 2020 with interpolated observed changes for the same intervals. Similar to the water-table elevation maps, the overall agreement between the simulated and observed changes is good across the core area of GMD4 with some areas having local mismatches. The largest discrepancy tends to be found in southwestern Sherman County. The model does a favorable job simulating the static to slightly rising water levels seen in the thinner saturated portions of the HPA along the eastern and northern edges of GMD4.

Figure 43 plots monitoring well locations, labeled by the row and column of the model cell in which each well is located, that were used in the model calibration. The hydrographs for these wells are plotted in figs. 44 to 53 and show the water levels labeled by the internal ID number of the observation well and the simulated water levels of the cell, labeled by row and column, in which it is located. The transient model simulates water levels within 25 feet for most of the wells in the active areas. There are examples of wells, specifically in Cheyenne and Sherman counties, where the simulated values over- or underestimate the observed water levels; however, in most cases, they still mimic the trends. Water levels in and around the SD6 LEMA area are represented very well both in terms of absolute values and relative change.

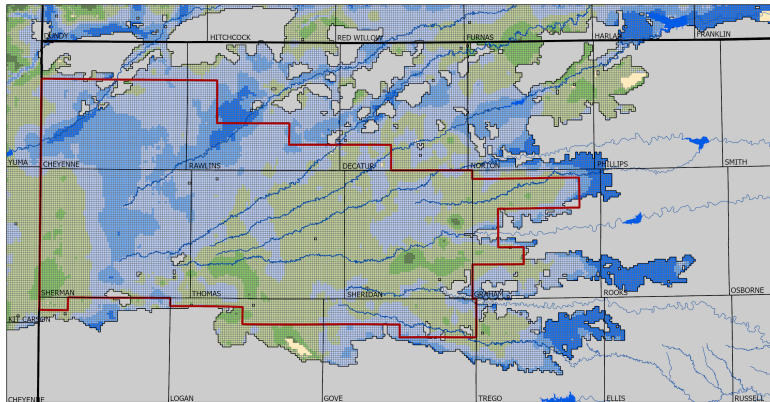


(a) Predevelopment

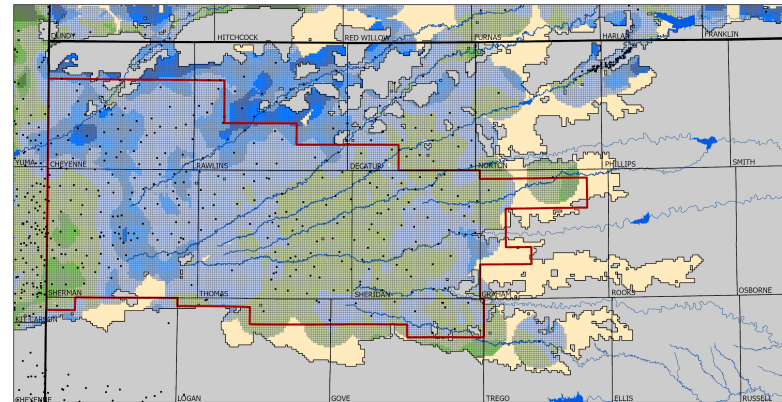


(c) 1970

 Observed
 Model Simulated



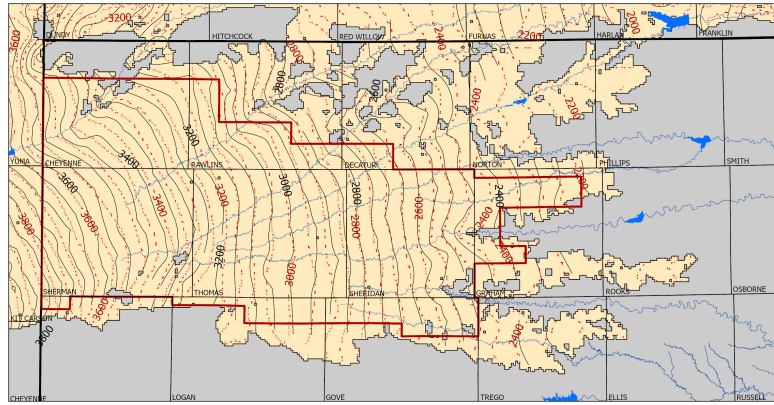
(b) Predevelopment



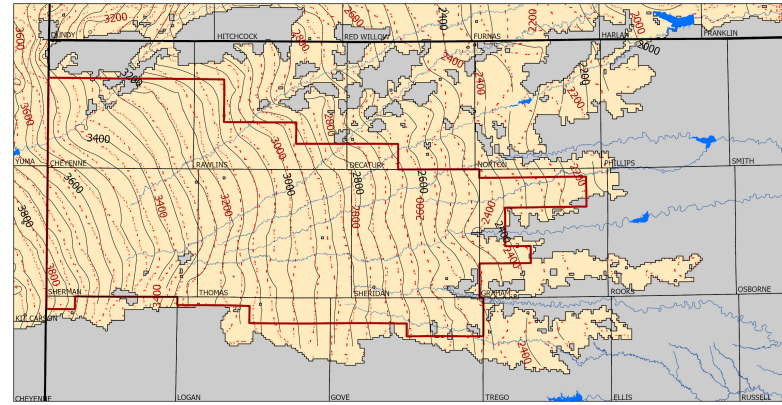
(d) 1970

 Underestimates \leq -50
 -25 to -50
 0 to -25
 0 to 25
 25 to 50
 Overestimates $>$ 50

Figure 35. Comparison of simulated versus observed water-table elevations, in feet, predevelopment and 1970.

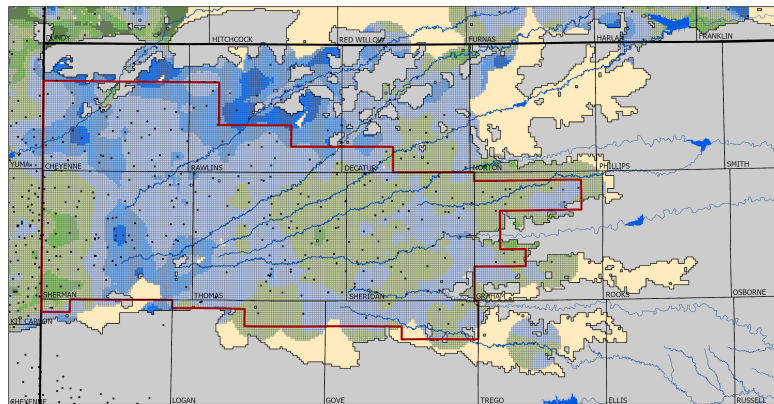


(a) 1980

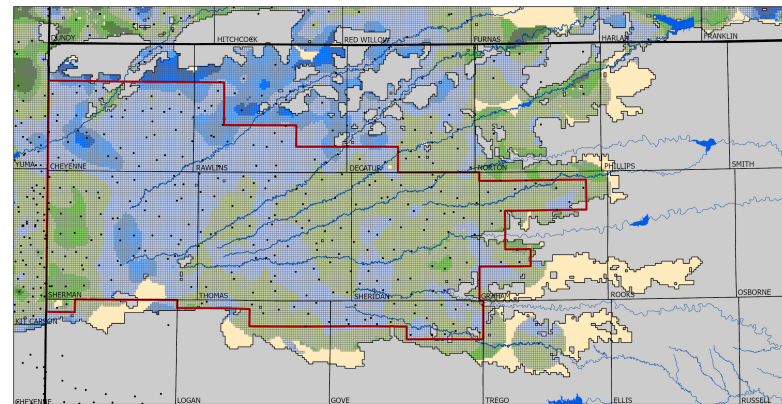


(c) 1990

Observed
Model Simulated



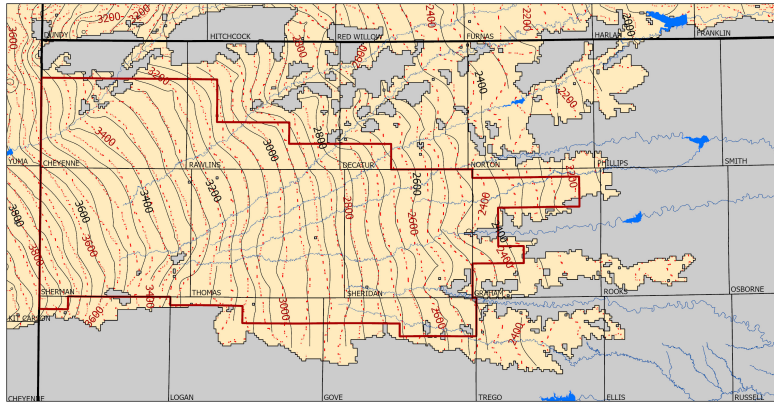
(b) 1980



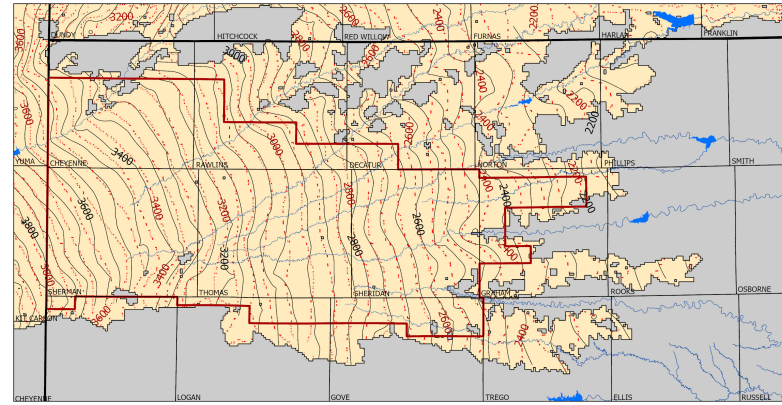
(d) 1990

Underestimates \leq -50
-25 to -50
0 to -25
0 to 25
25 to 50
Overestimates $>$ 50

Figure 36. Comparison of simulated versus observed water-table elevations, in feet, 1980 and 1990.

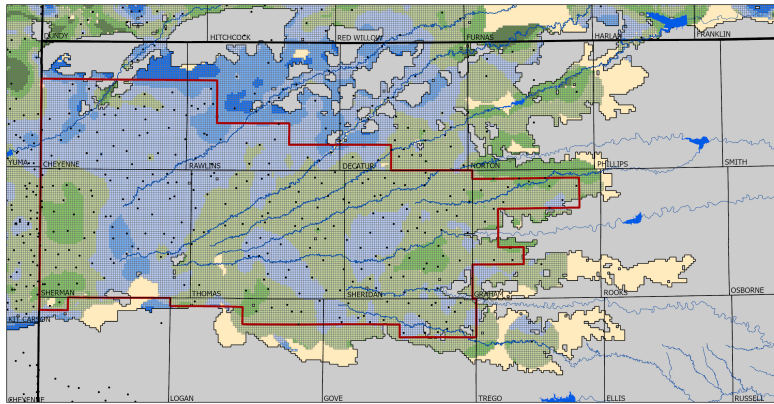


(a) 2000

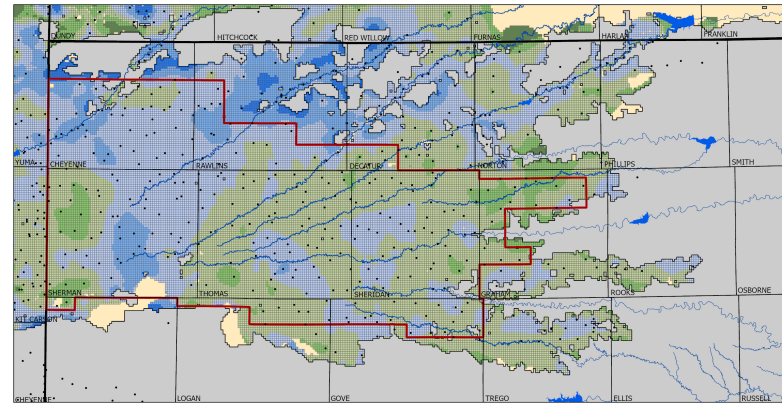


(c) 2010

Observed
 Model Simulated



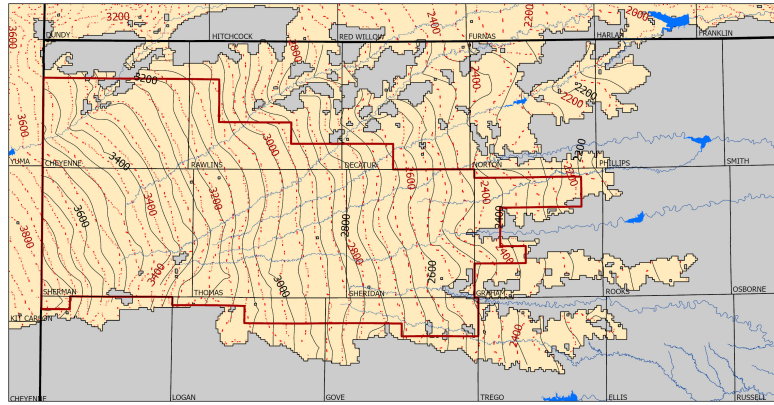
(b) 2000



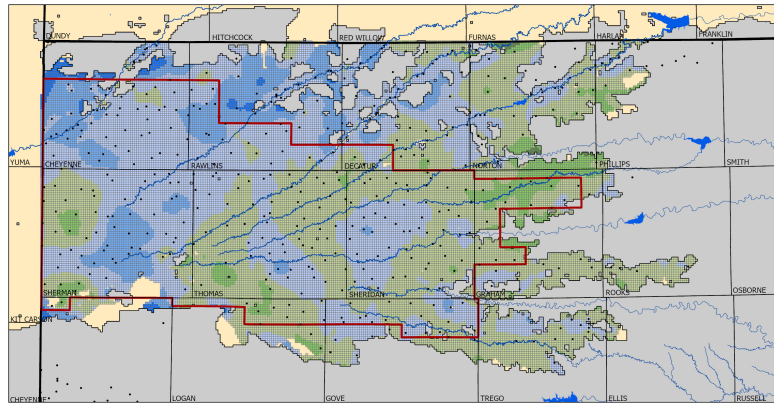
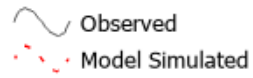
(d) 2010

Underestimates \leq -50
 -25 to -50
 0 to -25
 0 to 25
 25 to 50
 Overestimates $>$ 50

Figure 37. Comparison of simulated versus observed water-table elevations, in feet, 2000 and 2010.



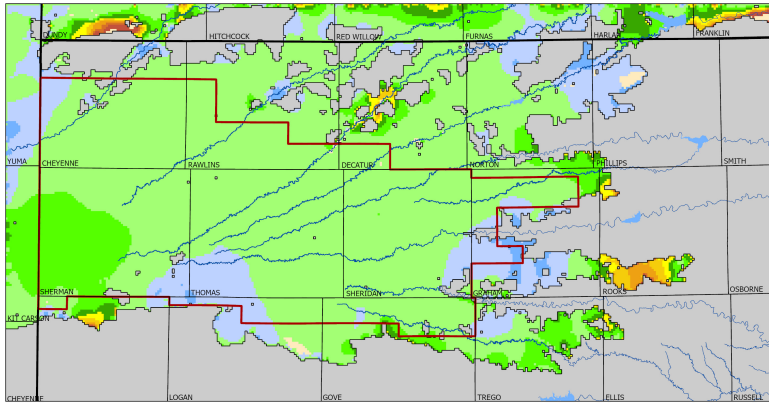
(a) 2020



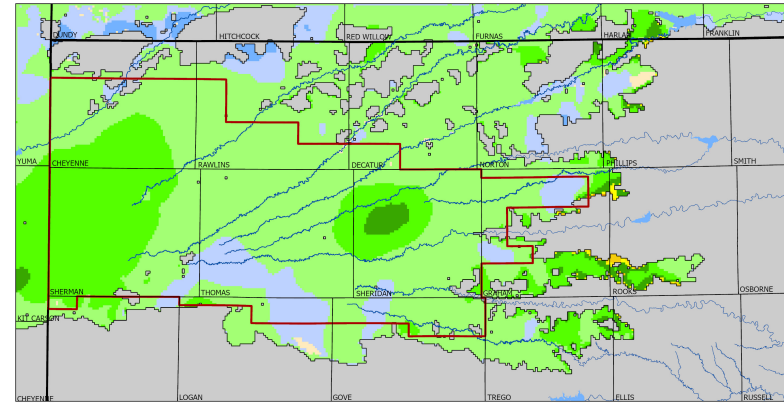
(b) 2020



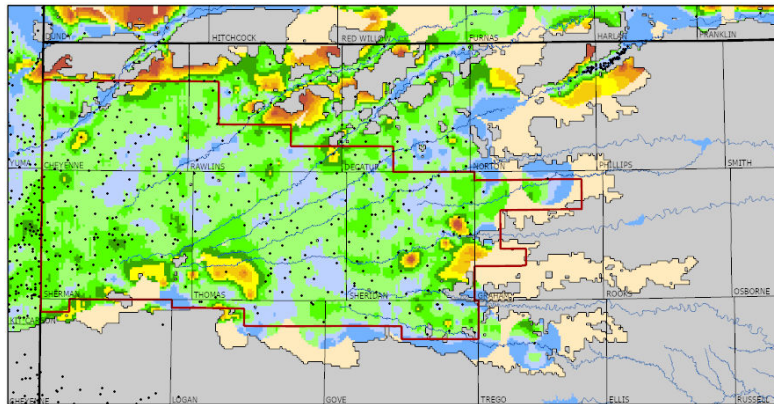
Figure 38. Comparison of simulated versus observed water-table elevations, in feet, 2020.



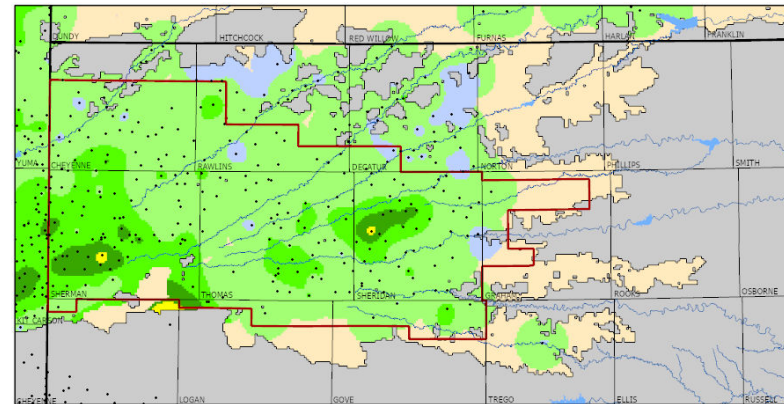
(a) Simulated predevelopment to 1970



(c) Simulated 1970 to 1980



(b) Observed predevelopment to 1970



(d) Observed 1970 to 1980

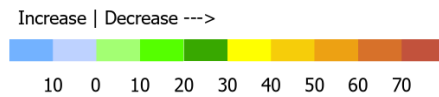
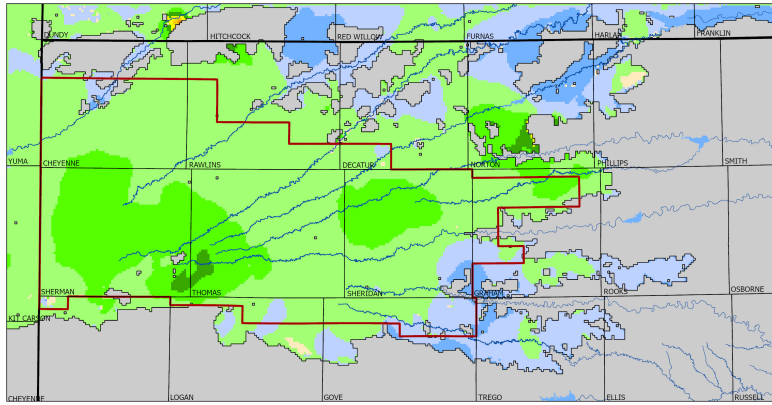
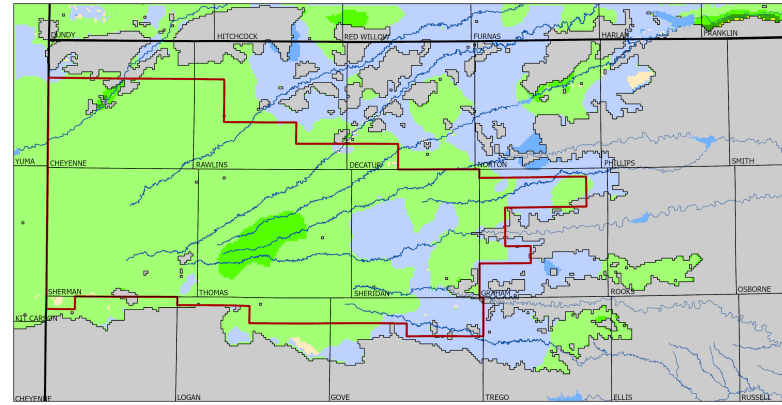


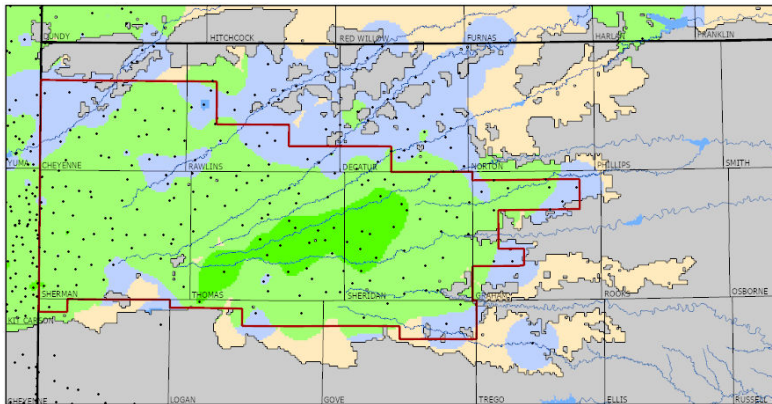
Figure 39. Simulated versus observed water-level changes, in feet, for the intervals predevelopment to 1970 and 1970 to 1980.



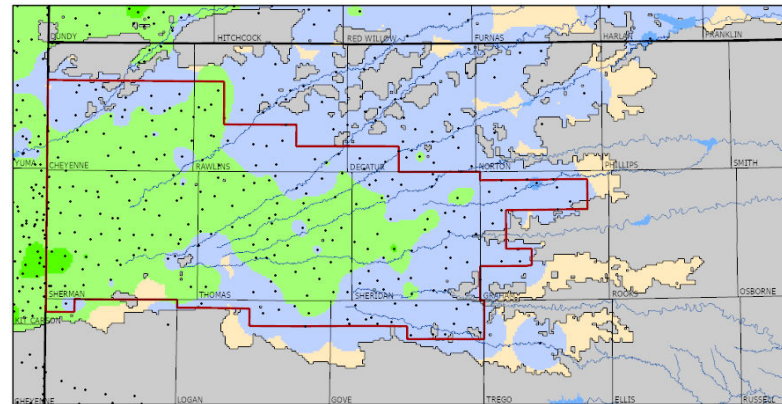
(a) Simulated 1980 to 1990



(c) Simulated 1990 to 2000



(b) Observed 1980 to 1990



(d) Observed 1990 to 2000

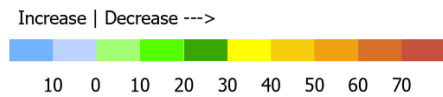
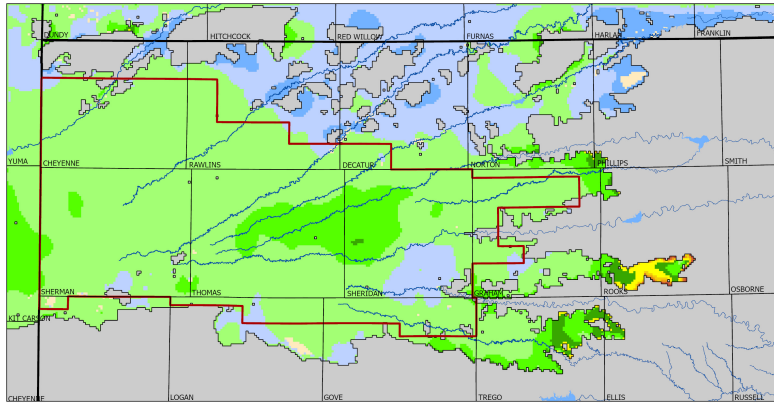
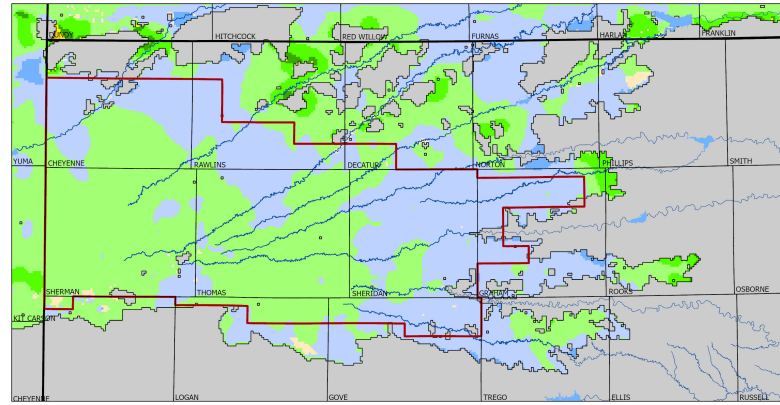


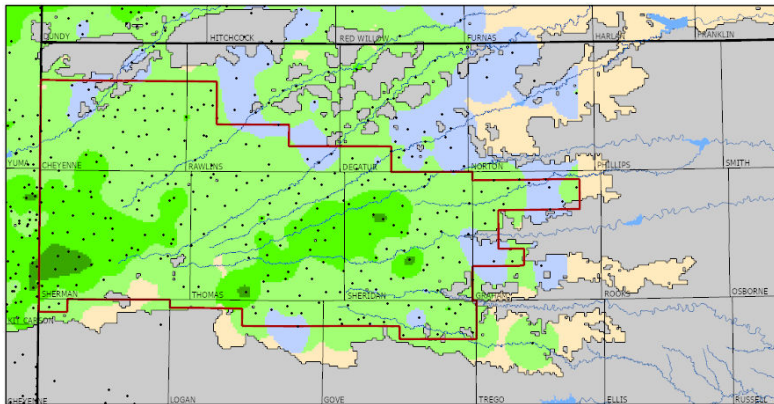
Figure 40. Simulated versus observed water-level changes, in feet, for the intervals 1980 to 1990 and 1990 to 2000.



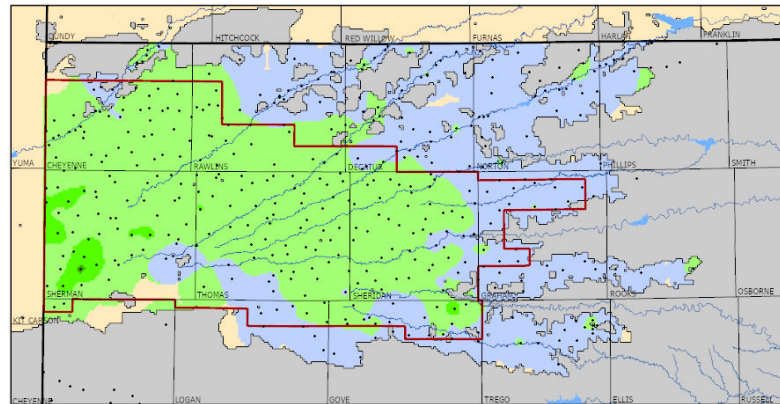
(a) Simulated 2000 to 2010



(c) Simulated 2010 to 2020



(b) Observed 2000 to 2010



(d) Observed 2010 to 2020

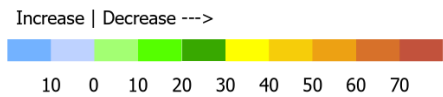
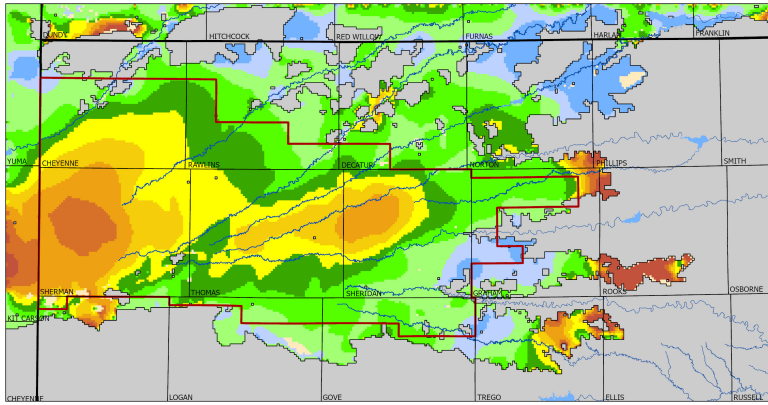
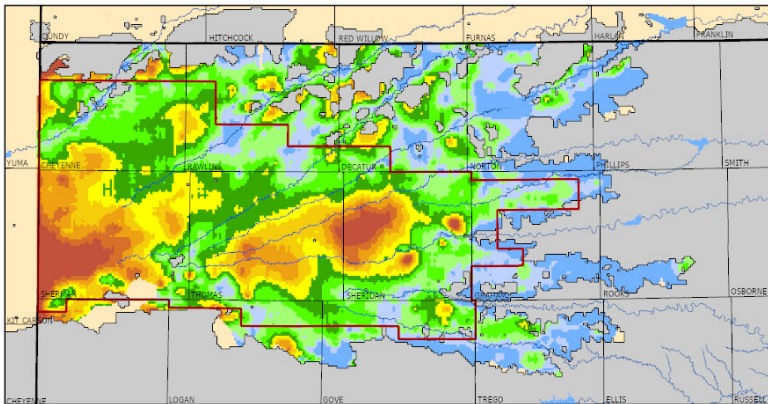


Figure 41. Simulated versus observed water-level changes, in feet, for the intervals 2000 to 2010 and 2010 to 2020.



(a) Simulated predevelopment to 2020



(b) Observed predevelopment to 2020

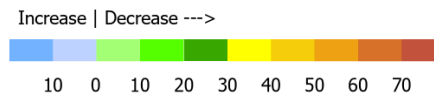


Figure 42. Simulated versus observed water-level changes, in feet, for the interval predevelopment to 2020.

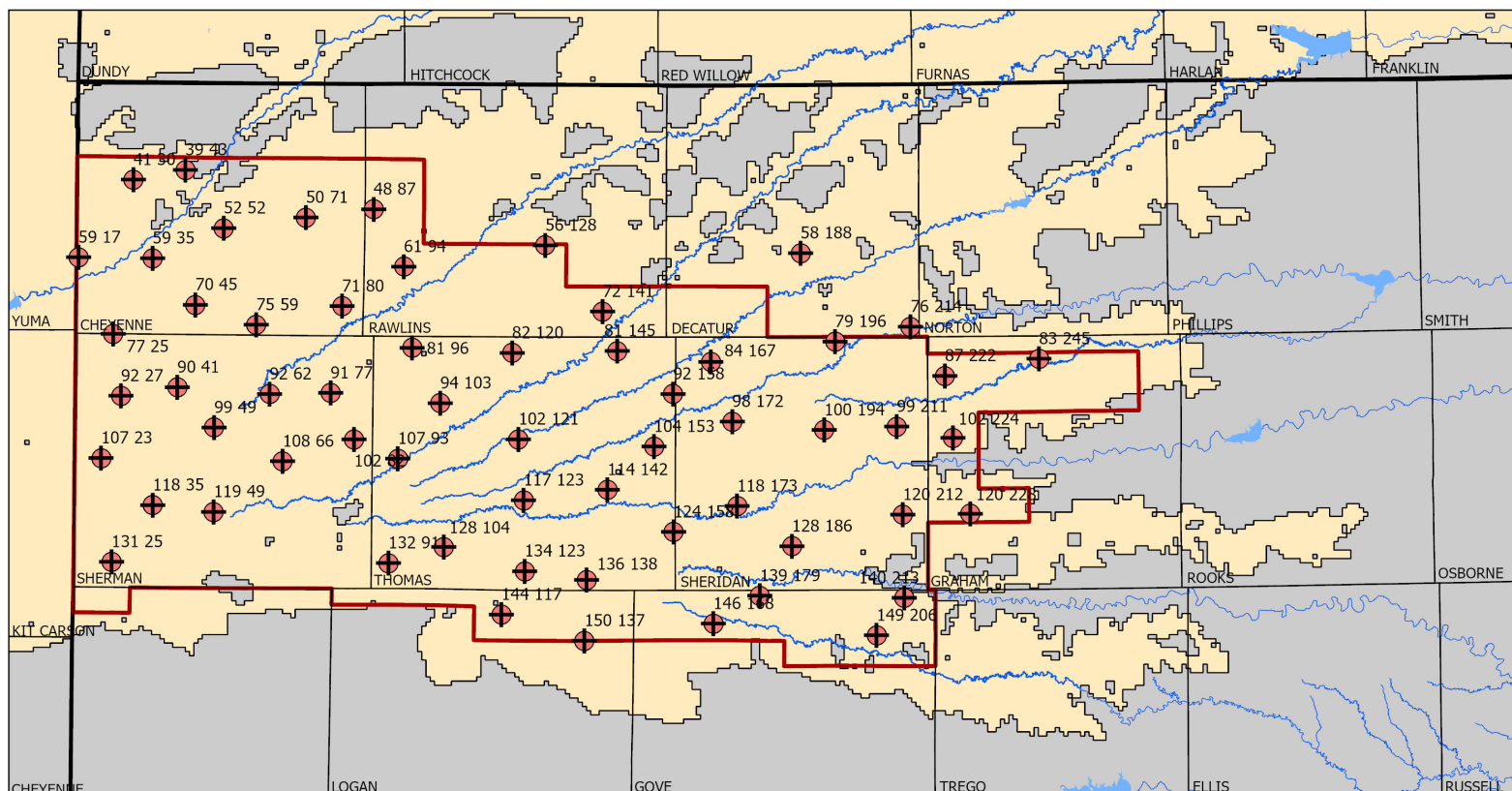


Figure 43. Wells with long-term measurement records used for model calibration, labeled by row and column of the model cell in which each well is located.

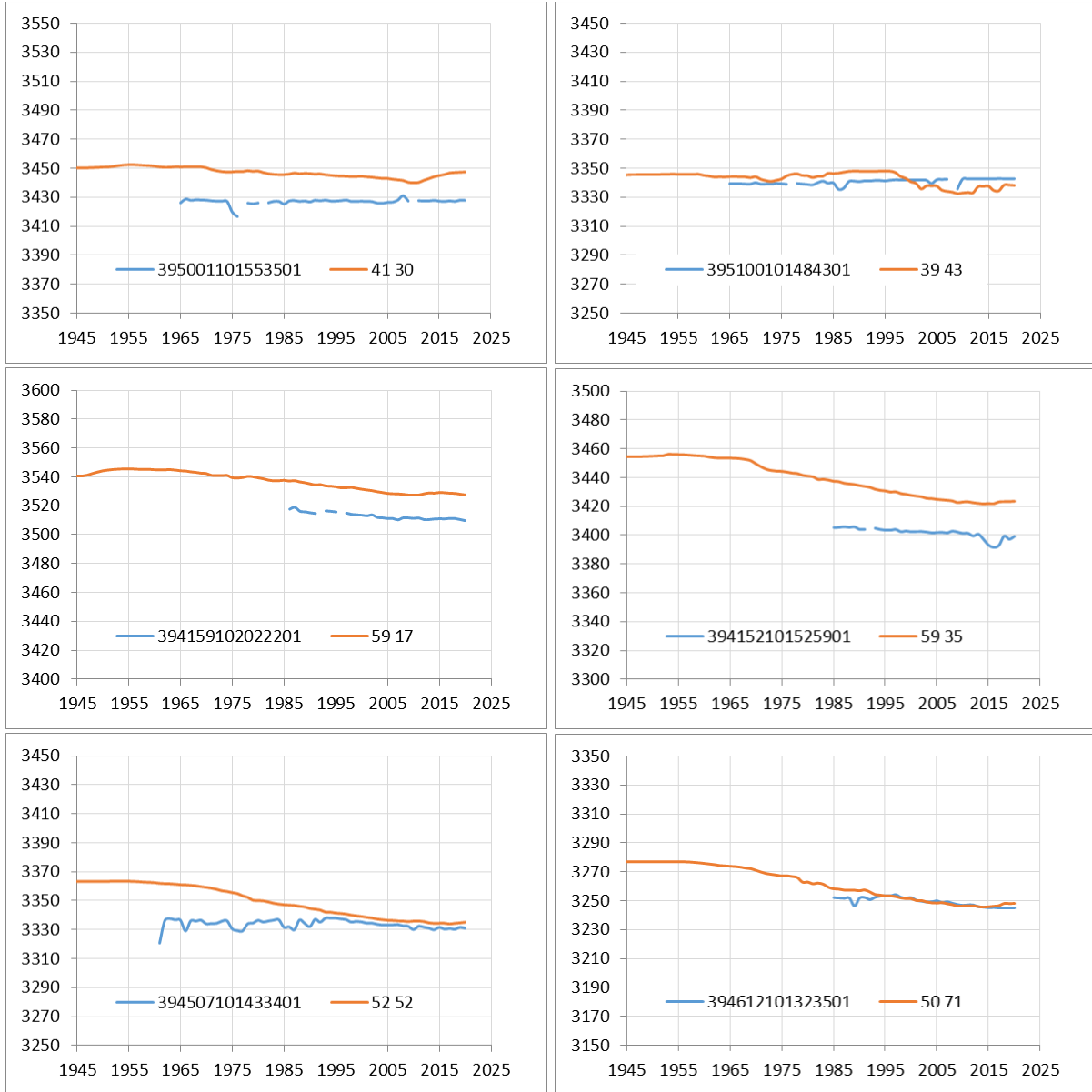


Figure 44. Simulated (orange line) versus observed (blue line) well hydrographs, northern Cheyenne County.

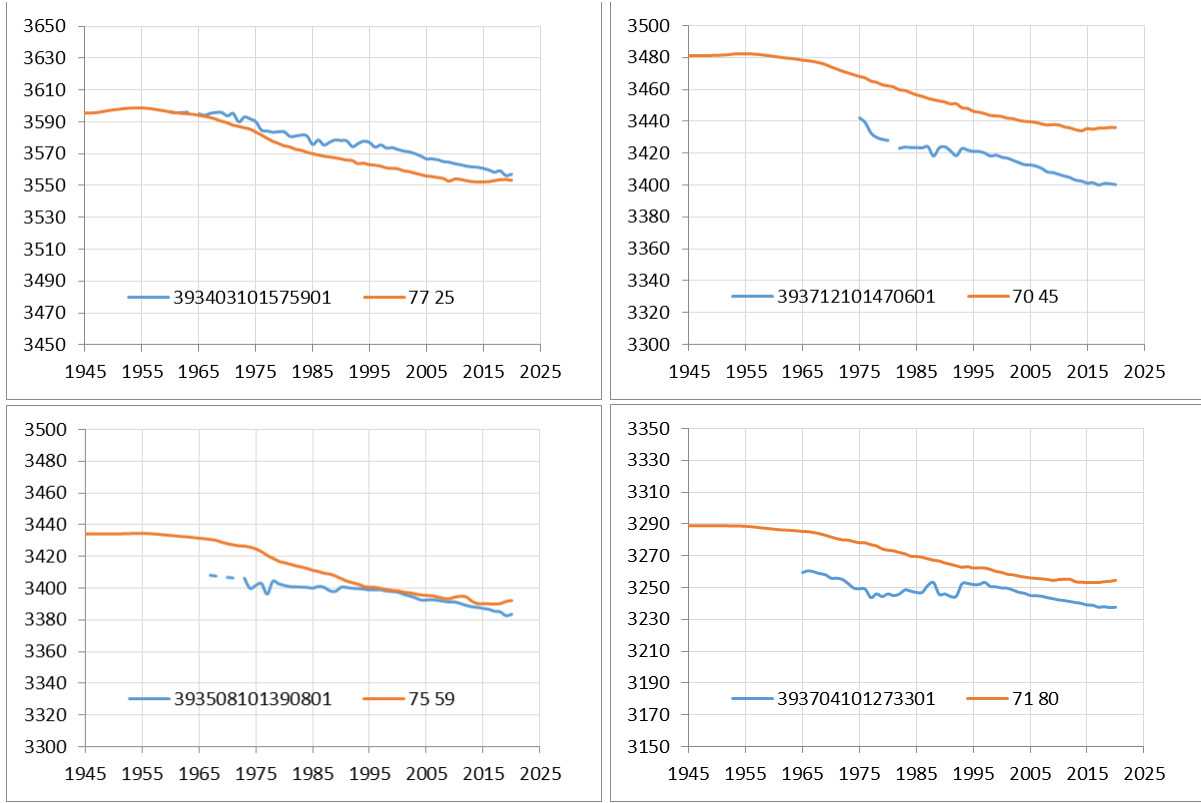


Figure 45. Simulated (orange line) versus observed (blue line) well hydrographs, southern Cheyenne County.

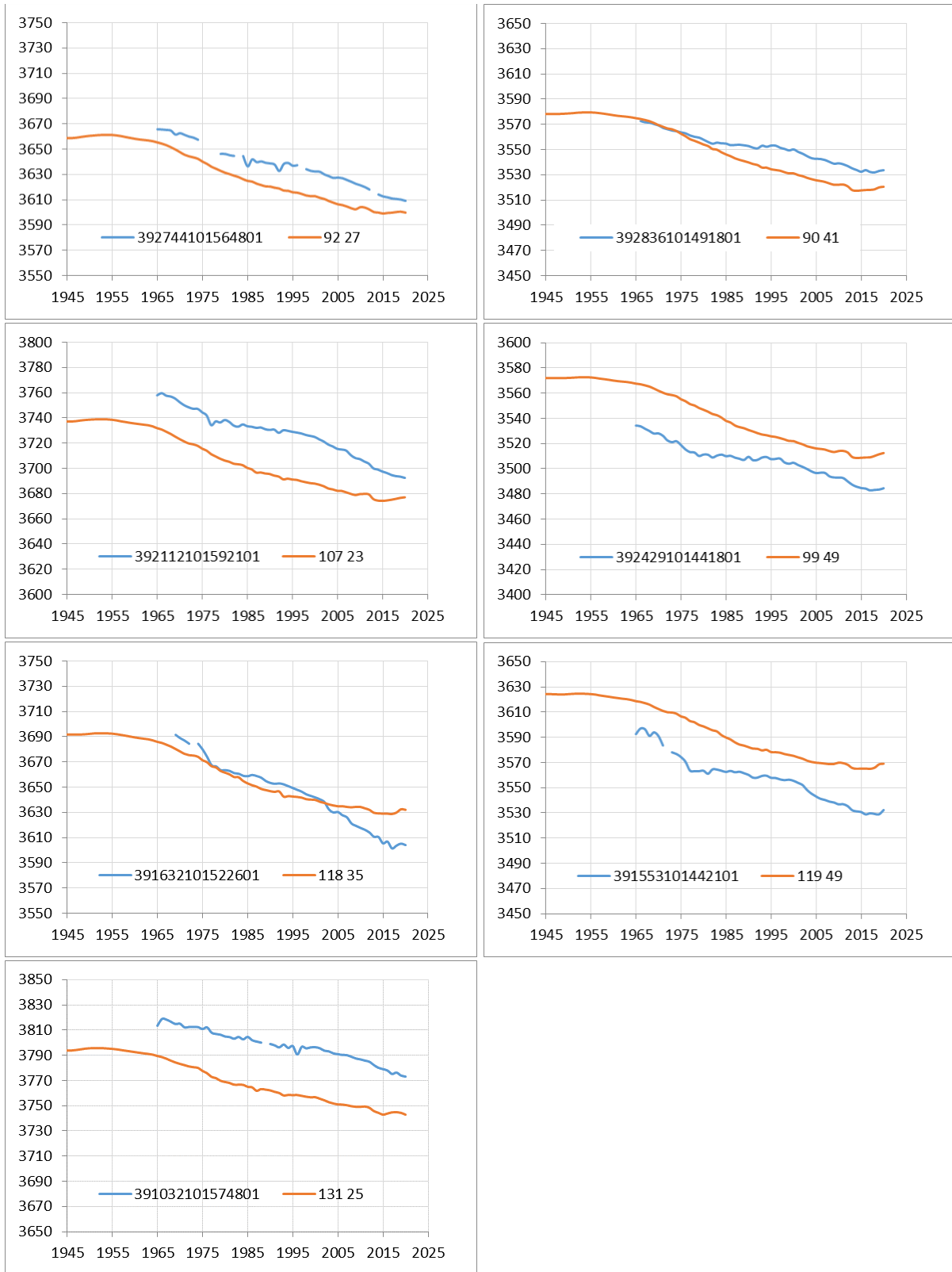


Figure 46. Simulated (orange line) versus observed (blue line) well hydrographs, western Sherman County.

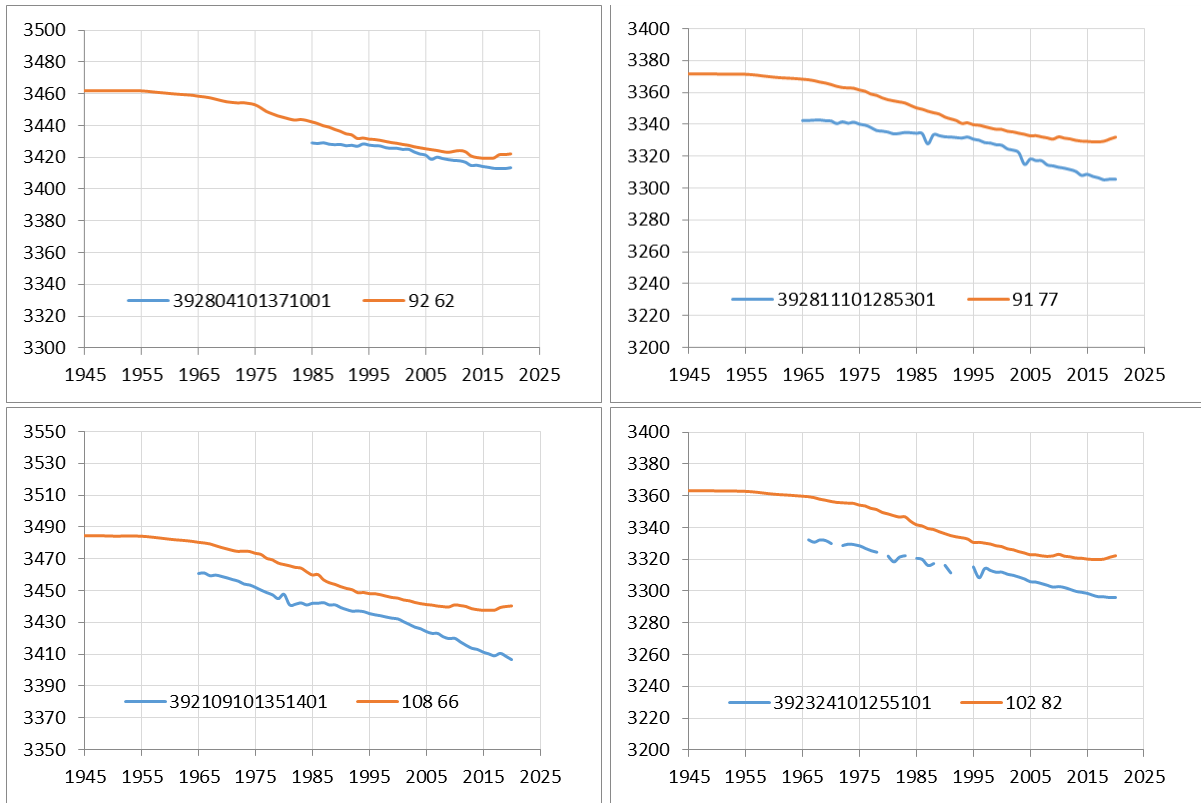


Figure 47. Simulated (orange line) versus observed (blue line) well hydrographs, northeast Sherman County.

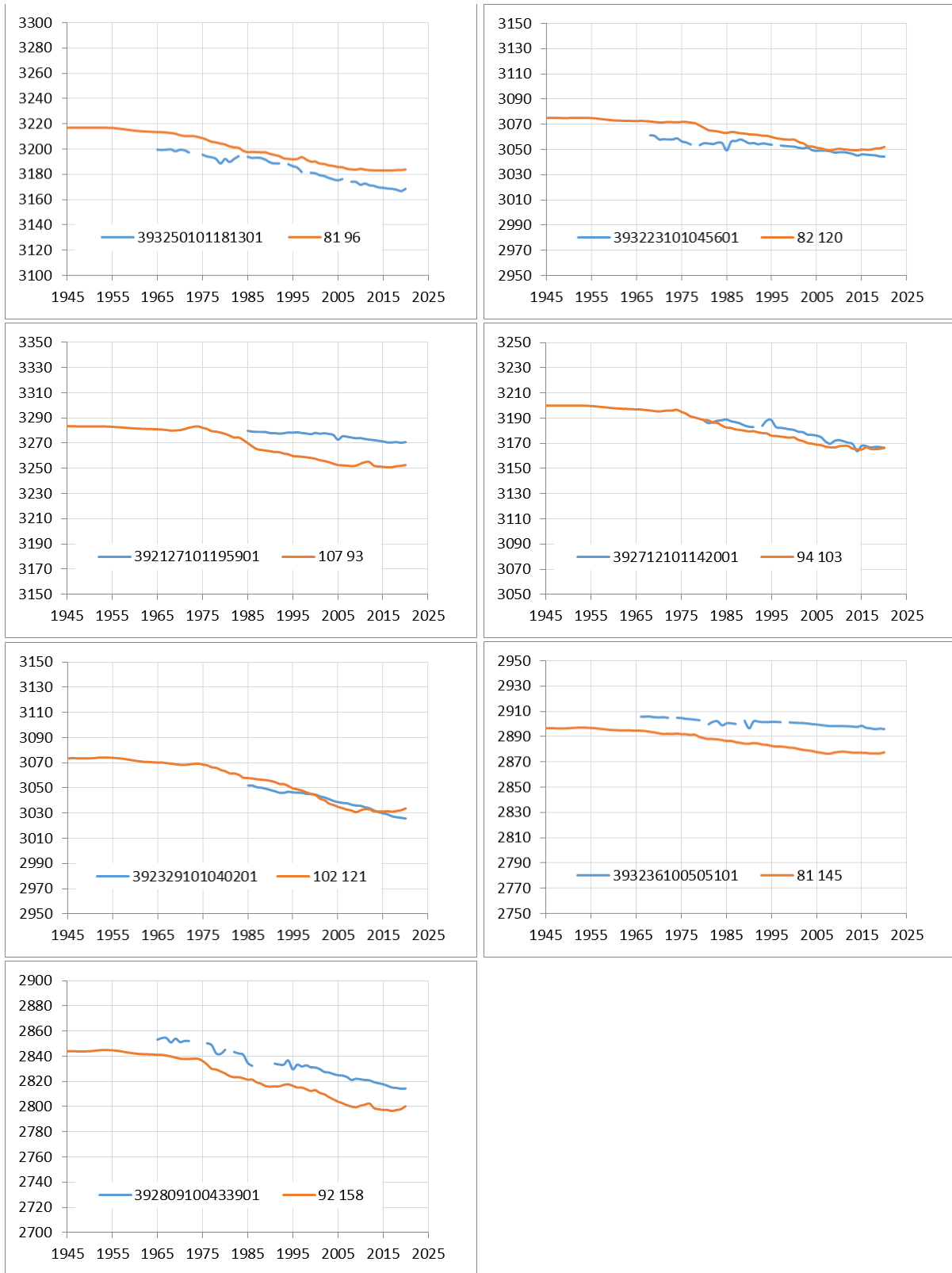


Figure 48. Simulated (orange line) versus observed (blue line) well hydrographs, northern Thomas County.



Figure 49. Simulated (orange line) versus observed (blue line) well hydrographs, southern Thomas County.

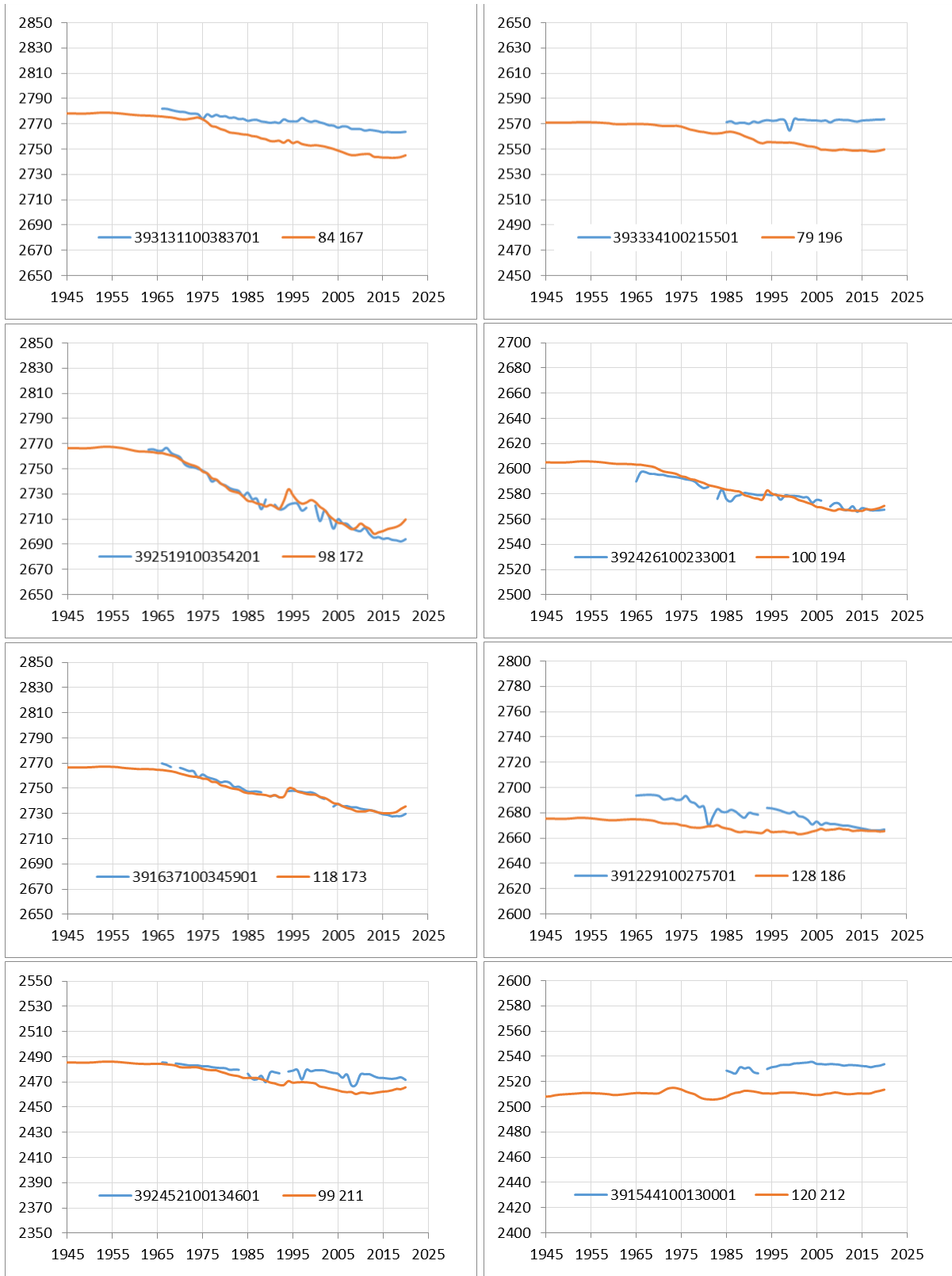


Figure 50. Simulated (orange line) versus observed (blue line) well hydrographs, Sheridan County.

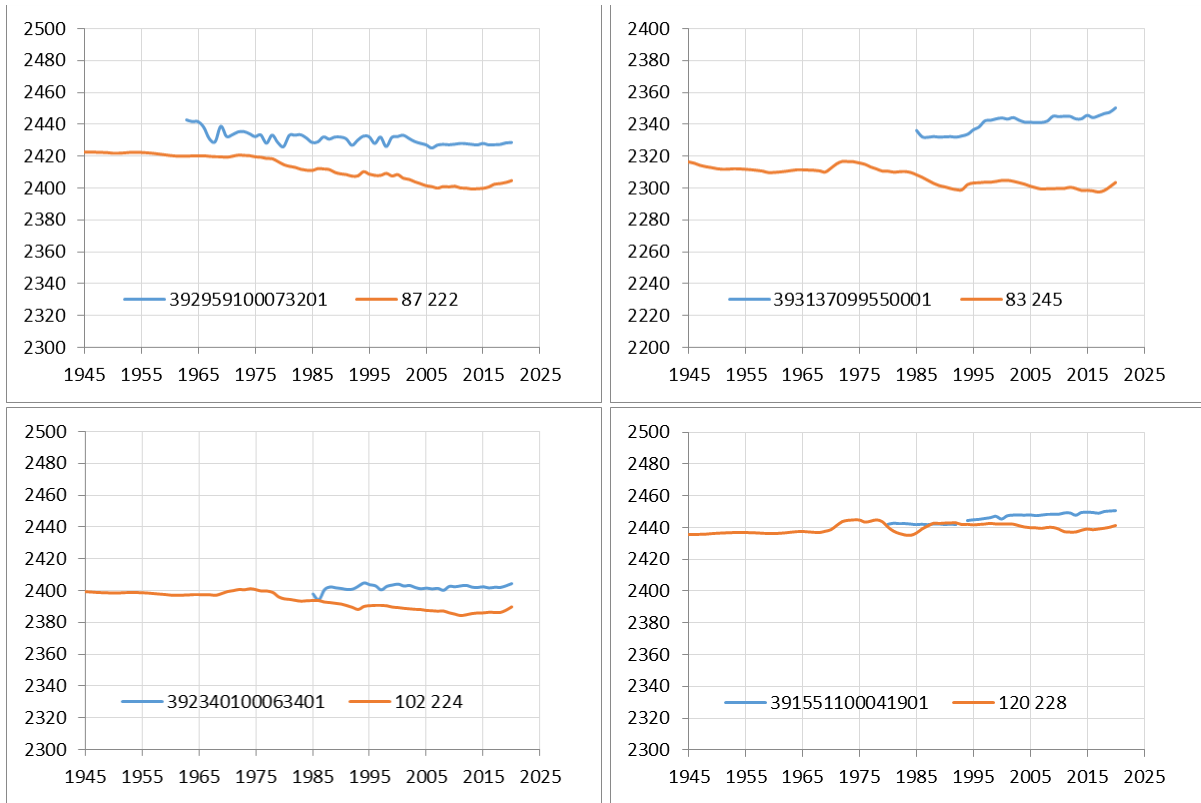


Figure 51. Simulated (orange line) versus observed (blue line) well hydrographs, Graham County.

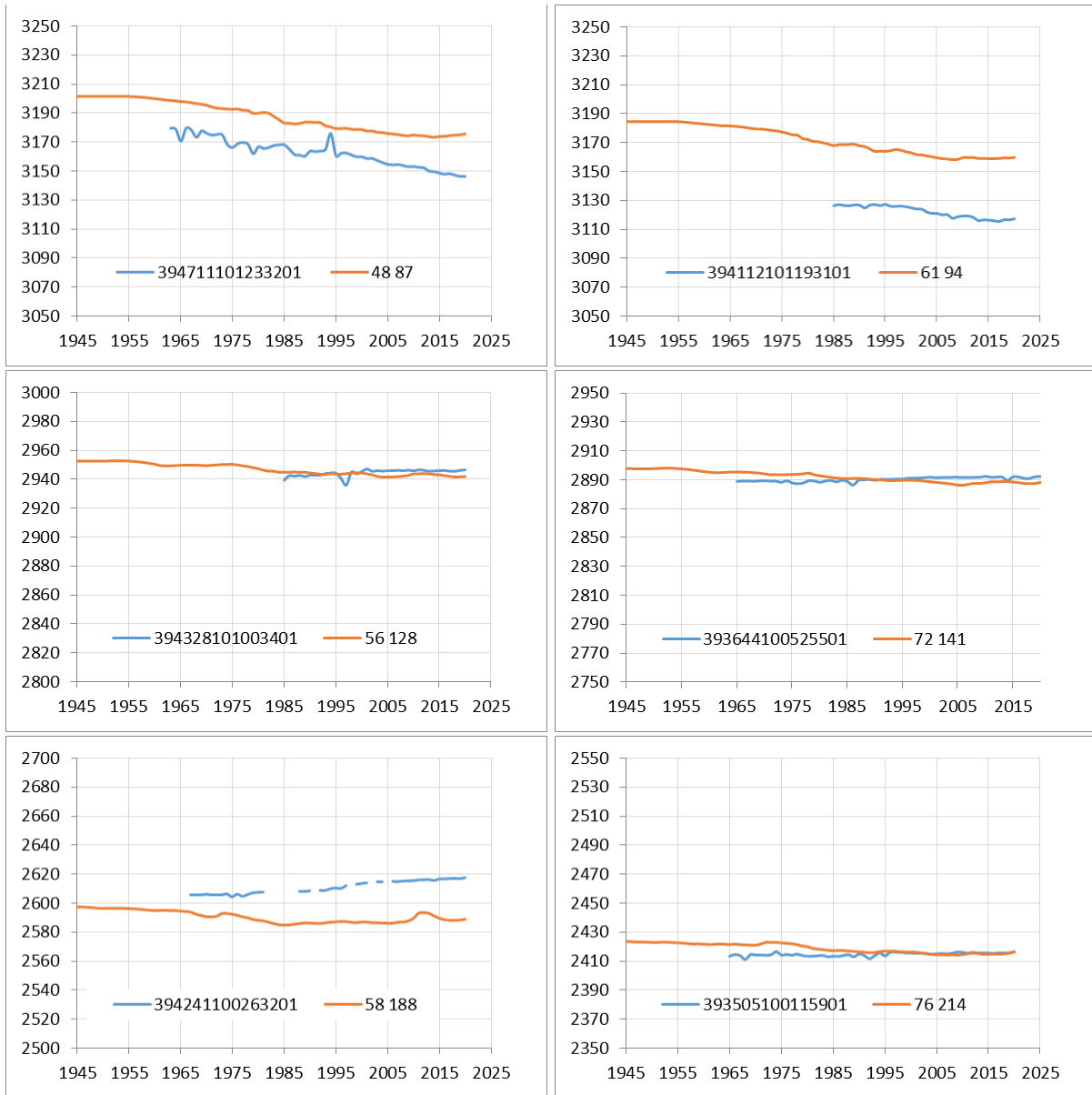


Figure 52. Simulated (orange line) versus observed (blue line) well hydrographs, Rawlins and Decatur counties.

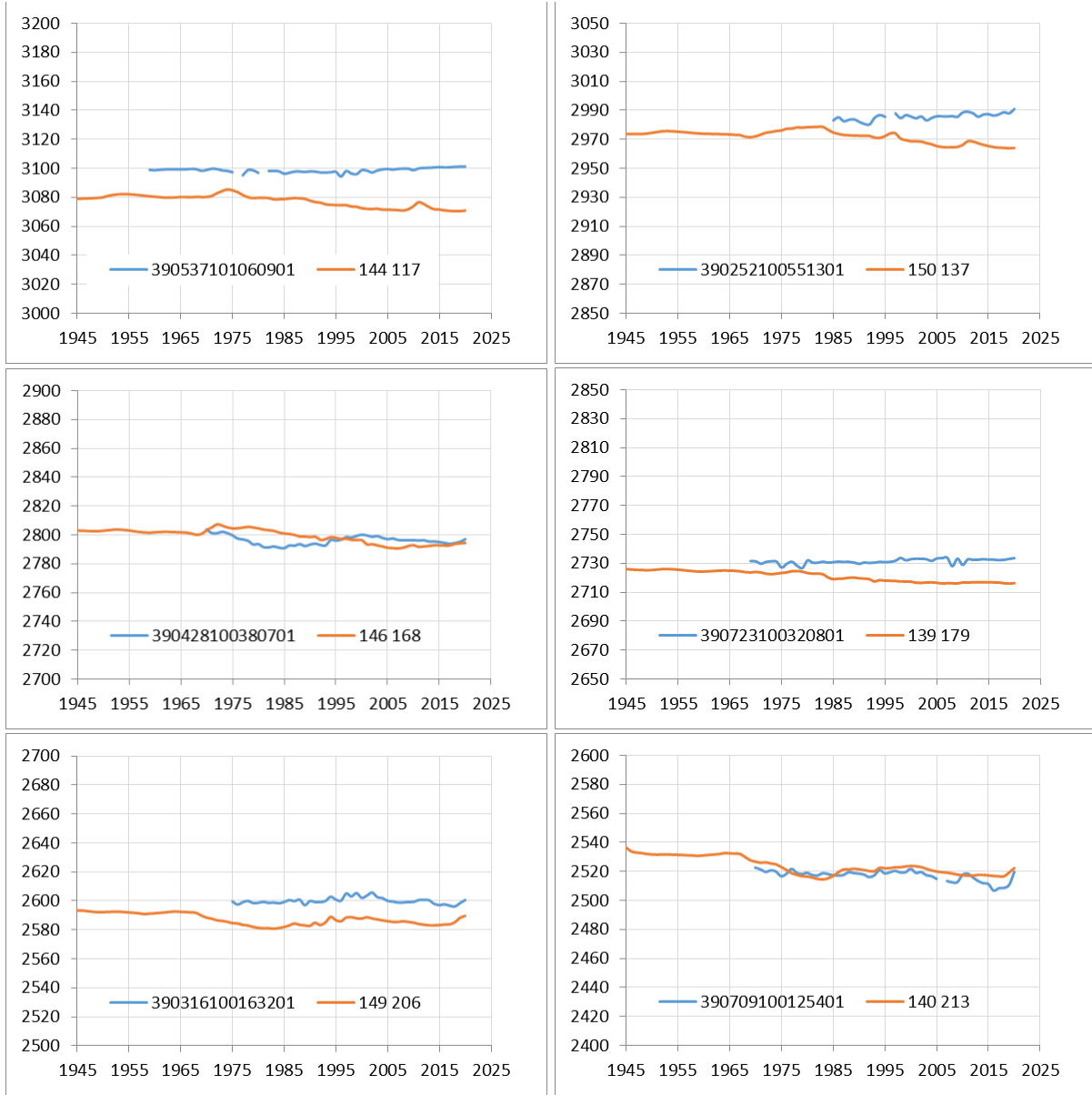


Figure 53. Simulated (orange line) versus observed (blue line) well hydrographs, Logan and Gove counties.

Model Budgets

Figure 54 shows the simulated groundwater budget for GMD4 over the transient period, including the net storage change, lateral flow across the GMD4 boundaries (lateral X and Y), well pumping, evapotranspiration (ET) loss, total areal recharge, drain cell loss, and stream leakage. Positive values indicate inflows of water to the aquifer system and negative values reflect outflows from the aquifer.

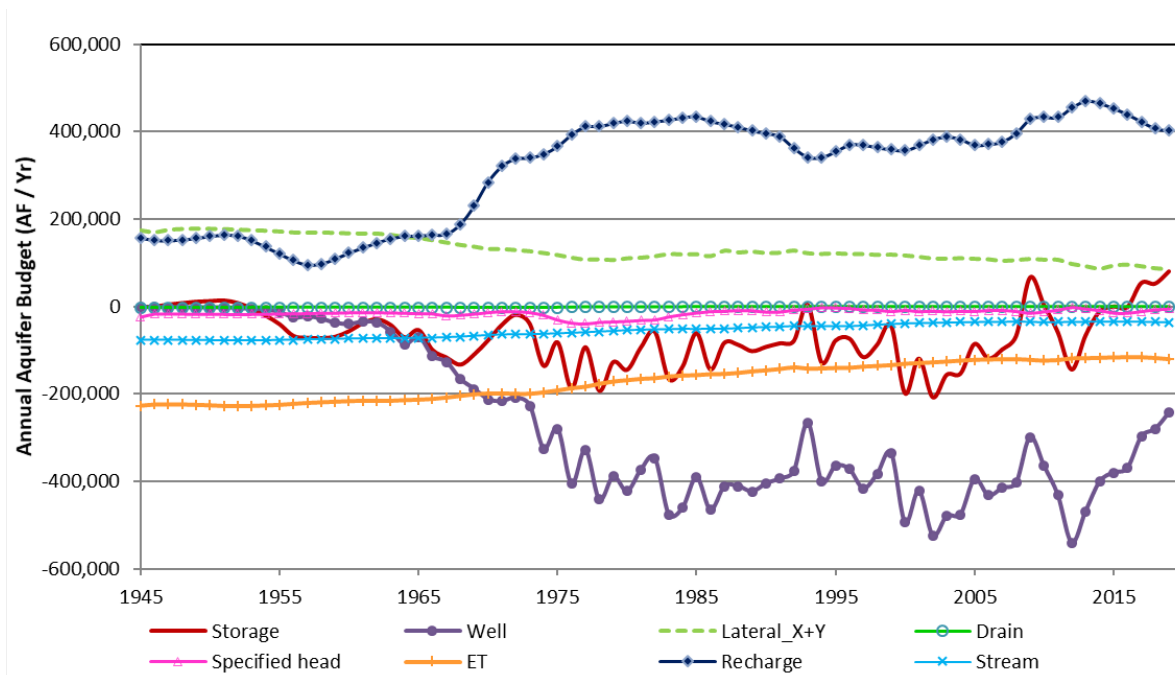


Figure 54. Annual aquifer budget for GMD4 from the calibrated model.

The largest inflows to the aquifer come from recharge, which represents the sum of all precipitation-based recharge, irrigation return flows, and lagged storage releases from low-permeability units, and the net lateral gradient inflow, which is the difference between gradient flows coming into GMD4 minus gradient outflows. Lateral flow of groundwater in and out of GMD4 decreases with time. The largest volume of lateral flow enters the district from Colorado. Water flows laterally following a general southwest-to-northeast gradient and exits the district through the northern and eastern district boundaries. The contributions of both the specified heads and drains to the district budget are small as most of those cells are located outside the district boundary.

Groundwater pumping (identified as “Well” in fig. 54) represents the largest outflow from the aquifer. Annual groundwater usage has been relatively constant since the 1980s, although there has been a shift to slightly less water usage in recent years. The amount of water loss from the aquifer to ET decreases during the transient period in response to water levels that have been declining over time (when water level is below the extinction depth, groundwater ET loss directly to plants and the atmosphere is no longer possible).

Aquifer storage changed over time as a result of the difference between groundwater inflows and outflows (fig. 54). Prior to the 1950s, groundwater pumping was insignificant, and the aquifer was in a relatively steady state with near zero storage change (stable water level for the district as a whole). Then the 1950s drought produced a noticeable decrease in precipitation recharge, which led to some storage loss despite groundwater pumping remaining small until the 1960s. After the 1960s, pumping significantly increased and caused continuous aquifer storage decline in most years except 1993, 2009, and years after 2014.

In our previous water-balance analysis for GMD4 (Bohling et al., 2021), the net inflow calculated from 1996 to 2017 water-level change and water-use data was 332,393 AF. To check for consistency between the calibrated model and water-balance analysis, simulated net inflow can be calculated as **storage change – pumping** in fig. 54. The average net inflow from the calibrated model between 1996 and 2017 is 337,508 AF, which is only 1.5% higher than the average value determined from the water-balance analysis.

Figure 55 plots the various recharge components originating from the land surface. Precipitation recharge is generated by the precipitation-recharge curves described earlier in this report and represents the amount of new water entering the aquifer system from both the upland areas of the aquifer and the higher rates of recharge for stream channels. Precipitation recharge averages 0.56 inches per year over the transient period. Recharge from irrigation return flows represents the amount of pumped irrigation water that infiltrates past the root zone of the irrigated crops, eventually reaching the water table. As the number of water rights and pumping volumes increase during the 1960s and 1970s, so does the amount of return flows. As water usage declines and irrigation systems become more and more efficient, the amount of return flow declines. Over the transient period, irrigation return flow averages 0.14 inches per year.

The final component is the amount of water coming from enhanced precipitation-based recharge occurring over irrigated fields. Compared to the precipitation recharge, the irrigation-enhanced precipitation recharge is relatively small because 1) irrigation enhancement to precipitation recharge only occurs during the growing season while precipitation recharge is calculated for both the growing and non-growing seasons and 2) the acreage of irrigated lands is much smaller than the active model area (fig. 25). Therefore, although irrigation doubles the precipitation recharge in the irrigated fields during the growing season, the amount of irrigation-enhanced precipitation recharge is small when compared to the overall precipitation recharge over the entire active model area.

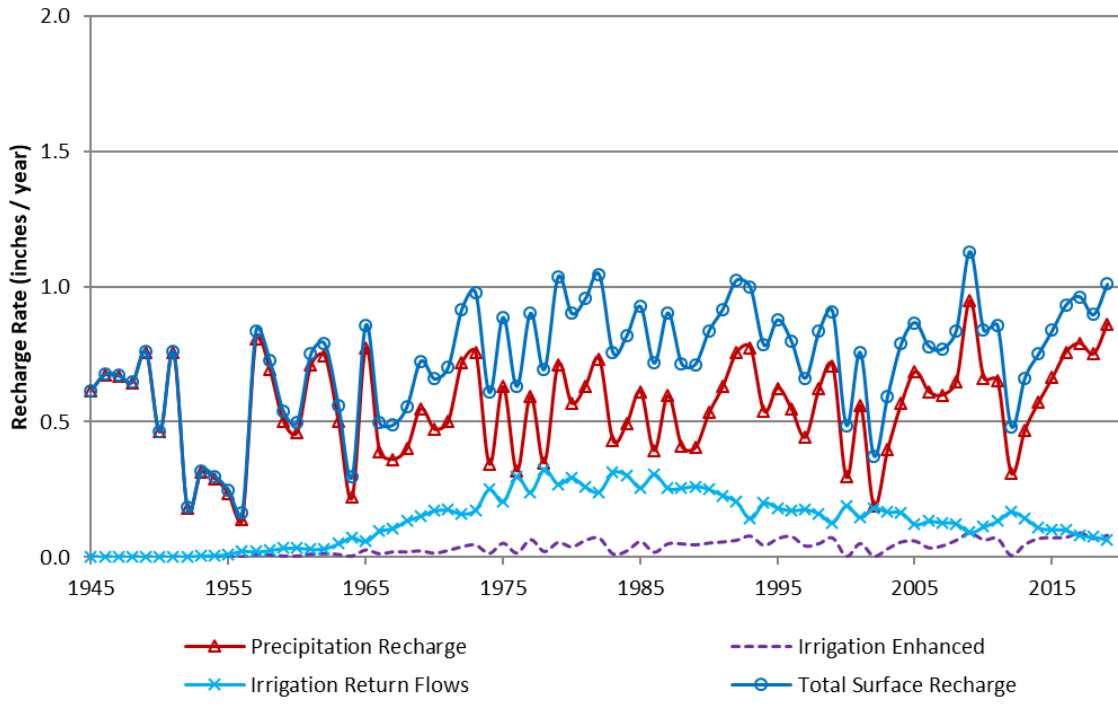


Figure 55. Recharge components originating from the land surface.

Each of the land-surface recharge components is subject to the model's delay function, and the total amount of water in each time step is tracked. Figure 56 illustrates the total amount of water derived from surface recharge that actually reaches the ever-changing water table. Compared to surface recharge, which is directly driven by precipitation and fluctuates significantly from year to year, the delayed recharge at the water table is smoother as the delay in the vadose zone has removed much of the annual fluctuation. Prior to the 1970s, delayed recharge from the surface was primarily controlled by precipitation recharge. During the 1970s and 1980s, it increased as irrigation return flows increased. Between the 1980s and 1990s, the delayed recharge from the surface remained stable, as the decline in irrigation return flows appeared to be offset by the increase in precipitation recharge. The relatively drier conditions during the late 1990s and early 2000s caused a decrease in surface recharge. Since the early 2000s, the delayed recharge from the surface has shown an overall increase in response to general increases in precipitation.

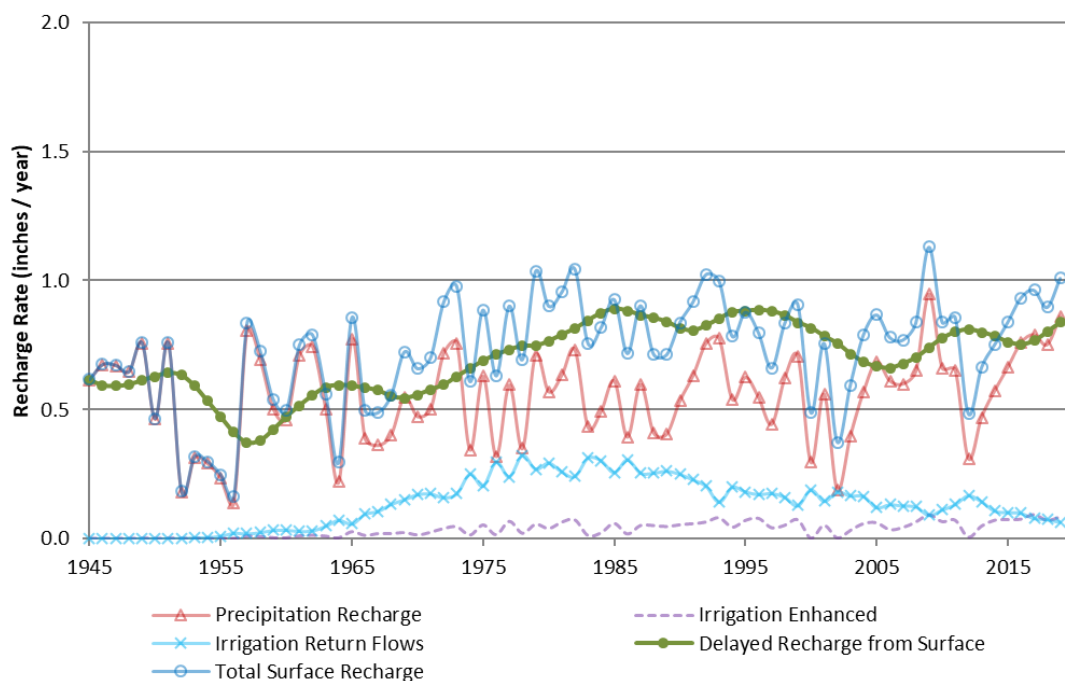


Figure 56. Total delayed recharge reaching the water table from the surface.

Figure 57 plots the amount of lagged drainage of water released from partially dewatered sediments. The total recharge to the water table is the sum of the lagged storage release and the delayed recharge from the surface. Given that lagged drainage occurs only when the water table declines, it does not start until the mid-1960s. Beginning in 1970, the amount of water released from the dewatered sediments averages 0.77 inches a year, which is equivalent to the total delayed recharge coming from the surface. The total inflows from all sources since 1980 average 1.57 inches a year, which is in line with computed net inflows from the data-driven water-balance methods (Butler et al., 2016, 2018).

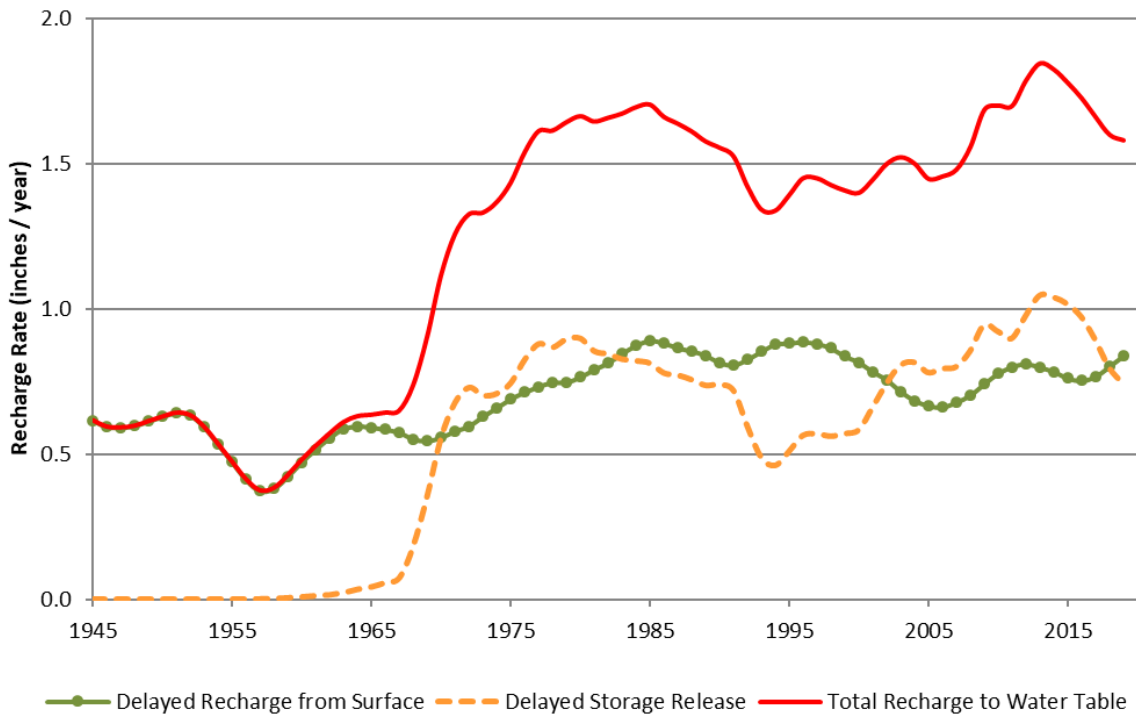


Figure 57. Lagged storage release and the total amount of recharge to the water table.

Figure 58 plots the cumulative change in the model’s groundwater budget. Aquifer storage is calculated for each model step based on the simulated water levels and specific yield values for the different HyDRA lithology groups. The computed total predevelopment aquifer storage within GMD4 is estimated to be 19.8 million acre-ft. The net effect of the model components produces an estimated 68,000 acre-ft average annual loss of storage. The simulated cumulative storage loss in 2020 is 29% of the predevelopment value.

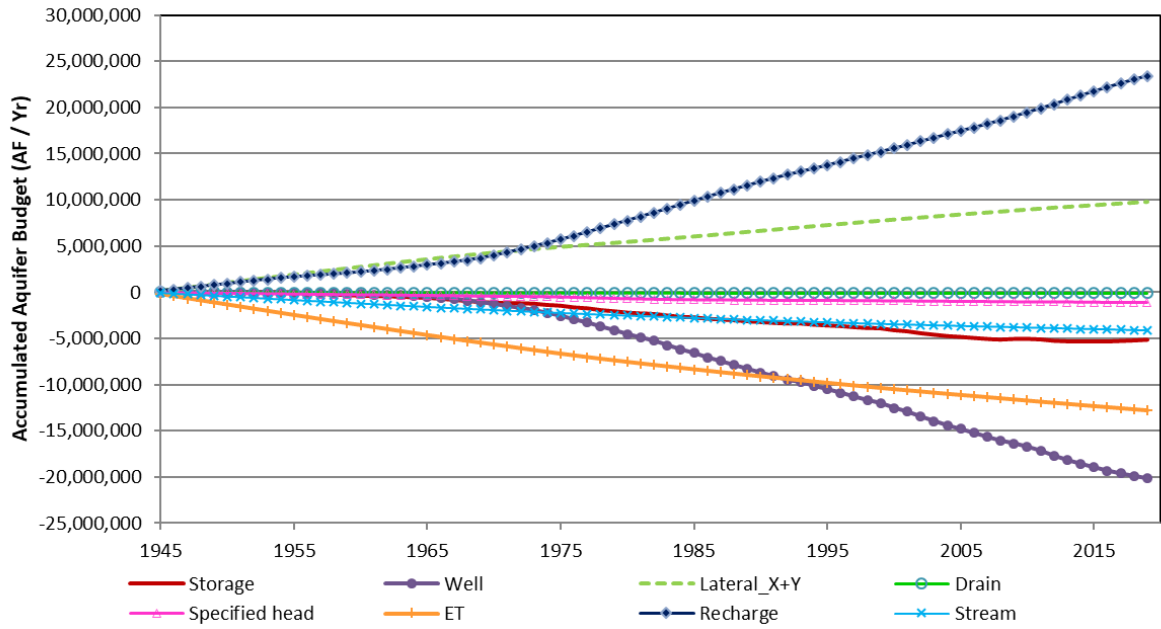


Figure 58. Accumulated groundwater budget, GMD4.

MODEL SCENARIOS

One of the valuable uses of a calibrated groundwater model is to assess the future responses of an aquifer to different water resources management and climatic scenarios. Four basic scenarios were considered in this study:

- 1) Status quo or no change in water-use policy.
- 2) 20% reduction in pumping.
- 3) 30% reduction in pumping.
- 4) GMD4 districtwide LEMA plan.

In all scenarios, the calibrated model is run from 2020 to 2093 with a repeat of the 1946 to 2019 climatic conditions. The irrigation system types are assumed to be the same as for 2019. For the specified head boundaries, the average water-level change over the last 10 years is used to project future water levels on these boundaries until a minimum saturated thickness of 10 ft is reached.

The first scenario assumes there is no change in the water-use policy with future pumping driven by current (2020) water rights. In the second and third scenario, pumping is reduced across the model to simulate the goal of the SD6 LEMA (20% reduction) and a comparison value more representative of what has actually been achieved (30% reduction). The final scenario explores the impact of a districtwide LEMA.

No Change in Future Water-Use Policy

This scenario uses the regression equation determined in the transient model calibration to compute the ratio of water use/authorized quantity, assuming there is no change in future water-use policy. For a given future year, the ratio, which is dependent on summer precipitation, is converted into the actual water-use demand by multiplying it by the present day (2020) authorized quantity. Pumping is not further adjusted based on conditions specified under the SD-6 or GMD4 districtwide LEMAs.

Figure 59 shows the annual aquifer budget for GMD4 based on the no change in future water-use policy scenario. Groundwater pumping, primarily for irrigation, continues to be the most significant outflow component of the aquifer budget. The total recharge, including both the delayed surface recharge (i.e., the water that has moved from surface recharge down to the water table) and lagged drainage release (fig. 57), is not sufficient to balance pumping. As a result, the HPA continues to lose water out of storage (annual storage budget is negative in most years). Water loss from computed ET and baseflow contributions to streams both decline in the future simulated period. Lateral flow across the district boundary switches from an inflow to an aquifer outflow component in 2060. This is because as the water level declines, the lateral inflow from Colorado declines at a faster rate than the lateral outflow through the northeast edge. However, the net lateral cross-boundary flow becomes very small as compared to either pumping or recharge. Overall, future pumping remains relatively constant during the simulation until roughly 2060, when it begins a gradual decrease as the percentage of area with total aquifer storage depletion increases and pumping in those model cells is turned off.

Figure 60 shows the contributions of the water-table recharge from delayed surface recharge and lagged drainage from partially dewatered sediments after water-table decline. Delayed recharge from the land surface shows a significant drop during the 2030s, which is due to the simulated drought during the 1950s. After the drought, the delayed recharge shows a gradual increase as the overall precipitation increases with time. Note that as the irrigation system efficiency improves in recent years, the amount of irrigation return flow is reduced. As a result of the drought-induced increase in pumping and return flows during the 2020s along with the fixed irrigation system efficiency, the delayed recharge from surface after 2030 is relatively stable but lower than that between 1980 and 2030.

The contributions from dewatered units are primarily a function of water-level decline. The repeat of the 1950s drought causes some increase in pumping, and the water level declines at a more significant rate during this time interval. Figure 60 shows that the contributions from dewatered units increase between 2020 and the late 2030s before showing a declining trend toward the end of the simulation (2094). The continuous decline of lagged drainage from dewatered units after the late 2030s is likely a result of both reduced water-level declines and more areas becoming depleted. The total average inflows (delayed recharge from surface plus lagged drainage from dewatered units) for the entire future scenario are projected to be 1.5 inches per year.

Figure 61 shows different surface recharge components. Consistent with the estimates in future pumping, irrigation return flows and enhanced recharge from irrigated field boundaries remain relatively stable. Precipitation-based recharge, the largest source of inflow from the land surface, shows an abrupt drop during the repeat of the 1950s drought followed by a gradual increase toward the end of the simulation.

Figure 62 shows the simulated head changes for selected time intervals for the no change in future water-use policy scenario. Most of the district will continue to see a certain amount of water-level decline with the largest occurring in Sherman County followed by Sheridan and Thomas counties. The average water-level change across GMD4 over the next 10 (2020 to 2030) and 20 (2020 to 2040) years is projected to be -3.87 ft and -9.03 feet, respectively.

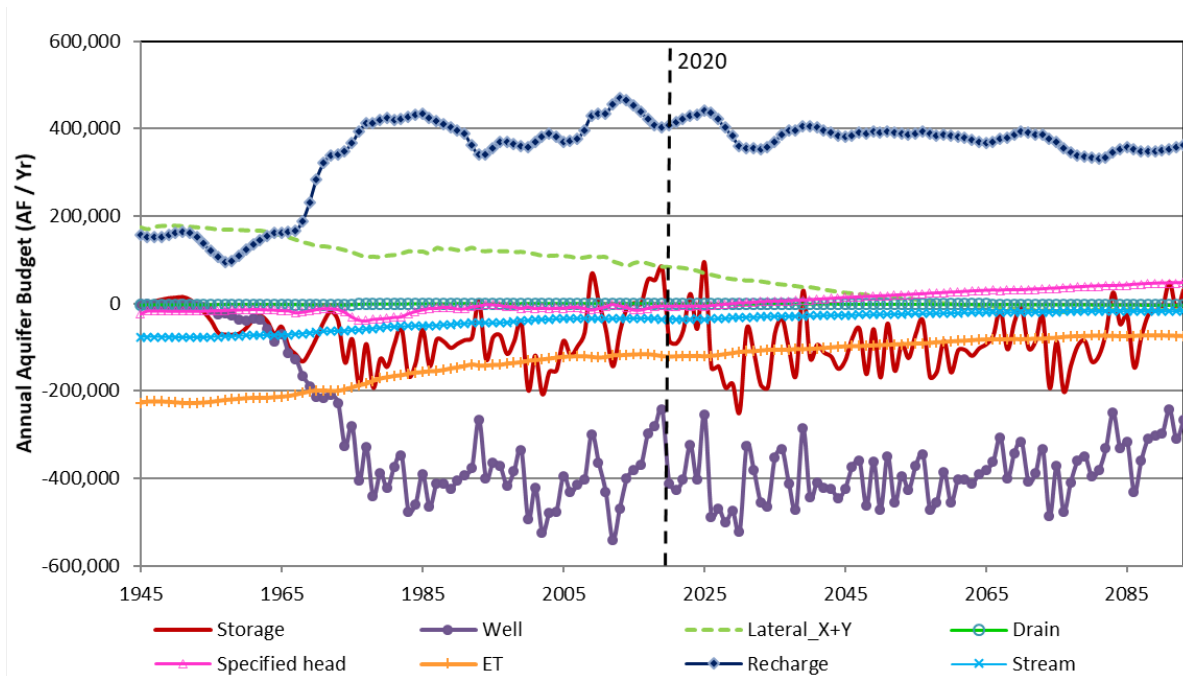


Figure 59. Annual aquifer budget for GMD4 under the no change in future water-use policy scenario. The calibrated model budget (predevelopment to 2019) is also plotted for comparison.

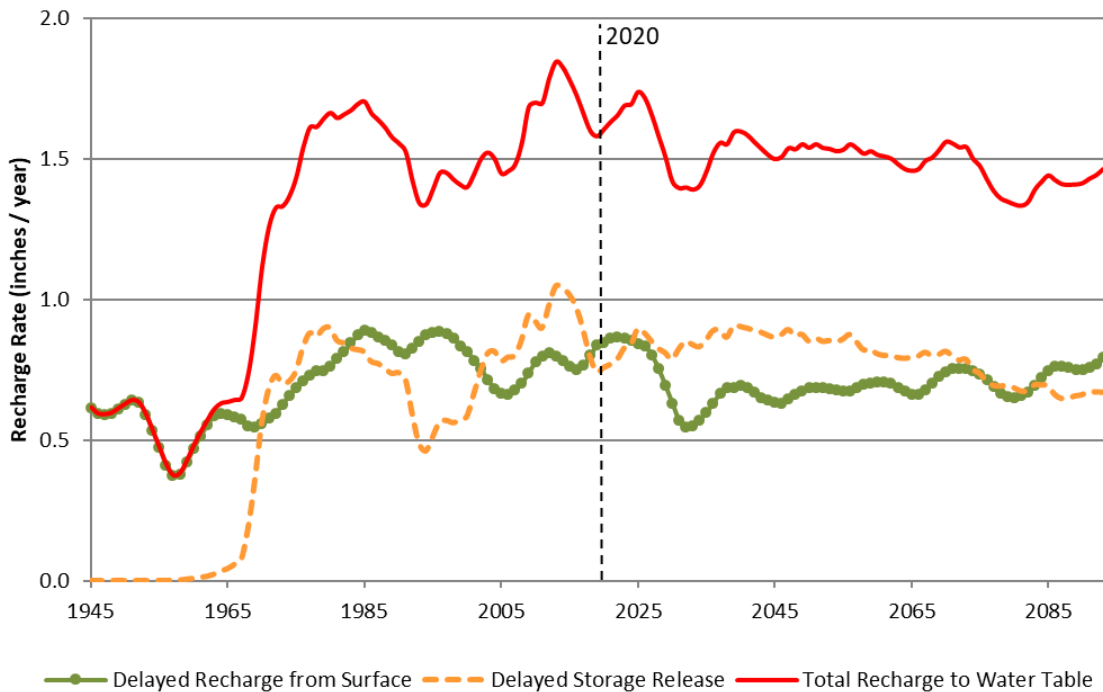


Figure 60. Water-table recharge in GMD4 under the no change in future water-use policy scenario.

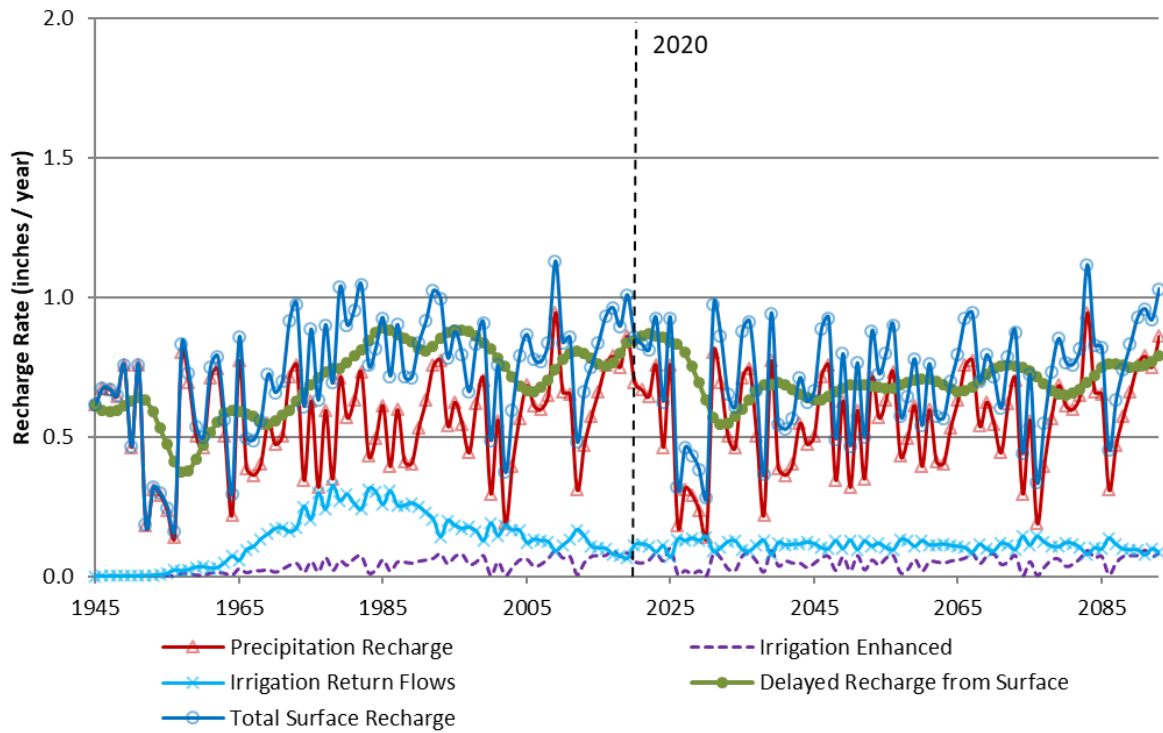
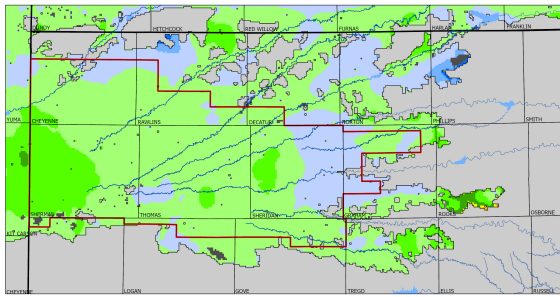
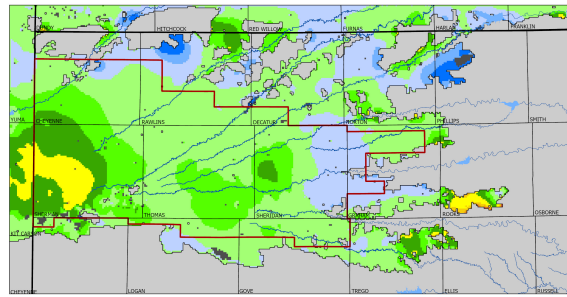


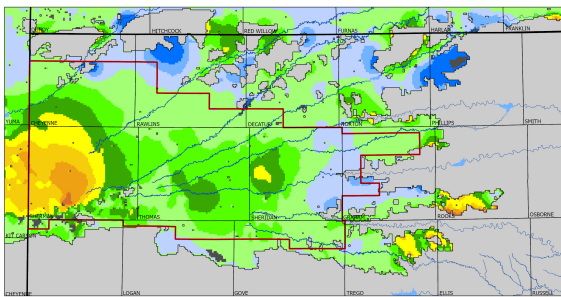
Figure 61. Different surface recharge components for GMD4 under the no change in future water-use policy scenario. The delayed surface recharge is also plotted for comparison.



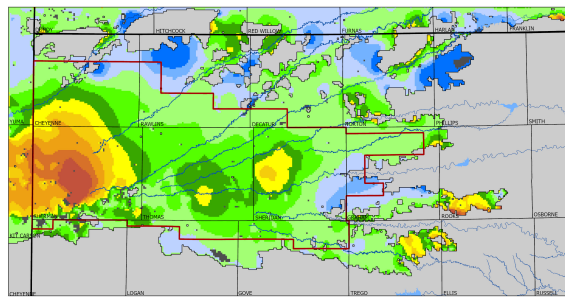
(a) 2020 to 2030



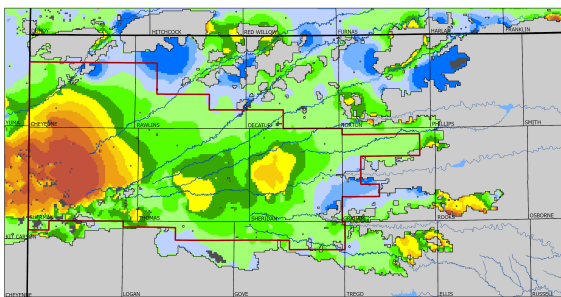
(b) 2020 to 2040



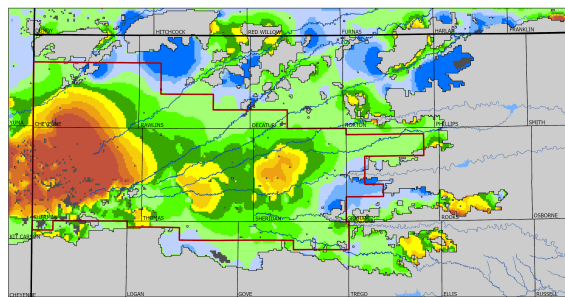
(c) 2020 to 2050



(d) 2020 to 2060



(e) 2020 to 2070



(f) 2020 to 2080

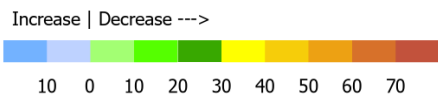


Figure 62. Simulated water-level change, in feet, for the no change in future water-use policy scenario.

Reduce Pumping by 20%

In this scenario, future pumping in all model cells is reduced by 20% from that used in the no change in future water-use policy scenario. This model run simulates what would happen if all areas achieved the targeted reduction goal listed under the SD6 LEMA plan.

Figure 63 shows the annual aquifer budget for the 20% irrigation pumping reduction scenario. Compared to the no change in water-use policy scenario, the overall aquifer pumping is reduced, and the rate of aquifer storage depletion is slowed, especially in the first couple of decades. The overall lateral flow across the district boundary switches from an inflow to an aquifer outflow component in 2070. Figure 64 shows the contribution of lagged drainage and delayed surface recharge for this scenario, and fig. 65 displays the different surface recharge components. As the pumping is reduced, so are the rates of irrigation return flow. Contributions from dewatered units are also reduced due to the moderated water-level declines. The total average inflows for the 20% reduction scenario are projected to be 1.38 inches per year.

Figure 66 shows the simulated head changes for selected time intervals for the 20% reduction in pumping. Water levels across the core of GMD4 are projected to moderate within the first decade and then, as the system adjusts to the reduced rates of recharge, transition into varying levels of declines. Under the 20 percent reduction in pumping scenario, the average water-level change across GMD4 over the next 10 (2020 to 2030) and 20 (2020 to 2040) years is projected to be -1.06 ft and -4.72 ft, respectively.

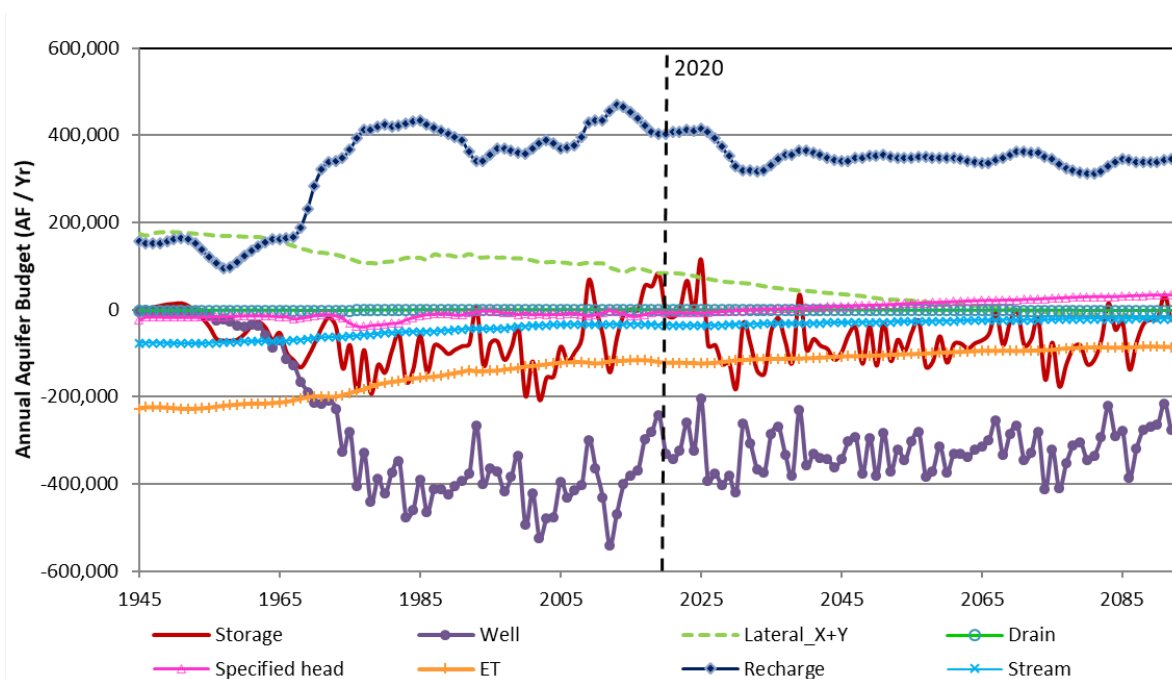


Figure 63. Annual aquifer budget for GMD4 under the 20% reduction in future water use scenario. The calibrated model budget (predevelopment to 2019) is also plotted for comparison.

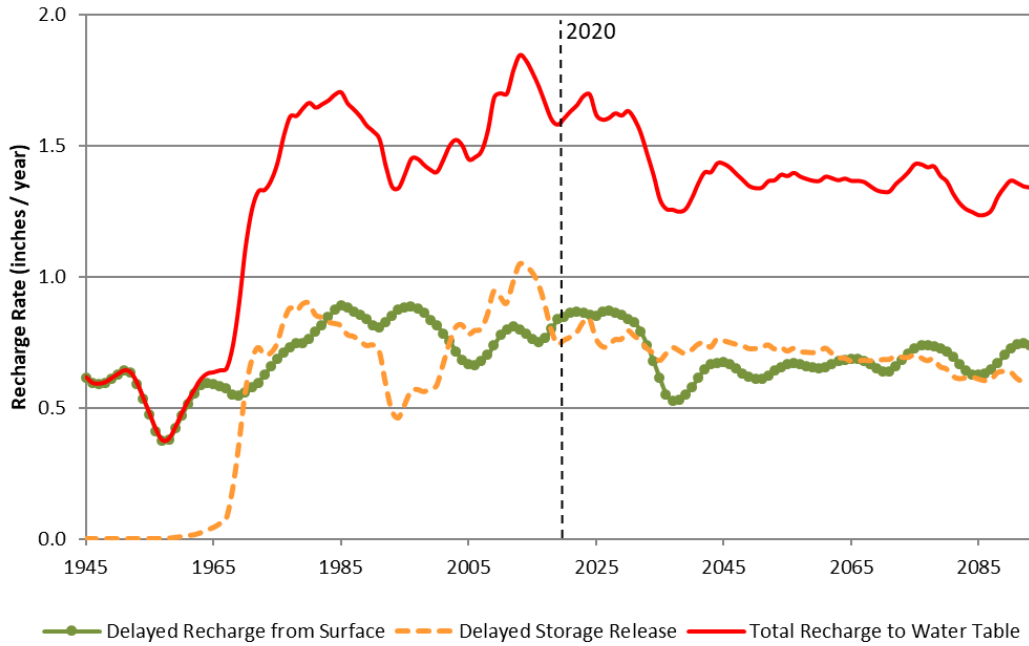


Figure 64. Water-table recharge in GMD4 under the 20% reduction in future water use scenario.

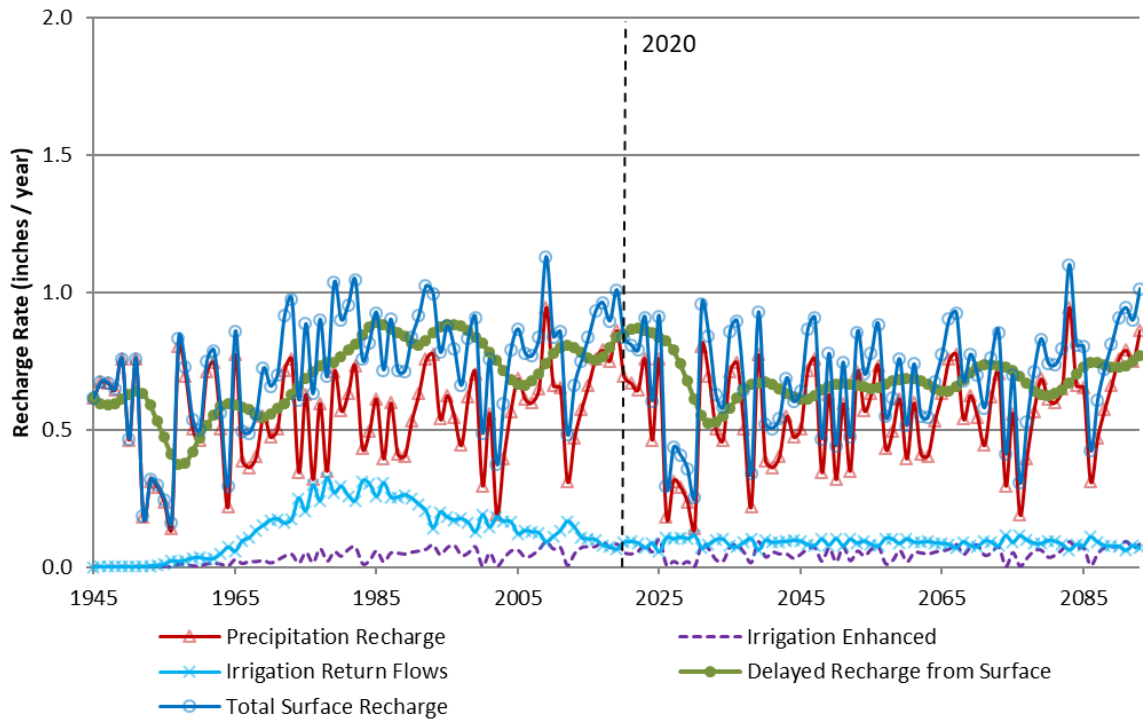
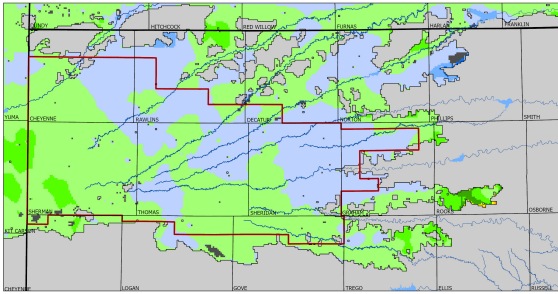
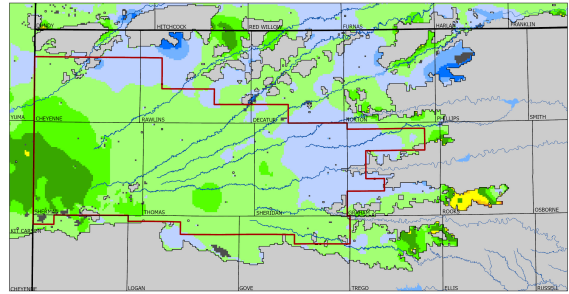


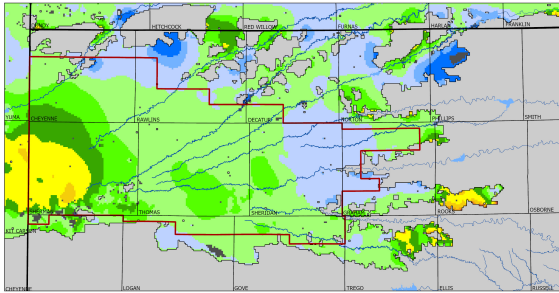
Figure 65. Different surface recharge components for GMD4 under the 20% reduction in future water use scenario. The delayed surface recharge is also plotted for comparison.



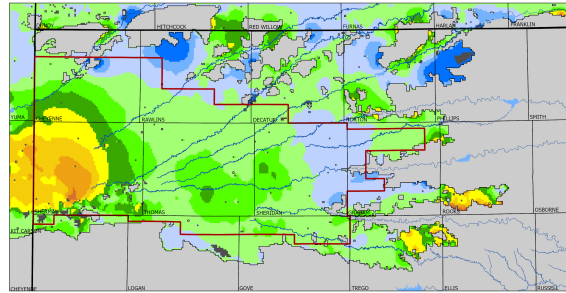
(a) 2020 to 2030



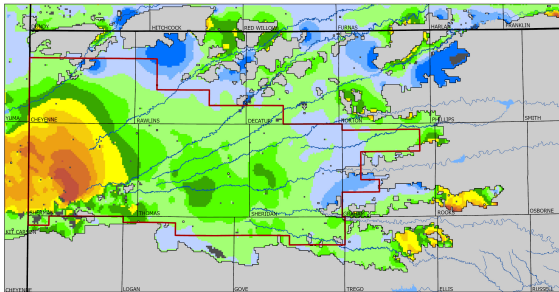
(b) 2020 to 2040



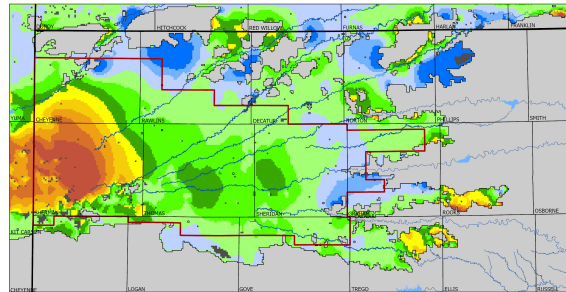
(c) 2020 to 2050



(d) 2020 to 2060



(e) 2020 to 2070



(f) 2020 to 2080

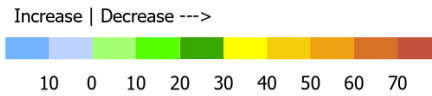


Figure 66. Simulated water-level change, in feet, for the 20% reduction in future water use scenario.

Reduce Pumping by 30%

In this scenario, future pumping in all model cells is reduced by 30% from that used in the no change in future water-use policy scenario. This model run simulates what would happen if all areas achieved the reductions more along the lines of what are actually occurring in the SD6 LEMA.

Figure 67 shows the annual aquifer budget for the 30% irrigation pumping reduction scenario. Compared to the previous two scenarios, the overall aquifer pumping is further reduced, and the rate of aquifer storage depletion is slowed, especially in the first several decades. The overall lateral flow across district boundary switches from an inflow to an aquifer outflow component in 2075. Figure 68 shows the contribution of lagged drainage and delayed surface recharge for this scenario, and fig. 69 displays the different surface recharge components. As the pumping is further reduced, so are the rates of irrigation return flows. In addition, contributions from dewatered units are reduced in response to the moderated water-level declines. The total average inflows over the 30% reduction scenario are projected to be 1.31 inches per year.

Figure 70 shows the simulated head changes for selected time intervals for the 30% reduction in pumping. Water levels across the core of GMD4 are projected to increase on average within the first decade, moderate for the next five years, and then, as the system adjusts to the reduced rates of recharge, transition into varying levels of declines. Under the 30 percent reduction in pumping scenario, the average water-level change across GMD4 over the next 10 (2020 to 2030) and 20 (2020 to 2040) years is projected to be 0.31 ft and -2.55 ft, respectively.

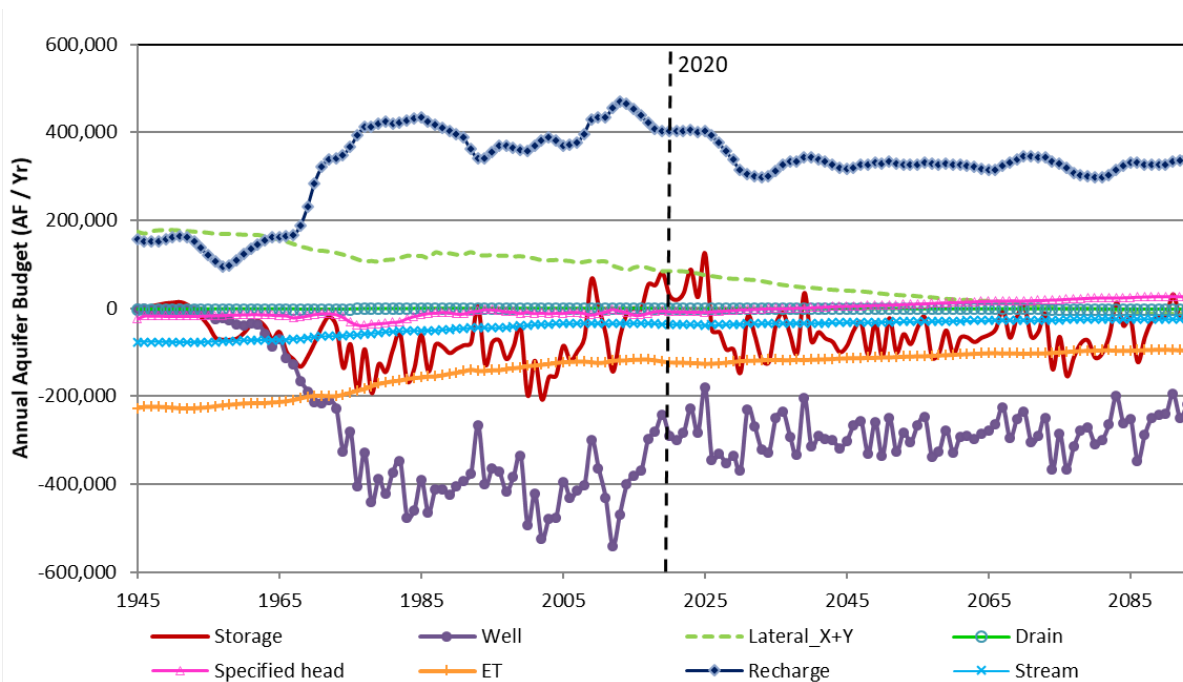


Figure 67. Annual aquifer budget for GMD4 under the 30% reduction in future water use scenario. The calibrated model budget (predevelopment to 2019) is also plotted for comparison.

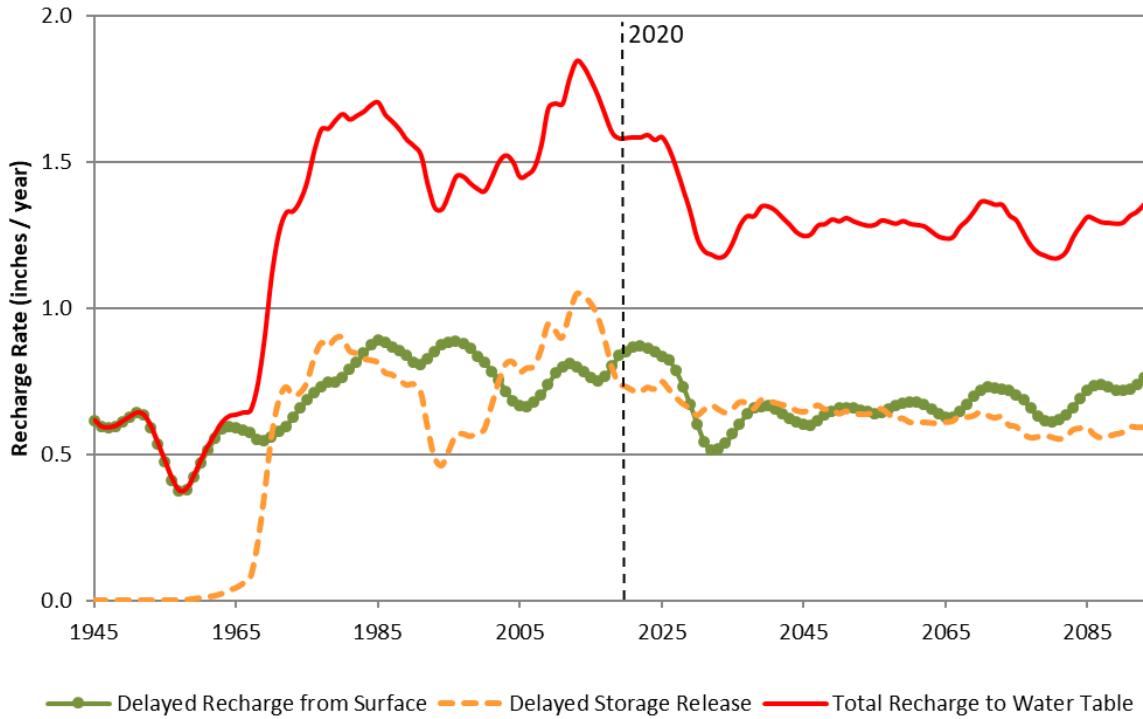


Figure 68. Water-table recharge in GMD4 under the 30% reduction in future water use scenario.

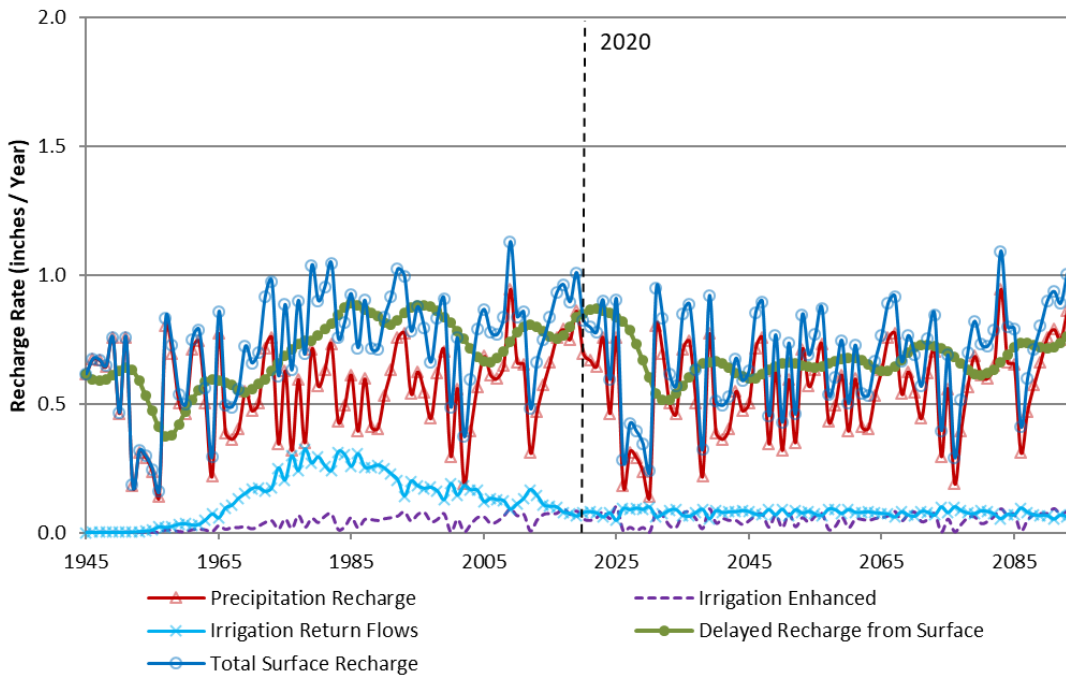
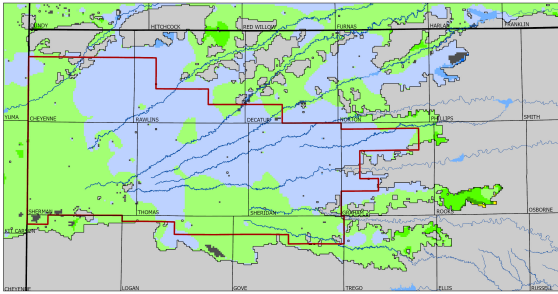
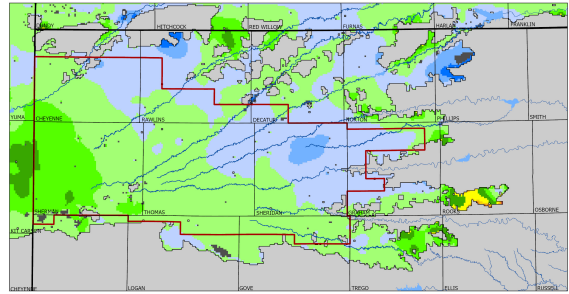


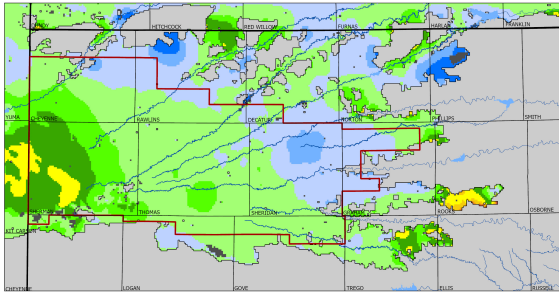
Figure 69. Different surface recharge components for GMD4 under the 30% reduction in future water use scenario. The delayed surface recharge is also plotted for comparison.



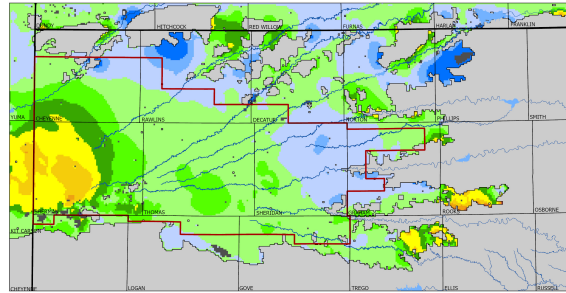
(a) 2020 to 2030



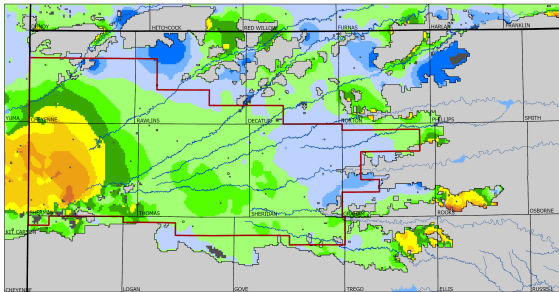
(b) 2020 to 2040



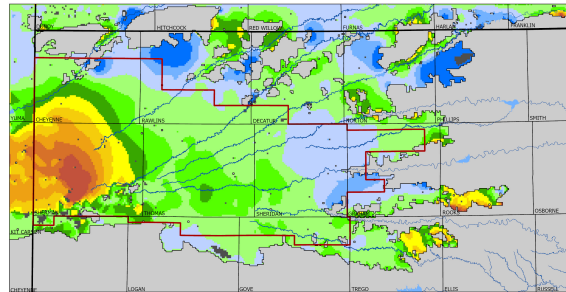
(c) 2020 to 2050



(d) 2020 to 2060



(e) 2020 to 2070



(f) 2020 to 2080

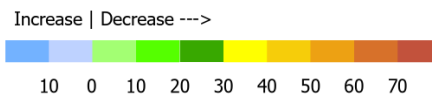


Figure 70. Simulated water-level change, in feet, for the 30% reduction in future water use scenario.

GMD4 Districtwide LEMA

In this scenario, the future pumping used in the no change in future water-use policy scenario is reduced in all cells to allocation amounts set by the GMD4 districtwide LEMA (pumping is not further adjusted based on conditions specified under the SD-6 LEMA). Under this management plan, new five-year allocations were established for water rights based on the rate of past groundwater declines occurring in specific townships. Within those townships, GMD4 and the KDA-DWR reviewed existing water rights (vested rights were excluded) to establish new LEMA allocations based on past irrigated acreage, current authorized quantity, and county-based net irrigation requirements for corn. This simulation applies the percent reduction, by township, computed by the KDA-DWR based on the new LEMA allocations (fig. 71) to the regressed pumping estimate in the no change in future water-use policy scenario.

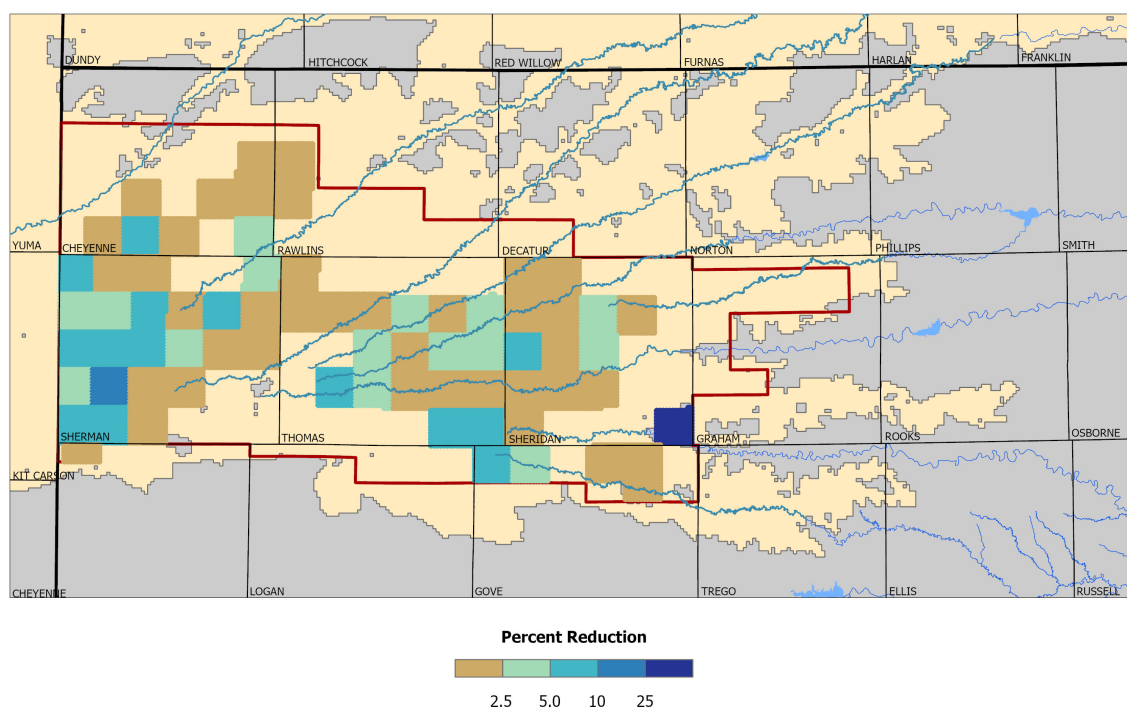


Figure 71. Percent reduction, by township, under the districtwide LEMA plan.

Figure 72 shows the annual aquifer budget for the districtwide LEMA plan reduction scenario. Most of the budget components are very similar to those in the no change in water-use policy scenario, with the overall aquifer pumping being reduced by an average of 1.74% over the simulated period. Figure 73 shows the contribution of lagged drainage and delayed surface recharge for this scenario, and fig. 74 displays the different surface recharge components. The small reduction in pumping results in very small changes to the other recharge components. The total average inflows over the districtwide scenario are projected to be 1.50 inches per year.

Figure 75 shows the simulated head changes at selected intervals for the districtwide LEMA scenario. Most of the district will continue to see varying levels of water-level declines. However,

even with the relatively small reductions in pumping, because the districtwide LEMA is focused on townships that have already shown relatively greater past levels of declines, future declines are noticeably less in those targeted areas. Under the districtwide LEMA scenario, the average water-level change across GMD4 over the next 10 (2020 to 2030) and 20 (2020 to 2040) years is projected to be 3.47 ft and -8.89 ft, respectively.

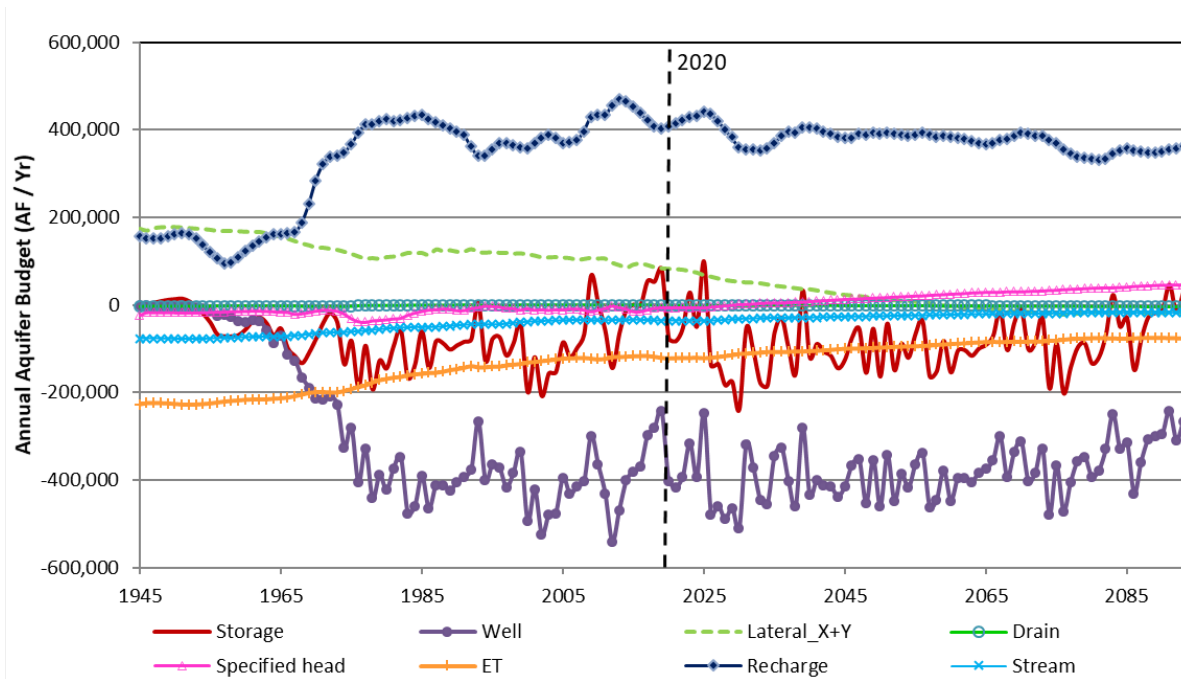


Figure 72. Annual aquifer budget for GMD4 under the districtwide LEMA plan future water use scenario. The calibrated model budget (predevelopment to 2019) is also plotted for comparison.

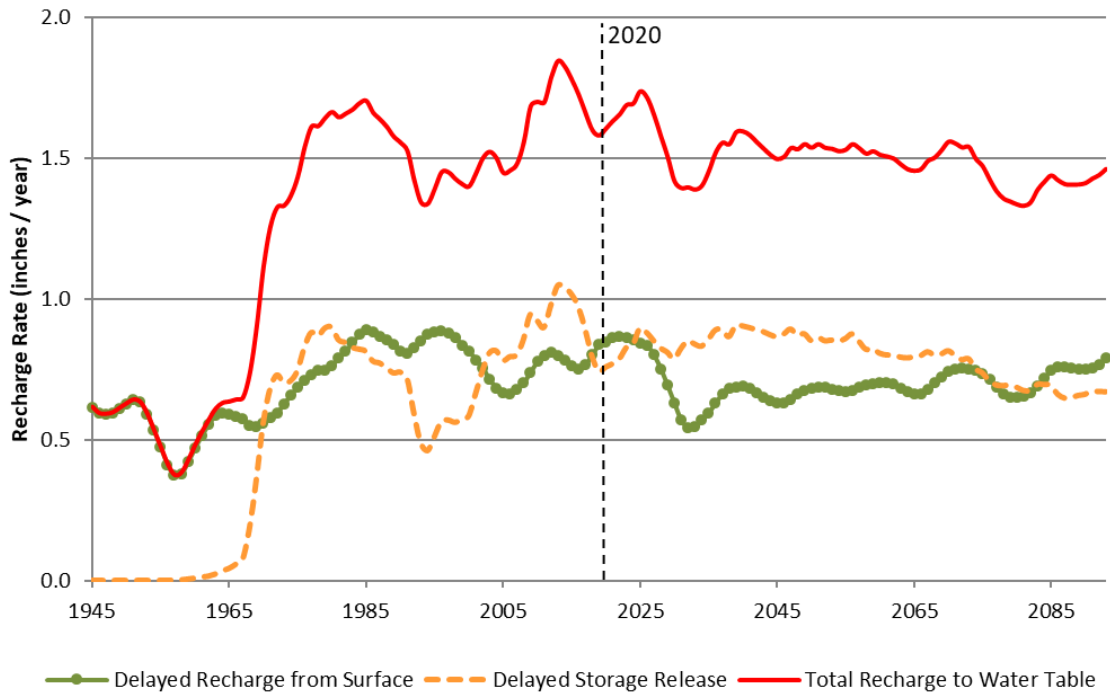


Figure 73. Water-table recharge in GMD4 under the districtwide LEMA plan future water use scenario.

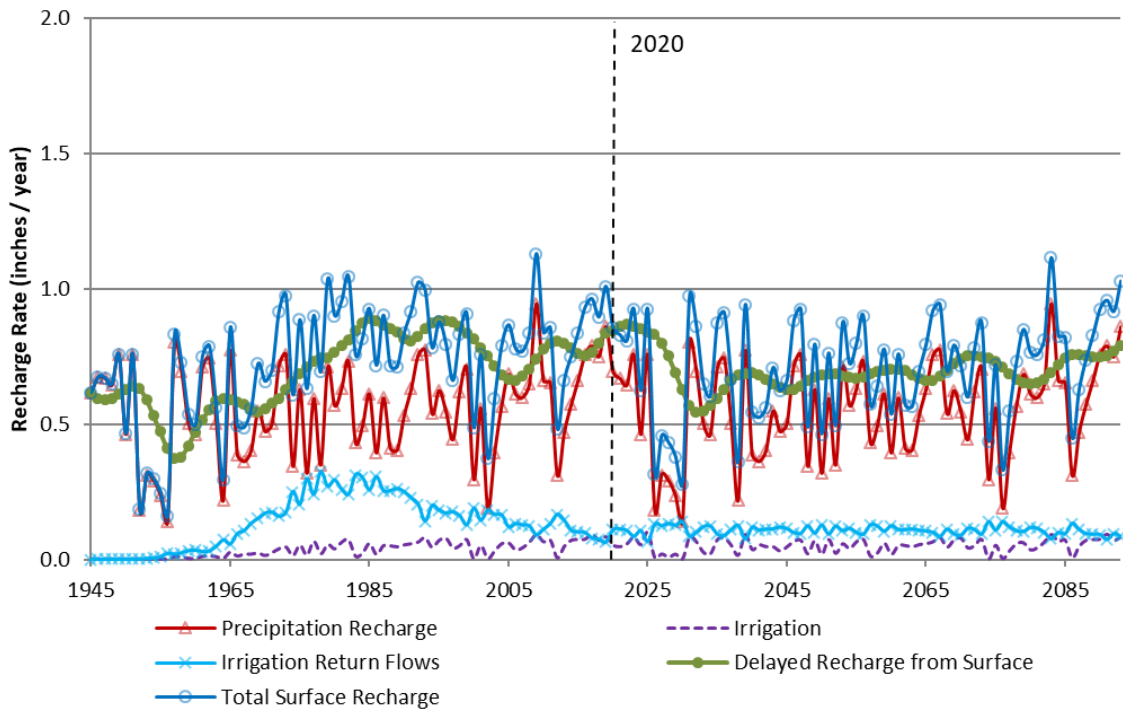
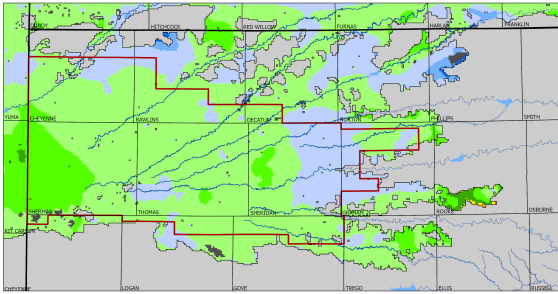
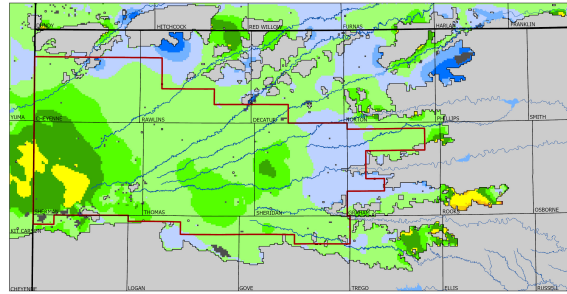


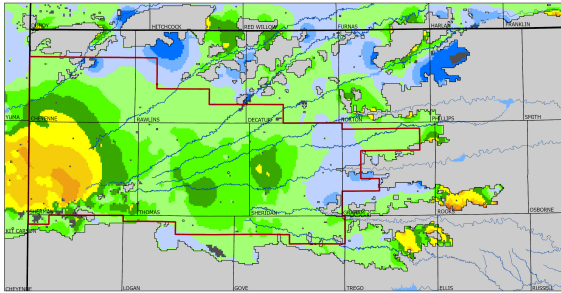
Figure 74. Different surface recharge components for GMD4 under the districtwide LEMA future water use scenario. The delayed surface recharge is also plotted for comparison.



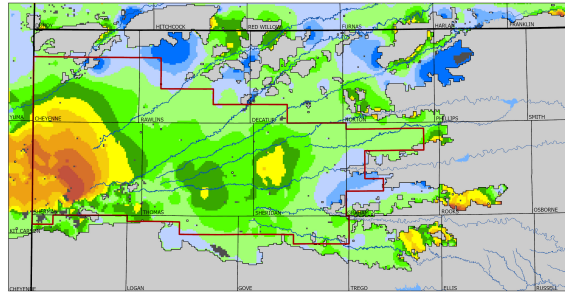
(a) 2020 to 2030



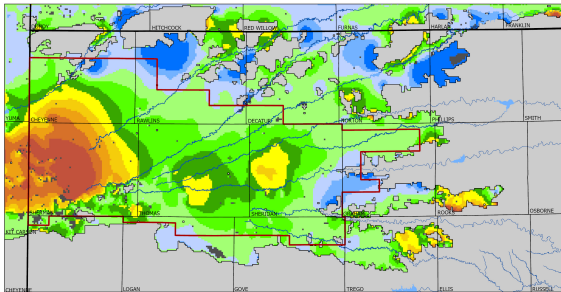
(b) 2020 to 2040



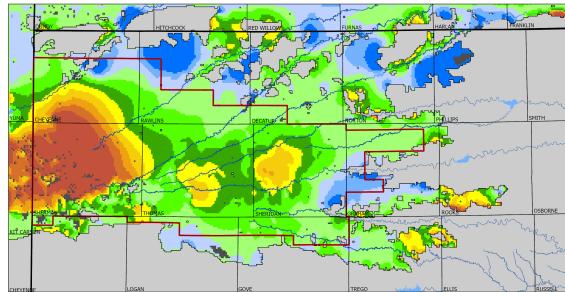
(c) 2020 to 2050



(d) 2020 to 2060



(e) 2020 to 2070



(f) 2020 to 2080

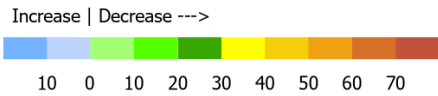


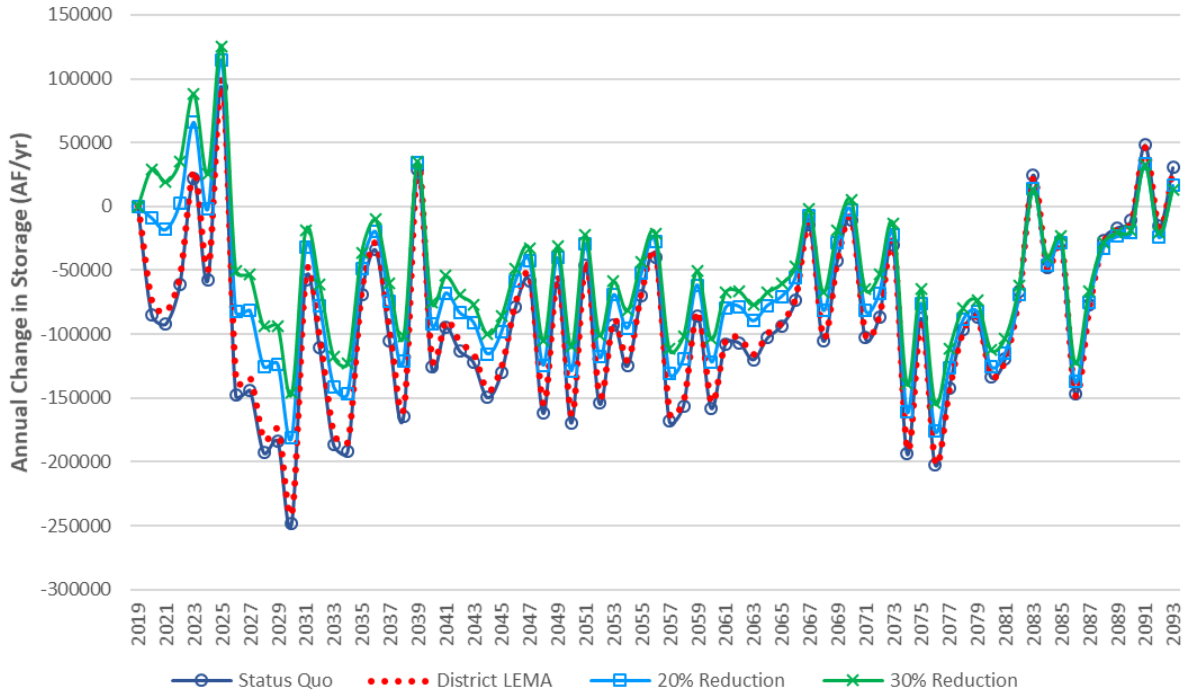
Figure 75. Simulated water-level change, in feet, for the districtwide LEMA future water use scenario.

Comparison of All Scenarios

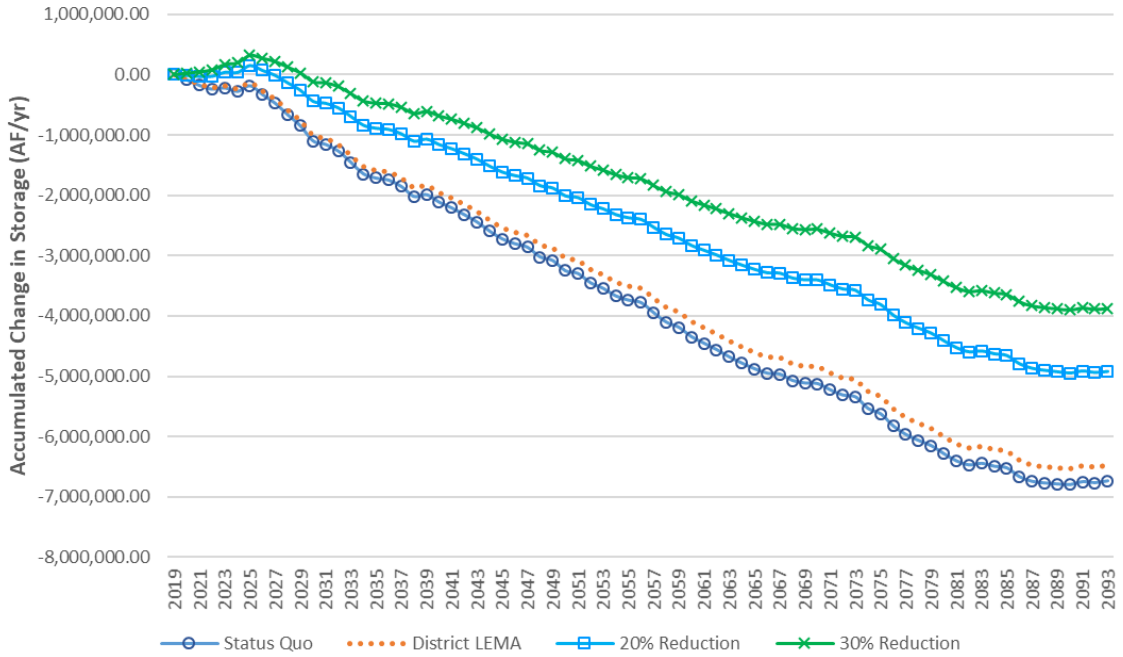
Figure 76 shows the annual and cumulative change in storage for GMD4 under all modeled scenarios. Changes to storage are very similar between the no change in water use and the districtwide LEMA scenarios, given the simulated reductions in pumping are small and targeted to specific townships. By contrast, aquifer loss caused by declining water levels is stabilized under both the 20% and 30% pumping reduction scenarios over the first decade, 2020 to 2030, despite having a repeat of 1950s drought conditions. As the components of the water budget adjust to the new pumping regimes, reduction in the rate of storage loss eventually slows. By the end of the scenario period (2094), the 20% and 30% pumping reduction have reduced storage loss by 27% and 43%, respectively.

Figures 77 and 78 show the projected aquifer thickness in 2050 and 2080 when the simulated water-level changes from 2020 to 2050 and from 2020 to 2080 are applied to the present day aquifer thickness. Under the no change in water use scenario, the average 2018 to 2020 aquifer thickness (fig. 16) in GMD4 is reduced from 69 ft to 55 ft in 2050 and 42 ft in 2080. Under the 30% pumping reduction scenario, average aquifer thickness across the district is projected to be 67 ft and 58 ft in 2050 and 2080, respectively.

A notable result from the future scenario simulations is that, due to spatial variations in hydrological conditions, aquifer responses to water-use management are different. For example, in western Sherman County, although there is more significant aquifer storage remaining due to the large saturated thickness, current pumping exceeds net inflow and, as a result, water levels continue to display a significant rate of decline even under a 30% reduction. In comparison, in portions of Thomas and Sheridan counties, groundwater declines are tempered by pumping reductions, resulting in extended aquifer lifetimes.

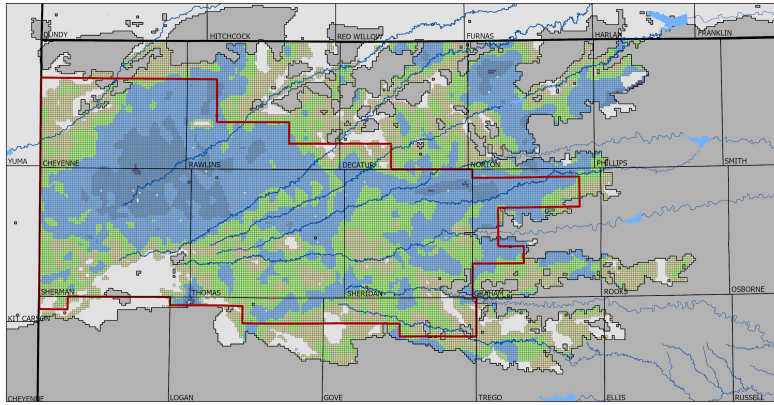


a) Annual

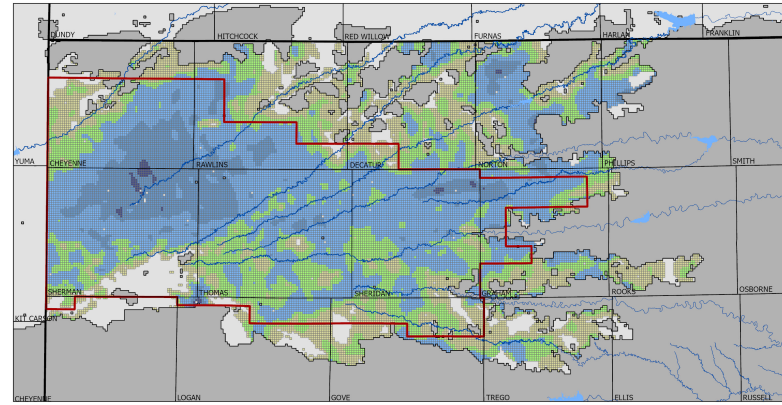


b) Accumulated

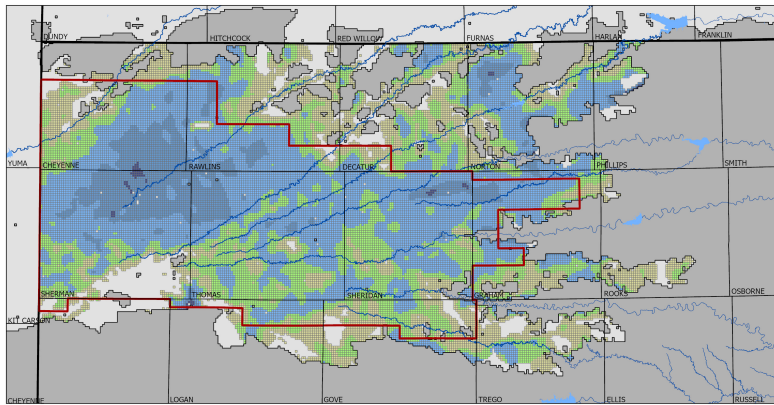
Figure 76. Change in GMD4 aquifer storage for all future scenarios.



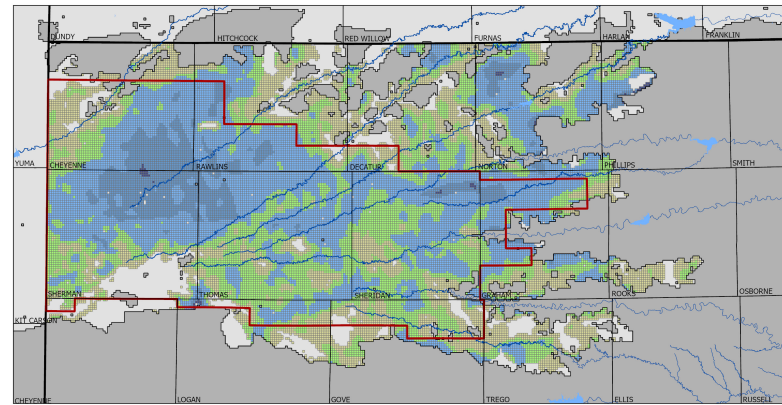
(a) Status quo or no change in water-use policy



(c) 30% reduction in pumping

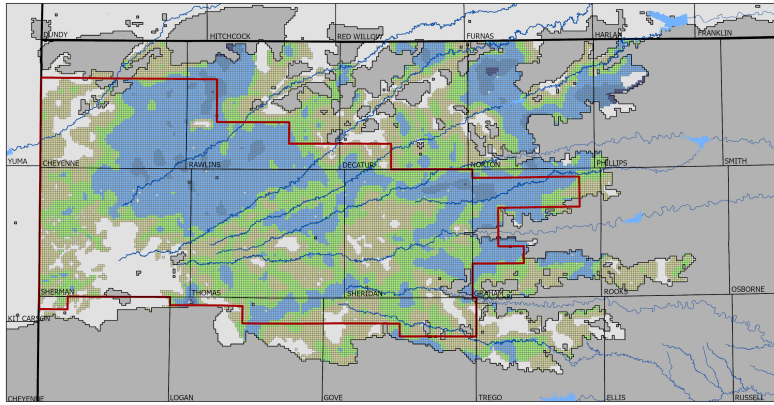


(b) 20% reduction in pumping

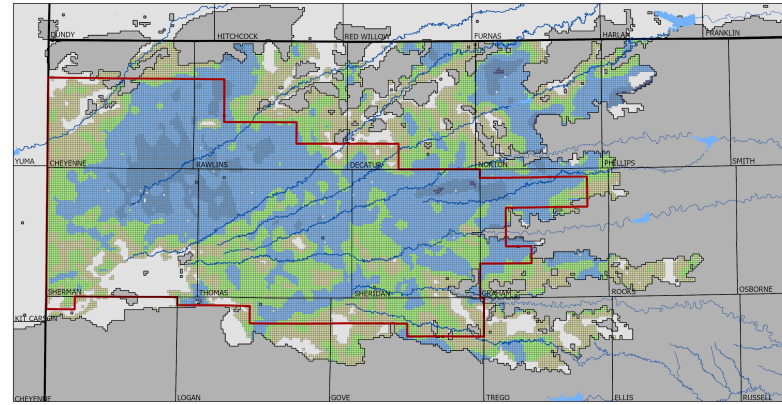


(d) GMD4 districtwide LEMA

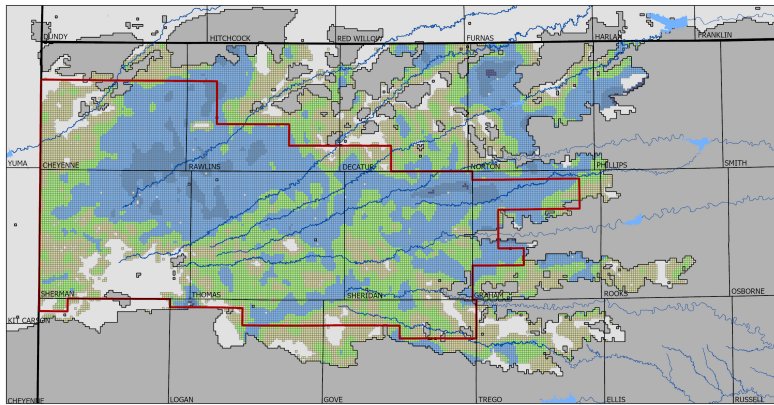
Figure 77. Simulated 2050 aquifer thickness, in feet, for all future scenarios.



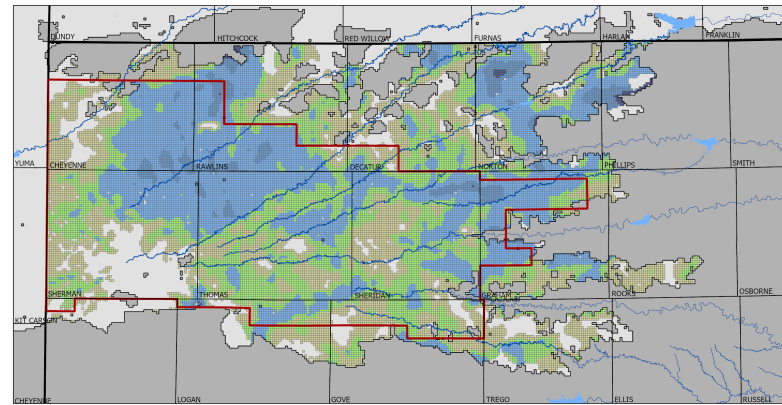
(a) Status quo or no change in water-use policy



(c) 30% reduction in pumping



(b) 20% reduction in pumping



(d) GMD4 districtwide LEMA

Figure 78. Simulated 2080 aquifer thickness, in feet, for all future scenarios.

Acknowledgments

The KGS modeling team acknowledges the funding support of the Kansas Water Office (and the State Water Plan Fund) and Northwest Kansas GMD4 for this project. The authors thank Josh Olson of the KWO and Shannon Kenyon of GMD4, who served as the primary contacts. In addition, we thank the GMD4 Board Members, who helped review the model's development. We also acknowledge KGS staff who contributed to this report. John Woods spent a substantial amount of time identifying stream elevations along the selected stream courses used in the project. We also thank Julie Tollefson, KGS editor, who reviewed the final report.

REFERENCES

- Bayne, C. K., 1956, Geology and ground-water resources of Sheridan County, Kansas: Kansas Geological Survey, Bulletin 116, 94 p.
- Becker, M. F., 1999, Digital map of predevelopment water levels for the High Plains aquifer in parts of Colorado, Kansas, Nebraska, New Mexico, Oklahoma, South Dakota, Texas, and Wyoming: U.S. Geological Survey, Open-File Report 99-264.
- Bohling, G. C., 2016, User's guide to Hydra_translate.xlsm: An Excel workbook for quantification of water well driller's logs: Kansas Geological Survey, Open-File Report 2016-30, 26 p.
- Bohling, G. C., Butler, J. J., Whittemore, D. O., and Wilson, B. B., 2021, Evaluation of data needs for assessments of aquifers supporting irrigated agriculture: *Water Resources Research*, v. 57, e2020WR028320. <https://doi.org/10.1029/2020WR028320>
- Bohling, G. C., Wilson, B. B., and Adkins-Heljeson, D., 2020, Explanation of quantitatively interpreted logs in the Kansas Geological Survey's WWC5 database: Kansas Geological Survey, Open-File Report 2020-13, 14 p.
- Butler, J. J., Jr., Whittemore, D. O., and Wilson, B. B., 2017, Equus Beds Groundwater Management District No. 2 sustainability assessment: Kansas Geological Survey, Open-File Report 2017-3, 93 p.
- Butler, J. J., Jr., Whittemore, D. O., Wilson, B. B., and Bohling, G. C., 2016, A new approach for assessing the future of aquifers supporting irrigated agriculture: *Geophysical Research Letters*, v. 43, no. 5, p. 2,004–2,010.
- Butler, J. J., Jr., Whittemore, D. O., Wilson, B. B., and Bohling, G. C., 2018, Sustainability of aquifers supporting irrigated agriculture: A case study of the High Plains aquifer in Kansas: *Water International*, v. 43, no. 6, p. 815–828.
- Doherty, J., 2004, PEST—Model-Independent Parameter Estimation. User Manual, 5th Edition: Watermark Numerical Computing, 333 p.
- Frye, J. C., 1945, Geology and ground-water resources of Thomas County, Kansas: Kansas Geological Survey, Bulletin 45, 110 p.
- Frye, J. C., and Leonard, A. R., 1949, Geology and ground-water resources of Norton County and northwestern Phillips County, Kansas: Kansas Geological Survey, Bulletin 81, 144 p.
- Hanson, R. L., 1991, Evapotranspiration and droughts: U.S. Geological Survey Water Supply Paper 2375, p. 99–104.
- Harbaugh, A. W., Banta, E. R., Hill, M. C., and McDonald, M. G., 2000, MODFLOW-2000, the U.S. Geological Survey modular ground-water model—User guide to modularization concepts and the ground-water flow process: U.S. Geological Survey, Open-File Report 00-92, 121 p.
- Hodson, W. G., 1963, Geology and ground-water resources of Wallace County, Kansas: Kansas Geological Survey, Bulletin 161, 108 p.
- Hodson, W. G., 1969, Geology and ground-water resources of Decatur County, Kansas: Kansas Geological Survey, Bulletin 196, 41 p.
- Hodson, W. G., and Wahl, K. D., 1960, Geology and ground-water resources of Gove County, Kansas: Kansas Geological Survey, Bulletin 145, 126 p.
- Homer, C. H., Fry, J. A., and Barnes C. A., 2012, The National Land Cover Database: U.S. Geological Survey Fact Sheet 2012-3020, 4 p.
- Johnson, C. R., 1958, Geology and ground-water resources of Logan County, Kansas: Kansas Geological Survey, Bulletin 129, 177 p.
- Liu, G., Wilson, B. B., Bohling, G. C., Whittemore, D. O., and Butler, J. J., Jr., 2021, Specific yield in regional groundwater modeling: Pitfalls, ramifications, and a promising path forward: *Water Resources Research*, in review, 35 p.
- Liu, G., Wilson, B. B., Whittemore, D. O., Wei Jin, W., and Butler, J. J., Jr., 2010, Ground-water model for Southwest Kansas Groundwater Management District No. 3: Kansas Geological Survey, Open-File Report 2010-18, 106 p.

- Ludvigson, G. A., Sawin, R. S., Franseen, E. K., Watney, W. L., West, R. R., and Smith, J. J., 2009, A review of the stratigraphy of the Ogallala Formation and revision of Neogene ("Tertiary") nomenclature in Kansas; *in*, Current Research in Earth Sciences: Kansas Geological Survey, Bulletin 256, part 2.
- Macfarlane, P. A., and Wilson, B. B., 2006, Enhancement of the bedrock-surface map beneath the Ogallala portion of the High Plains aquifer, western Kansas: Kansas Geological Survey, Technical Series Report 20, 28 p.
- Peterson, D. L., 2018 [2015], Kansas land cover patterns phase II — final report: Kansas Biological Survey, University of Kansas, 17 p.
- Prescott, G. C., Jr., 1952, Geology and ground-water resources of Cheyenne County, Kansas: Kansas Geological Survey, Bulletin 100, 106 p.
- Prescott, G. C., Jr., 1953, Geology and ground-water resources of Sherman County, Kansas: Kansas Geological Survey, Bulletin 105, 130 p.
- Prescott, G. C., Jr. 1955, Geology and ground-water resources of Graham County, Kansas: Kansas Geological Survey, Bulletin 110, 98 p.
- Prudic, D. E., Konikow, L. F., and Banta, E. R., 2004, A new streamflow-routing (SFR1) package to simulate stream-aquifer interaction with MODFLOW-2000: U.S. Geological Survey, Open-File Report 2004-1042, 104 p.
- Republican River Compact Administration (2003), Republican River Compact Administration Ground Water Model, June 30, 2003.
<http://www.republicanrivercompact.org/v12p/RRCAModelDocumentation.pdf>
- Walters, K. L., 1956, Geology and ground-water resources of Rawlins County, Kansas: Kansas Geological Survey, Bulletin 117, 100 p.
- Whittemore, D. O., Butler, J. J., Jr., and Wilson, B. B., 2016, Assessing the major drivers of water-level declines: New insights into the future of heavily stressed aquifers: Hydrologic. Science Journal, v. 61, no. 1, p. 134–145.
- Whittemore, D. O., Macfarlane, P. A., and Wilson, B. B., 2014, Water resources of the Dakota aquifer in Kansas: Kansas Geological Survey, Bulletin 260, 68 p.
- Wilson, B. B., and Bohling, G. C., 2003, Assessment of reported water use and total annual precipitation, State of Kansas: Kansas Geological Survey, Open-File Report 2003-55C, 39 p.
- Wilson, B. B., Liu, G., Bohling, G. C., Whittemore, D. O., and Butler, J. J., Jr., 2015, West Central Kansas GMD1 Model: Kansas Geological Survey, Open-File Report 2015-33, 137 p.
- Wilson, B. B., Liu, G., Bohling, G. C., Whittemore, D. O., and Butler, J. J., Jr., 2020, GMD2 Groundwater Flow Model: Kansas Geological Survey, Open-File Report 2020-1, 93 p.
- Wilson, B. B., Liu, G., Whittemore, D. O., and Butler, J. J., 2008, Smoky Hill River ground-water model: Kansas Geological Survey, Open-File Report 2008-20, 99 p.